MOLECULAR PHYSIOLOGY OF TICK SALIVARY SECRETION AND TRANSCRIPTOMICS OF TICK IN INTERACTION WITH TICK-BORNE PATHOGEN

by

DONGHUN KIM

B.S., Kyungpook National University, 2006
M.S., Kyungpook National University, 2008

AN ABSTRACT OF A DISSERTATION

submitted in partial fulfillment of the requirements for the degree

DOCTOR OF PHILOSOPHY

Department of Entomology
College of Agriculture

KANSAS STATE UNIVERSITY
Manhattan, Kansas

2016

Abstract

Tick salivary secretion is crucial for survival and for successful feeding. Tick saliva includes excretory water/ions and bioactive components for compromising the hosts' immune responses, and provides a direct route for pathogen transmission. Control of the tick salivation involves autocrine/paracrine dopamine, the most potent stimulator of tick salivation. Our research group reported the presence of two dopamine receptors in the salivary glands of the blacklegged tick (*Ixodes scapularis*): dopamine receptor (D1) and invertebrate specific D1-like dopamine receptor (InvD1L).

Dopamine-induced salivary secretion was orchestrated by two distinct physiological roles via activation of the two dopamine receptors (Chapter 2). Low concentration of dopamine activated D1 receptor on epithelial cells of salivary gland acini leading inward fluid transport. High concentration of dopamine activated InvD1L receptors on axonal projections innervating myoepithelial cells modulating pumping/gating actions for emptying luminal saliva into the main duct. Thus, ticks coordinated salivary secretion with duo dopamine receptors.

Dopamine-mediated saliva production involves an important downstream component, Na/K-ATPase (Chapter 3). Na/K-ATPase was found in the epithelial cells of all types of acini. However, Na/K-ATPase had two different functions in salivary secretion in different acini: 1) dopamine-mediated production of primary saliva in distally located salivary gland acini type-2/-3, and 2) dopamine-independent resorption in proximally located salivary gland acini type-1. Type-1 acini were also found to function in direct water absorption of off-host ticks, which could be a potential route for delivery of acaricides.

Chapter 4 investigated the comparative transcriptomics of the lone star tick underlying the processes of pathogen acquisition. Differential expression analyses in pathogen-exposed

ticks revealed a number of transcripts that are important in the tick-pathogen interaction. These included genes for tick immunity against pathogen and for modulation of tick physiology facilitating a pathogen's invasion and proliferation.

My study expanded the understanding of physiological mechanisms controlling tick salivation. In addition, transcriptomics of ticks in interaction with pathogen identified several genes that are relevant in vector/pathogen interactions. The knowledge obtained in my study will facilitate to the development of novel methods for the disruption of tick feeding and pathogen transmission.

MOLECULAR PHYSIOLOGY OF TICK SALIVARY SECRETION AND TRANSCRIPTOMICS OF TICK IN INTERACTION WITH TICK-BORNE PATHOGEN

by

DONGHUN KIM

B.S., Kyungpook National University, 2006
M.S., Kyungpook National University, 2008

A DISSERTATION

submitted in partial fulfillment of the requirements for the degree

DOCTOR OF PHILOSOPHY

Department of Entomology
College of Agriculture

KANSAS STATE UNIVERSITY
Manhattan, Kansas

2016

Approved by:

Major Professor
Yoonseong Park

Abstract

Tick salivary secretion is crucial for survival and for successful feeding. Tick saliva includes excretory water/ions and bioactive components for compromising the hosts' immune responses, and provides a direct route for pathogen transmission. Control of the tick salivation involves autocrine/paracrine dopamine, the most potent stimulator of tick salivation. Our research group reported the presence of two dopamine receptors in the salivary glands of the blacklegged tick (*Ixodes scapularis*): dopamine receptor (D1) and invertebrate specific D1-like dopamine receptor (InvD1L).

Dopamine-induced salivary secretion was orchestrated by two distinct physiological roles via activation of the two dopamine receptors (Chapter 2). Low concentration of dopamine activated D1 receptor on epithelial cells of salivary gland acini leading inward fluid transport. High concentration of dopamine activated InvD1L receptors on axonal projections innervating myoepithelial cells modulating pumping/gating actions for emptying luminal saliva into the main duct. Thus, ticks coordinated salivary secretion with duo dopamine receptors.

Dopamine-mediated saliva production involves an important downstream component, Na/K-ATPase (Chapter 3). Na/K-ATPase was found in the epithelial cells of all types of acini. However, Na/K-ATPase had two different functions in salivary secretion in different acini: 1) dopamine-mediated production of primary saliva in distally located salivary gland acini type-2/-3, and 2) dopamine-independent resorption in proximally located salivary gland acini type-1. Type-1 acini were also found to function in direct water absorption of off-host ticks, which could be a potential route for delivery of acaricides.

Chapter 4 investigated the comparative transcriptomics of the lone star tick underlying the processes of pathogen acquisition. Differential expression analyses in pathogen-exposed

ticks revealed a number of transcripts that are important in the tick-pathogen interaction. These included genes for tick immunity against pathogen and for modulation of tick physiology facilitating a pathogen's invasion and proliferation.

My study expanded the understanding of physiological mechanisms controlling tick salivation. In addition, transcriptomics of ticks in interaction with pathogen identified several genes that are relevant in vector/pathogen interactions. The knowledge obtained in my study will facilitate to the development of novel methods for the disruption of tick feeding and pathogen transmission.

Table of Contents

List of Figures

List of Tables

Acknowledgements

This dissertation could not have been completed without the great support that I have received from so many people over the years.

To my advisor, Dr. Yoonseong Park, I deeply appreciate you for the advice, support, patience, and willingness that allowed me to pursue on research topics for tick salivary glands physiology and transcriptomics. The joy and enthusiasm he has for his research was contagious and motivational for me. I am dreaming to become a scientist and advisor like him in near future.

I would like to thank my Ph.D. committee members: Drs. Michael Kanost, Kun Yan Zhu, and Gregory Ragland for their time, interest, and helpful comments.

I thank all my lab members. I always enjoyed the time with you and love our environment in Park lab. I also thank to all Korean graduate students and their families for their warm words and encouragement. I learned a lot from you.

Lastly, I would like to thank my family for all their love and support. My parents always support me in all my pursuits. Most of all for my loving, supportive, encouraging and respecting wife Eunkyung Shin whose faithful support during the doctoral degree is so appreciated. To my son Ian Kim, you are the best present in my life. Thank you for coming into my life and giving your mom and dad joy.

Chapter 1 - Introduction

Ticks

Ticks belong to the Phylum Arthropoda, Class Arachnida, Subclass Acari, which is characterized by an envelope like body, rather than having numerous body segments as in other arthropods. Acari are further divided into two superorders: Parasitiformes and Acariformes. Parasitiformes includes ticks under the order Ixodida, which has 899 valid species divided into three Families: Ixodidae (hard ticks), Argasidae (soft ticks), and Nuttalliellidae (monospecific family)(Barker and Murrell, 2004).

Ticks have four developmental stages: egg, larva, nymph and adult. During the transition from the larval stage into a nymph, ticks go from possessing three pairs of legs to having four pairs of legs, which are retained into the adult stage. Ticks are obligatory hematophagous arthropods, requiring blood meals in order to transition between each life stage. After blood feeding on a given host, ticks drop off of the host and molt into the next stage or, in the case of adult female ticks, lay their eggs. All developmental stages require blood meals, with the exception of the egg stage. Hard ticks are further classified based upon the number of hosts required in order to progress through their developmental stages: one-, two-, or three-host ticks. One-host ticks attach and feed on a single host for the duration of all of their developmental stages (e.g. *Boophilus microplus*). Two-host ticks feed on a single host for the duration of the larval and nymphal stages before dropping off of the host. After molting from a nymph, the adult attaches to a second host (e.g. *Hyalomma dromedarii*) to take its final blood meal before dropping off the host to lay eggs. Three-host ticks require different hosts for each life stage: larva, nymph, and adult. Most ticks in the United States are three-host ticks, as are the cases with the blacklegged tick (*Ixodes scapularis*), lone star tick (*Amblyomma americanum*), and the brown dog tick (*Rhipicephalus sanguineus*). Soft ticks have more than one nymphal stage, requiring additional blood feedings. With the exception of having an increased number of nymphal stages, soft ticks undergo all of the same developmental stages as hard ticks (Hoogstraal, 1985).

Vector of diseases

Ticks are obligatory hematophagous ectoparasites, which feed numerous times throughout their development. During blood meals, ticks imbibe large amounts of blood, sometimes feeding for upwards of two weeks, increasing their body mass by up to 100 times their unfed weight (Kaufman, 2007). Pharmacological agents secreted along with the tick's saliva help to facilitate the completion of blood feeding by inhibiting the host's immune response, including reducing inflammation, and circumventing the hemostatic response of the host. This compromised state of the host immune system inadvertently provides opportunistic pathogens an ample means for successful transmission (Francischetti et al., 2009; Hovius et al., 2007; Ribeiro, 1987). Tick blood digestion occurs in midgut cells expose pathogen in limited chance to proteinases. A small portion of an ingested blood is retained in the midgut as ticks undergo the molting process between life stages, enabling pathogens to survive in the gut for future transmission into the next host. Taken altogether, the exclusive blood feeding behaviors of ticks makes them very efficient vectors of blood-borne pathogens.

Hard ticks are major vectors of diseases in the United States and throughout the world, although both hard and soft ticks are known to transmit diseases, such as Lyme disease and tick-borne relapsing fever (TBRF), respectively. Ticks transmit various microbial disease causing agents, including protozoans, bacteria, and viruses to humans, as well as animals, including pets, livestock, and wildlife.

Lyme disease, which is caused by the spirochete, *Borrelia burgdorferi*, is the most commonly reported vector-borne disease transmitted by *Ixodes scapularis* in the United States. First reported as a new inflammatory arthritis in Old Lyme, Connecticut in the mid-1970s, Lyme disease often manifests with flu-like symptoms, but is often accompanied by a characteristic skin rash in the shape of a "bull's eye". It was later described by Dr. Burgdorfer in 1981 that the culprit for Lyme disease, the spirochete, *B. burgdorferi,* is transmitted by *I. scapularis* (Burgdorfer et al., 1982). The nymphal stage of *I. scapularis* is the major vector for Lyme disease, which the CDC reports has afflicted just over 25,000 individuals per year over the last 10 years (2005-2014). Additionally, Lyme disease has a large geographical distribution along the eastern coast of the United States, and is steadily spreading into the Midwest.

Human monocytic ehrlichiosis is caused by the obligatory intracellular bacteria, *Ehrlichia chaffeensis*, which is transmitted by the lone star tick, *Amblyomma americanum*

(Anderson et al., 1993). This species of tick has a large geographic distribution, spanning nearly the entire eastern half of the United States, posing a real risk to the residents of numerous southeastern states of being exposed to ehrlichiosis. Annual cases of ehrlichiosis keep increasing every year, and according to CDC reports, the cases of ehrlichiosis were almost five times higher in 2008 (961 cases) than in 2000 (200 cases) (http://www.cdc.gov/ehrlichiosis/stats/), although the numbers of annual ehrlichiosis cases have decreased slightly in subsequent years.

Tick salivary glands in the feeding and osmoregulation

Ticks salivary secretion is crucial for successful feeding on the vertebrate host. Tick saliva includes excretory water/ions and bioactive components for compromising the hosts' immune responses (Kaufman and Phillips, 1973a; Ribeiro, 1989; Schoeler and Wikel, 2001; Valenzuela, 2004) and also provides a direct route for pathogen transmission. Understanding the physiology of salivary secretion may provide an insight into the development of novel methods to disrupt tick feeding and pathogen transmission.

Tick salivary glands are located in the anterolateral region of the tick, each resembling a cluster of grape, and consisting of one agranular and two types of granular acini (aveoli) (Fig. 1-1A) (Binnington, 1978). Agranular acini are commonly referred to as type 1 acini, which are located along the proximal end of the main duct near to the mouth parts (Krolak et al., 1982; Needham et al., 1990). The location of type 1 acini suggests that they function in the secretion of hygroscopic saliva in order to capture atmospheric water vapor while in the off-host phase (Rudolph and Knulle, 1974). Four types of cells are included in type 1 acini: central lamellate, peripheral lamellate, peritubular, and circumluminal cells (Fig. 1- 1B). Peripheral lamellate cells have a highly complex labyrinth structure with dense mitochondria and are thought to be the major functional cells for ion and water transport. Granular acini are type-2 and type-3, which are located in the secondary and tertiary branches of the salivary glands, respectively (Binnington, 1978), and function in the secretion of bioactive molecules to suppress the host immune response and of excess ions and water from the ingested blood meal. The basic structures of type-2 and type-3 acini are similar to each other in their composition of granular cells, acinar valve, and myoepithelial-like cells (adluminal cell) (Fig. 1- 1C&D) (Coons et al., 1994; Coons and Roshdy, 1973; Fawcett et al., 1981a; Fawcett et al., 1981b; Krolak et al., 1982; Needham et al., 1990). Multiple axons (~2 to 3) innervating acini types 2 and 3 have been

identified in the classic ultrastructural studies and also in our immunohistochemistries of neuropeptides (Šimo et al., 2009a; Šimo et al., 2009b). Interestingly, male ticks have an additional acini, type-4, which include similar cellular structure to other acini types, but consist of only a single type of granular cell (Binnington, 1978; Walker et al., 1985), for which the function is yet unclear.

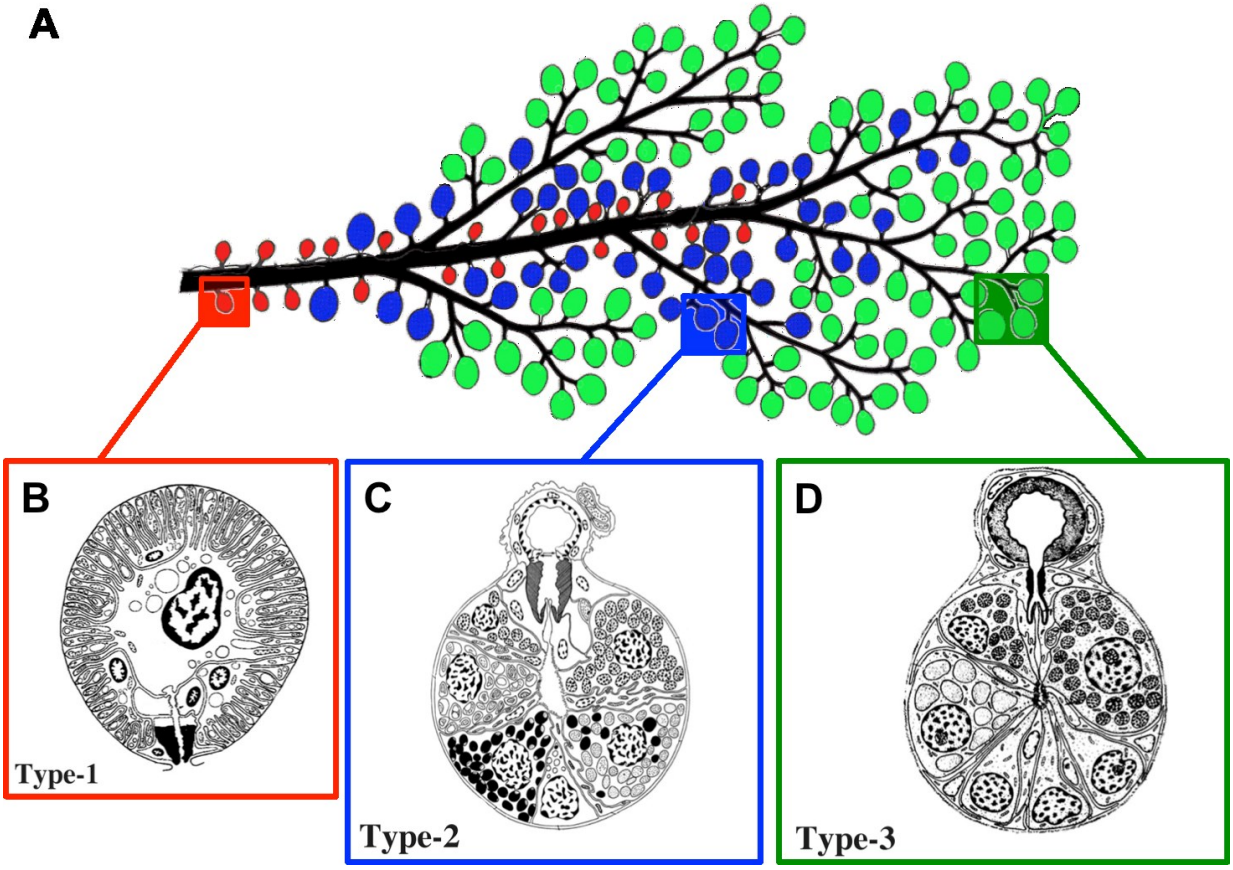

Figure 1-1. Tick salivary glands and cell structure of different types of acini.

(A) Whole salivary gland, type-1 in red, type-2 in blue, and type-3 in green(Binnington, 1978), (B) Cellular structure of type-1 acini in red box(Needham et al., 1990), (C) Cellular structure of type-2 acini in blue box(Coons and Roshdy, 1973), (D) Cellular structure of type-3 acini in green box(Fawcett et al., 1981a)

Tick salivary glands as an excretory organ

In blood-feeding arthropods, the elimination of excess water and ions obtained from a blood meal is vital to maintaining homeostasis and osmoregulation. In insects, diuresis occurs via the Malpighian tubules and hindgut, which is controlled by the concerted action of numerous neuropeptide hormones: diuretic hormones (CRF-like and calcitonin-like), kinin, and CAP_{2b}/periviscerokinin (Beyenbach, 2003; Coast, 2007; Gäde, 2003). These hormonal factors act on the membrane receptors (mainly G protein-coupled receptors; GPCR) and trigger the intracellular signaling cascades, resulting in active fluid transport by generating electrochemical gradients (Davies et al., 1995; Davies et al., 1997; Gade, 2004; MacPherson et al., 2001; Pollock et al., 2004; Pollock et al., 2003; Rosay et al., 1997).

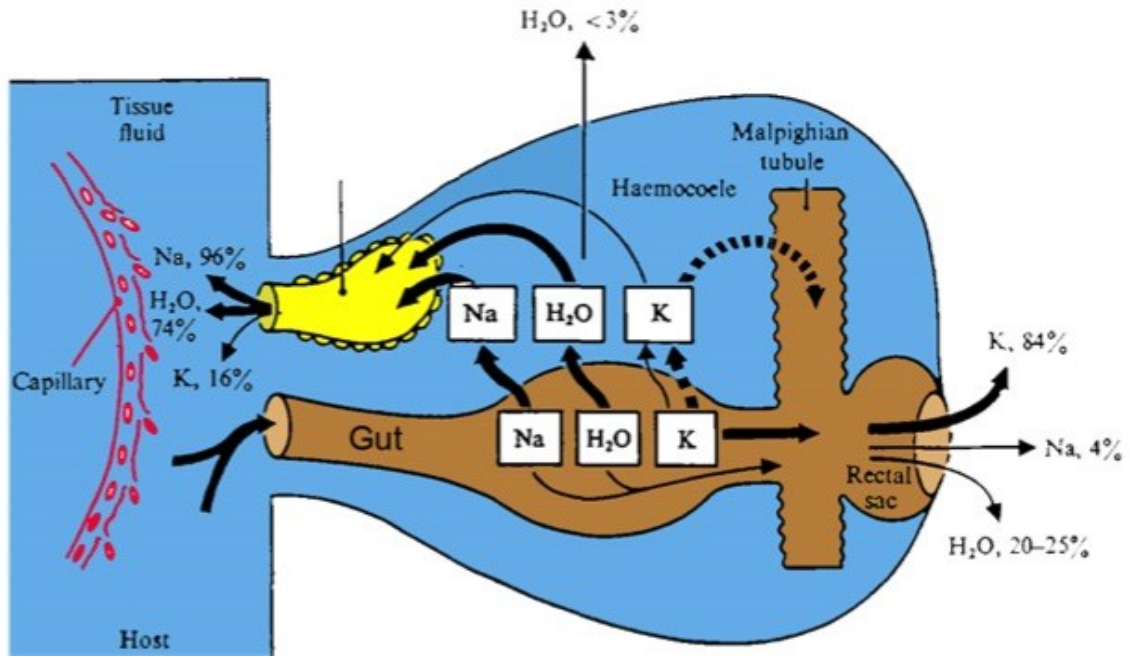

Figure 1-2. Salivary glands (yellow) play a critical role in elimination of excess water and ions obtained from blood digestion (Kaufman and Phillips, 1973a).

In ticks, the major mechanism for removal of excess fluids and ions (diuresis) occurs via the salivary glands (Binnington, 1978), while nitrogenous wastes obtained from digestion of the blood meal are excreted as a form of guanine-rich excreta via the hind gut, consisting of the Malpighian tubules, rectum, rectal sac, and anus (Hamdy, 1977; Sonenshine, 2014). In hard ticks, about 80% of the total imbibed blood meal is excreted through the salivary glands

(Kaufman and Phillips, 1973a; Tatchell, 1967). For example, the saliva in the Rocky Mountain wood tick, *Dermacentor andersoni,* contains 74% of its total secreted water, 96% of its total secreted sodium, and 16% of the total secreted potassium, while feces contains the remainder of the water and ions (Kaufman and Phillips, 1973a). Fluid secretion via the salivary glands has been induced by catecholamines (dopamine, adrenaline, and noradrenaline), ergot alkaloids (ergonovine and ergotamine), and homogenates of synganglion (tick brain), but not by the hemolymph of salivating ticks or the homogenate of the Malpighian tubules or ovary (Kaufman, 1976; Kaufman, 1977; Kaufman and Phillips, 1973b; Needham and Sauer, 1975; Sauer et al., 1976). Among these salivation elicitors, dopamine is the most potent molecule to induce fluid secretion in isolated salivary glands, while serotonin, glutamate, histamine, acetylcholine, and pilocarpine (an agonist of the muscarinic acetylcholine receptor) has no direct effect on fluid secretion in isolated salivary glands.

Dynamic control of salivary secretion: two distinct dopamine receptors

Earlier studies found that dopamine induced activity of adenylate cyclase and increased cAMP level in tick salivary glands (Hume et al., 1984; Schmidt et al., 1981). In addition, dopamine-induced salivary secretion was inhibited by dopamine receptor antagonist (Kaufman, 1977; Kaufman and Phillips, 1973b; Needham and Sauer, 1975). Based on these studies, it had been proposed that tick salivary glands express at least one dopamine receptor in the salivary glands (Sauer et al., 2000).

In recent studies however, our group identified two distinct dopamine receptors from *Ixodes scapularis*, activated by autocrine/paracrine dopamine. These were characterized from the tick salivary glands based on their sequence similarities to vertebrate dopamine receptors and were named as dopamine receptor (D1) and Invertebrate-specific D1-like dopamine receptor (InvD1L) (Koči et al., 2014; Šimo et al., 2014; Šimo et al., 2011). Immunohistochemistry revealed immunoreactivity of these two dopamine receptors at different regions of the salivary gland acini. D1 receptor is localized at the epithelial cellular junctions that face the lumen of the acini, whereas InvD1L receptor is likely localized on neuronal projection within the acinar lumen (Šimo et al., 2014; Šimo et al., 2011). Using a heterologous expression system, D1 receptor was demonstrated to activate both the calcium and cAMP signaling pathways, while InvD1L receptor

triggered exclusively the calcium pathway and not the cAMP pathway (Šimo et al., 2011). The fact that D1 and InvD1L receptors were located in different cells and seemed to be activating two different downstream pathways, suggested their having distinct functions in dopamine induced salivation. My study investigating the dynamic responses of salivary gland acini to dopamine supported this hypothesis in Chapter 2. D1 located in epithelial cells, facing the lumen of the acini, activated the epithelial cells for influx of fluid into the lumen of salivary gland acini, while InvD1L, localized in the neuronal projections, modulated myoepithelial cell activities for the expulsion of luminal saliva into the main duct, emptying the lumen through a pumping/gating action of acini (Kim et al., 2014). Based on the sensitivity of these two different receptors, these two distinct dopamine actions are likely controlled by local dopamine concentrations; low concentrations are sufficient for the activation of the D1 receptor for inward fluid transport, while high concentrations are required for the activation of InvD1L, inducing a pumping/gating action.

Downstream pathways of dopamine signaling for tick salivary secretion

I have investigated the downstream candidates of dopamine-induced salivation: Na/K-ATPase and V-ATPase. Previously, dopamine induced salivary secretion in isolated salivary glands were partially or completely inhibited by ouabain, a Na/K-ATPase blocker, in a dose dependent manner (Kaufman and Phillips, 1973c; McSwain et al., 1997; Rutti et al., 1980), while bafilomycin A1, a V-ATPase blocker, inhibited dopamine-induced salivation at a limited level (~20% reduction) (McSwain et al., 1997). Silencing of Na/K-ATPase in the salivary glands and synganglion by RNA interference (RNAi) caused incomplete blood feeding and reduced oviposition rate (Karim et al., 2008). Based on these previous studies, I aimed to uncover further details of the functions of Na/K-ATPase in dopamine-induced salivary secretion.

My study using immunohistochemistry showed that Na/K-ATPase is localized to the epithelial cells in all types of salivary gland acini. Further physiological study using pharmacological agents demonstrated that Na/K-ATPase is a major molecular component in tick salivary secretion, forming an electrochemical gradient across the epithelial cells, energizing fluid transport as a downstream action of dopamine. However, I also found that Na/K-ATPase had dual functions depending on acini type: fluid transport in type 2 and 3 acini for primary saliva production, and water/ion resorption from the primary saliva in type 1 acini (Kim et al.,

2016). My study is currently expanded to investigate the function(s) of V-ATPase, localized in the myoepithelial cells of type 2 and 3 acini.

Other controllers of tick salivary glands

In addition to dopamine, other controllers might be involved in tick salivary secretion as well. In *A. americanum*, octopamine induced salivary secretion of isolated salivary glands, although it required 100 times higher concentration than dopamine (Needham and Pannabecker, 1983; Pannabecker and Needham, 1985). In *A. hebraeum*, gamma-aminobutyric acid (GABA) potentiated dopamine-induced salivary secretion as a synergist, while GABA itself had no effects on salivary secretion (Lindsay and Kaufman, 1986). GABA was putatively suggested to function as a neuromodulator of dopamine-induced salivary secretion. Pilocarpine, a cholinomimetic drug, induced salivary secretion by injection into the tick, while salivary glands without synganglion (tick brain) were not activated for the fluid secretion from *A. hebraeum* (Kaufman, 1978). This indicated that salivary secretion is indirectly controlled via the central nervous system. Interestingly, alkaloid ergots, unlikely endogenous molecules in ticks, induced salivary secretion at levels comparable to dopamine in the isolated salivary glands of *A. hebraeum* (Kaufman and Wong, 1983). In recent studies, it was discovered that neuropeptidergic axons innervate the salivary glands from the tick brain (synganglion). At least five neuropeptides showed immunoreactivity in the salivary glands: myoinhibitory peptide (MIP), SIFamide, pigment-dispersing factor (PDF), RFamide and tachykinin (TK) (Šimo et al., 2009a; Šimo et al., 2009b). Of these, SIFamide and MIP were co-expressed in the protocerebral salivary gland neurons, which reached the neck region, including the acinar valve, in both type 2 and 3 acini (Šimo et al., 2009a; Šimo et al., 2014). The receptors for SIFamide and MIP were also characterized in type 2 and 3 acini(Šimo et al., 2013), which indicated signal cascades of SIFamide and MIP in the salivary glands. However, the functions of these neuropeptides in salivary secretion are yet unknown.

Studies in genomics and transcriptomics of ticks

In the genomic era, modern technologies, such as sequencing and molecular biology, have been attempting to understand various biological aspects of organisms. Advances in sequencing technology continue to expand the pools of available genomic information in arthropods, including ticks. Recently, the first tick genome was released for *I. scapularis*, and is available through Vectorbase (http://www.vectorbase.org) (Giraldo-Calderón et al., 2015; Pagel Van Zee et al., 2007). Furthermore, the with the advent of next generation sequencing techniques, the doors have been opened to further investigations into understanding both what kinds of bioactive molecules are secreted via the salivary glands and how vectors and pathogens interact with each other at the genomic level.

Tick salivary glands secrete biological compounds in their saliva, aimed at suppressing the host immune response, including processes like hemostasis and inflammation, but they also inadvertently enhance pathogen transmission (Gillespie et al., 2000; Mejri et al., 2002; Ribeiro, 1995; Ribeiro, 1989; Wikel, 1999; Wikel and Alarcon-Chaidez, 2001). Therefore, the study of salivary gland transcripts from ticks is believed to be a key target in developing potential vaccines, as well as pharmacological molecules. Over the last 10 years, studies of tick sialomes have been performed in various tick species (soft ticks and hard ticks), which include Ixodes, Amblyomma, Dermacentor, and Rhipicephalus (Alarcon-Chaidez et al., 2007; Aljamali et al., 2009; Anatriello et al., 2010; Batista et al., 2008; Bissinger et al., 2011; Calvo et al., 2006; Chmelař et al., 2008; Francischetti et al., 2011; Francischetti et al., 2008a; Francischetti et al., 2008b; Francischetti et al., 2005; Jaworski et al., 2010; Mans et al., 2008a; Mans et al., 2008b; Nene et al., 2004; Nene et al., 2002; Ribeiro et al., 2006; Valenzuela et al., 2002). These studies show that transcripts have been fundamentally categorized as housekeeping, secreted protein, unknown, and transposable elements. Secreted proteins in various species of ticks include mainly Kunitz domain-containing proteins, antimicrobial peptides, protease inhibitors, lipocalins, various enzymes, and unknown function proteins.

Unlike studies of sialomes in ticks, our current knowledge is very limited in regards to the interactions taking place between ticks and the pathogens they transmit. Although research at the molecular level has revealed that some proteins, Salp16 and Salp15 of *I. scapularis*, are interacting with outer surface proteins of the pathogens, *Anaplasma phagocytophilum* and *Borrelia burgdorferi* (Anguita et al., 2002; Hovius et al., 2007; Sukumaran et al., 2006), there are

limited studies aimed at understanding the tick/pathogen interaction at the genomic level. Although a transcript analysis was studied for the interaction between *R. appendiculus* and *Theileria parva*, pathogen infection in ticks did not induce any transcriptional changes in the tick (Nene et al., 2004). A more complete understanding of transcriptional changes in ticks, depending on pathogen infection, at the genomic level might shade off the difficulties in the development of novel methods for the disruption of tick feeding and pathogen transmission.

Need novel methods to disrupt tick feeding and pathogen transmission

Ticks not only transmit a number of important human diseases, but ticks also cause an important, direct, devastating economic loss to the livestock industry (Angus, 1996). In the earlier days, the use of various classes of acaricides was the only viable means to control ticks on livestock animals, such as cattle. However, overuse of acaricides has caused ticks to develop resistance to most known acaricides: pyrethroid, organophosphate, carbamate, and formamidines (George, 2000; George et al., 2004; Rosario-Cruz et al., 2005). In the meantime, a vaccine to control ticks for livestock was introduced in the late 1990s. Bm86, which is a membrane-bound glycoprotein, localized on the surface of midgut cells, was discovered as an antigen from partially fed female gut extracts of *B. microplus* (Gough and Kemp, 1993; Willadsen and Kemp, 1988; Willadsen et al., 1989). A commercial vaccine of anti-Bm86 is now in use, named as TickGARD and TickGARD Plus in Australia, and Gavac and Gavac Plus in Cuba. The combinatory treatment of vaccine with acaricide had synergistic effects to reduce tick infestation on cattle (Canales et al., 1997; Lodos et al., 1999; Willadsen et al., 1995). However, the presence of ticks from the same species living in geographically different regions has sequence variation in the antigen, which caused a reduction in efficacy of the vaccine (García-García et al., 1999). Like Bm86, a vaccine for Lyme disease was developed in the earlier days(Livey et al., 2011). However, manufacturer because of low number of use voluntarily withdrew the vaccine(Shen et al., 2011). Current ways of protection against Lyme disease are landscaping, use of acaricides, management of deer (pathogen reservoir), and personal protection.

In conclusion, we have faced the demand for the development of new acaricides with a novel mode of action. Understanding the physiological mechanisms controlling salivary secretion via dopamine receptors and their downstream signal cascade in ticks, and how to regulate transcription levels in ticks against pathogen invasion, may provide us the critical keys

to disrupting tick-infestation and/or pathogen transmission in order to save not only human health but also the livestock industry.

Research objectives

Ticks are obligatory ectoparasites of many vertebrates and are known to transmit numerous pathogens, causing diseases such as Lyme disease and human monocytic ehrlichiosis. Tick salivary secretions are crucial, not only for successful feedings, but also for the injection of bioactive salivary components into the host and for osmoregulation following the ingestion of large amounts of blood. Pathogens are transmitted into the host alongside the salivary secretion. Control of the salivary glands involves dopamine, which is the most potent inducer of salivation. Two distinct dopamine receptors have been characterized from the salivary glands and named as dopamine receptor (D1) and Invertebrate specific D1-like dopamine receptor (InvD1L) based on their sequence similarities to the vertebrate dopamine receptors. Immunoreactive localization of two dopamine receptors and the number of dopamine receptors contrasts the previous conjecture that one dopamine receptor might be located on the surface of salivary glands and plays a role in salivary secretion. The lonestar tick, *Amblyomma americanum*, is known as the major vector of human monocytic ehrlichiosis due to transmitting the obligatory intracellular rickettsiales, *Ehrlichia chaffeensis*, although vegetation ticks (host-seeking ticks) in nature only exhibit infection rates as low as 1% by *Ehrlichia chaffeensis*, indicating that tick acquisition of the pathogen may be a limiting step for the prevalence of the pathogen. I hypothesize that the two distinct dopamine receptors, D1 and InvD1L, play critical roles in different physiological processes responsible for fluid secretions in *Ixodes scapularis*, and that ticks regulate gene expression to defend against pathogen introduction or vice-versa in the interaction between *Amblyomma americanum* and *Ehrlichia chaffeensis*. In this study, I will test the hypotheses and investigate the physiological processes of each dopamine receptor and the genomic levels of gene regulation underlying the processes of pathogen acquisition and development of immunity towards the pathogen using next-generation sequencing (NGS) analysis.

Objective 1. To investigate the different physiological functions of the two distinct dopamine receptors, D1 and InvD1L, in dopamine induced salivary secretion by using subtype specific agonists and antagonists on dissected salivary glands. I will identify a receptor specific agonist and antagonist via the heterologous expression system, which can then be applied towards an investigation of the responses of salivary glands at the level of acini and entire salivary glands.

Objective 2. To characterize the role of Na/K-ATPase in intracellular signaling for dopamine in the salivary glands of *Ixodes scapularis*, by building gene structure, immunolocalization, and use of a specific antagonist of Na/K-ATPase on the dissected salivary glands. I will clone and sequence missing portions of the Na/K-ATPase gene, localize Na/K-ATPase by way of immunereactivity, observe and record the responses of both acini and entire salivary glands, and quantify ion concentrations in secreted saliva by SEM.

Objective 3. To investigate the interaction between the vector (tick) and the bacterial pathogen (Rickettsiales) at the genomic level via sequencing, de novo assembly, and differential expression analysis. I will sequence libraries using Illumina HiSeq2500, assemble sequence reads using Trinity, and analyze differential expression based on the FPKM values of each library.

The results of this research are important for expanding our knowledge of not only tick salivary gland physiology, but also of the interaction(s) between ticks as a vector and the pathogens they transmit at the genomic level. In addition, understanding the complexity of tick salivary mechanisms and interaction(s) of the vector and pathogen will help us to develop the novel methods for the disruption of tick feeding.

Reference

Alarcon-Chaidez, F. J., Sun, J. and Wikel, S. K. (2007). Transcriptome analysis of the salivary glands of Dermacentor andersoni Stiles (Acari: Ixodidae). *Insect Biochem Mol Biol* **37**, 48-71.

Aljamali, M. N., Hern, L., Kupfer, D., Downard, S., So, S., Roe, B. A., Sauer, J. R. and Essenberg, R. C. (2009). Transcriptome analysis of the salivary glands of the female tick Amblyomma americanum (Acari: Ixodidae). *Insect Mol. Biol.* **18**, 129-54.

Anatriello, E., Ribeiro, J. M. C., de Miranda-Santos, I. K. F., Brandao, L. G., Anderson, J. M., Valenzuela, J. G., Maruyama, S. R., Silva, J. S. and Ferreira, B. R. (2010). An insight into the sialotranscriptome of the brown dog tick, Rhipicephalus sanguineus. *BMC Genomics* **11**.

Anderson, B. E., Sims, K. G., Olson, J. G., Childs, J. E., Piesman, J. F., Happ, C. M., Maupin, G. O. and Johnson, B. J. (1993). Amblyomma americanum: a potential vector of human ehrlichiosis. *The American journal of tropical medicine and hygiene* **49**, 239-244.

Anguita, J., Ramamoorthi, N., Hovius, J. W., Das, S., Thomas, V., Persinski, R., Conze, D., Askenase, P. W., Rincon, M., Kantor, F. S. et al. (2002). Salp15, an ixodes scapularis salivary protein, inhibits CD4(+) T cell activation. *Immunity* **16**, 849-59.

Angus, B. M. (1996). The history of the cattle tick Boophilus microplus in Australia and achievements in its control. *Int J Parasitol* **26**, 1341-55.

Barker, S. C. and Murrell, A. (2004). Systematics and evolution of ticks with a list of valid genus and species names. *Parasitology* **129**, S15-S36.

Batista, I. F. C., Chudzinski-Tavassi, A. M., Faria, F., Simons, S. M., Barros-Batestti, D. M., Labruna, M. B., Leão, L. I., Ho, P. L. and Junqueira-de-Azevedo, I. L. M. (2008). Expressed sequence tags (ESTs) from the salivary glands of the tick Amblyomma cajennense (Acari: Ixodidae). *Toxicon* **51**, 823-834.

Beyenbach, K. W. (2003). Transport mechanisms of diuresis in Malpighian tubules of insects. *J. Exp. Biol.* **206**, 3845-3856.

Binnington, K. C. (1978). Sequential changes in salivary gland structure during attachment and feeding of the cattle tick, Boophilus microplus. *Int. J. Parasitol.* **8**, 97-115.

Bissinger, B. W., Donohue, K. V., Khalil, S. M., Grozinger, C. M., Sonenshine, D. E., Zhu, J. and Roe, R. M. (2011). Synganglion transcriptome and developmental global gene expression in adult females of the American dog tick, Dermacentor variabilis (Acari: Ixodidae). *Insect Mol. Biol.* **20**, 465-91.

Burgdorfer, W., Barbour, A. G., Hayes, S. F., Benach, J. L., Grunwaldt, E. and Davis, J. P. (1982). Lyme disease-a tick-borne spirochetosis? *Science* **216**, 1317-1319.

Calvo, E., Pham, V. M., Lombardo, F., Arca, B. and Ribeiro, J. M. (2006). The sialotranscriptome of adult male Anopheles gambiae mosquitoes. *Insect Biochem. Mol. Biol.* **36**, 570-5.

Canales, M., Enriquez, A., Ramos, E., Cabrera, D., Dandie, H., Soto, A., Falcon, V., Rodriguez, M. and de la Fuente, J. (1997). Large-scale production in Pichia pastoris of the recombinant vaccine Gavac against cattle tick. *Vaccine* **15**, 414-22.

Chmelař, J., Anderson, J. M., Mu, J., Jochim, R. C., Valenzuela, J. G. and Kopecký, J. (2008). Insight into the sialome of the castor bean tick, Ixodes ricinus. *BMC Genomics* **9**.

Coast, G. (2007). The endocrine control of salt balance in insects. *Gen. Comp. Endocrinol.* **152**, 332-338.
Coons, L. B., Lessman, C. A., Ward, M. W., Berg, R. H. and Lamoreaux, W. J. (1994). Evidence of a myoepithelial cell in tick salivary glands. *Int. J. Parasitol.* **24**, 551-62.
Coons, L. B. and Roshdy, M. A. (1973). Fine Structure of the Salivary Glands of Unfed Male Dermacentor variabilis (Say) (Ixodoidea: Ixodidae). *J. Parasitol.* **59**, 900-912.
Davies, S. A., Huesmann, G. R., Maddrell, S. H., O'Donnell, M. J., Skaer, N. J., Dow, J. A. and Tublitz, N. J. (1995). CAP2b, a cardioacceleratory peptide, is present in Drosophila and stimulates tubule fluid secretion via cGMP. *Am J Physiol* **269**, R1321-6.
Davies, S. A., Stewart, E. J., Huesmann, G. R., Skaer, N. J., Maddrell, S. H., Tublitz, N. J. and Dow, J. A. (1997). Neuropeptide stimulation of the nitric oxide signaling pathway in Drosophila melanogaster Malpighian tubules. *Am J Physiol* **273**, R823-7.
Fawcett, D. W., Doxsey, S. and Büscher, G. (1981a). Salivary gland of the tick vector (R. appendiculatus) of East Coast fever. I. Ultrastructure of the type III acinus. *Tissue Cell* **13**, 209-230.
Fawcett, D. W., Doxsey, S. and Büscher, G. (1981b). Salivary gland of the tick vector (R. appendiculatus) of East Coast fever. II. Cellular basis for fluid secretion in the type III acinus. *Tissue Cell* **13**, 231-253.
Francischetti, I. M., Sa-Nunes, A., Mans, B. J., Santos, I. M. and Ribeiro, J. M. (2009). The role of saliva in tick feeding. *Front. Biosci.* **14**, 2051-88.
Francischetti, I. M. B., Anderson, J. M., Manoukis, N., Pham, V. M. and Ribeiro, J. M. C. (2011). An insight into the sialotranscriptome and proteome of the coarse bontlegged tick, Hyalomma marginatum rufipes. *J. Proteomics* **74**, 2892-2908.
Francischetti, I. M. B., Mans, B. J., Meng, Z., Gudderra, N., Veenstra, T. D., Pham, V. M. and Ribeiro, J. M. C. (2008a). An insight into the sialome of the soft tick, Ornithodorus parkeri. *Insect Biochem. Mol. Biol.* **38**, 1-21.
Francischetti, I. M. B., Meng, Z., Mans, B. J., Gudderra, N., Hall, M., Veenstra, T. D., Pham, V. M., Kotsyfakis, M. and Ribeiro, J. M. C. (2008b). An insight into the salivary transcriptome and proteome of the soft tick and vector of epizootic bovine abortion, Ornithodoros coriaceus. *J. Proteomics* **71**, 493-512.
Francischetti, I. M. B., Pham, V. M., Mans, B. J., Andersen, J. F., Mather, T. N., Lane, R. S. and Ribeiro, J. M. C. (2005). The transcriptome of the salivary glands of the female western black-legged tick Ixodes pacificus (Acari: Ixodidae). *Insect Biochem Mol Biol* **35**, 1142-1161.
Gade, G. (2004). Regulation of intermediary metabolism and water balance of insects by neuropeptides. *Annu Rev Entomol* **49**, 93-113.
Gäde, G. (2003). REGULATION OF INTERMEDIARY METABOLISM AND WATER BALANCE OF INSECTS BY NEUROPEPTIDES. *Annu. Rev. Entomol.* **49**, 93-113.
García-García, J. C., Gonzalez, I. L., González, D. M., Valdés, M., Méndez, L., Lamberti, J., D'Agostino, B., Citroni, D., Fragoso, H., Ortiz, M. et al. (1999). Sequence Variations in the Boophilus Microplus Bm86 Locus and Implications for Immunoprotection in Cattle Vaccinated with this Antigen. *Exp. Appl. Acarol.* **23**, 883-895.
George, J. E. (2000). Present and future technologies for tick control. *Ann N Y Acad Sci* **916**, 583-8.
George, J. E., Pound, J. M. and Davey, R. B. (2004). Chemical control of ticks on cattle and the resistance of these parasites to acaricides. *Parasitology* **129 Suppl**, S353-66.

Gillespie, R. D., Mbow, M. L. and Titus, R. G. (2000). The immunomodulatory factors of bloodfeeding arthropod saliva. *Parasite Immunol.* **22**, 319-31.
Giraldo-Calderón, G. I., Emrich, S. J., MacCallum, R. M., Maslen, G., Dialynas, E., Topalis, P., Ho, N., Gesing, S., Consortium, t. V., Madey, G. et al. (2015). VectorBase: an updated bioinformatics resource for invertebrate vectors and other organisms related with human diseases. *Nucleic Acids Res.* **43**, D707-D713.
Gough, J. M. and Kemp, D. H. (1993). Localization of a Low Abundance Membrane Protein (Bm86) on the Gut Cells of the Cattle Tick Boophilus microplus by Immunogold Labeling. *The Journal of Parasitology* **79**, 900-907.
Hamdy, B. H. (1977). Biochemical and Physiological Studies of Certain Ticks (Ixodoidea). Excretion during ixodid feeding. *J. Med. Entomol.* **14**, 15-18.
Hoogstraal, H. (1985). Argasid and Nuttalliellid Ticks as Parasites and Vectors1. In *Adv. Parasitol.*, vol. Volume 24 eds. J. R. Baker and R. Muller), pp. 135-238: Academic Press.
Hovius, J. W. R., van Dam, A. P. and Fikrig, E. (2007). Tick–host–pathogen interactions in Lyme borreliosis. *Trends Parasitol.* **23**, 434-438.
Hume, M. E., Essenberg, R. C., McNew, R. W., Bantle, J. A. and Sauer, J. R. (1984). Adenosine-3',5'-monophosphate in salivary glands of unfed and feeding female lone star ticks, Amblyomma americanum (L.). *Comp. Biochem. Physiol.* **79**, 47-50.
Jaworski, D. C., Zou, Z., Bowen, C. J., Wasala, N. B., Madden, R., Wang, Y., Kocan, K. M., Jiang, H. and Dillwith, J. W. (2010). Pyrosequencing and characterization of immune response genes from the American dog tick, Dermacentor variabilis (L.). *Insect Mol. Biol.* **19**, 617-30.
Karim, S., Kenny, B., Troiano, E. and Mather, T. (2008). RNAi-mediated gene silencing in tick synganglia: A proof of concept study. *BMC Biotechnol.* **8**, 30.
Kaufman, W. R. (1976). The influence of various factors on fluid secretion by in vitro salivary glands of ixodid Ticks. *J. Exp. Biol.* **64**, 727-742.
Kaufman, W. R. (1977). The influence of adrenergic agonists and their antagonists on isolated salivary glands of ixodid ticks. *Eur. J. Pharmacol.* **45**, 61-8.
Kaufman, W. R. (1978). Actions of some transmitters and their antagonists on salivary secretion in a tick. *Am. J. Physiol.* **235**, R76-81.
Kaufman, W. R. (2007). Gluttony and sex in female ixodid ticks: How do they compare to other blood-sucking arthropods? *J. Insect Physiol.* **53**, 264-273.
Kaufman, W. R. and Phillips, J. E. (1973a). Ion and Water-Balance in Ixodid Tick Dermacentor-Andersoni .1. Routes of Ion and Water Excretion. *J. Exp. Biol.* **58**, 523-536.
Kaufman, W. R. and Phillips, J. E. (1973b). Ion and Water-Balance in Ixodid Tick Dermacentor-Andersoni .2. Mechanism and Control of Salivary Secretion. *J. Exp. Biol.* **58**, 537-547.
Kaufman, W. R. and Phillips, J. E. (1973c). Ion and Water-Balance in Ixodid Tick Dermacentor-Andersoni .3. Influence of Monovalent Ions and Osmotic Pressure on Salivary Secretion. *J. Exp. Biol.* **58**, 549-564.
Kaufman, W. R. and Wong, D. L. (1983). Evidence for multiple receptors mediating fluid secretion in salivary glands of ticks. *Eur. J. Pharmacol.* **87**, 43-52.
Kim, D., Šimo, L. and Park, Y. (2014). Orchestration of salivary secretion mediated by two different dopamine receptors in the blacklegged tick Ixodes scapularis. *J. Exp. Biol.* **217**, 3656-3663.

Kim, D., Urban, J., Boyle, D. L. and Park, Y. (2016). Multiple functions of Na/K-ATPase in dopamine-induced salivation of the Blacklegged tick, Ixodes scapularis. *Sci. Rep.* **6**, 21047.
Koči, J., Šimo, L. and Park, Y. (2014). Autocrine/paracrine dopamine in the salivary glands of the blacklegged tick Ixodes scapularis. *J. Insect Physiol.*
Krolak, J. M., Ownby, C. L. and Sauer, J. R. (1982). Alveolar structure of salivary glands of the lone star tick, Amblyomma americanum (L.): unfed females. *J. Parasitol.* **68**, 61-82.
Lindsay, P. J. and Kaufman, W. R. (1986). Potentiation of salivary fluid secretion in ixodid ticks: a new receptor system for gamma-aminobutyric acid. *Can. J. Physiol. Pharmacol.* **64**, 1119-26.
Livey, I., O'Rourke, M., Traweger, A., Savidis-Dacho, H., Crowe, B. A., Barrett, P. N., Yang, X., Dunn, J. J. and Luft, B. J. (2011). A New Approach to a Lyme Disease Vaccine. *Clin. Infect. Dis.* **52**, s266-s270.
Lodos, J., Ochagavia, M. E., Rodriguez, M. and De La Fuente, J. (1999). A simulation study of the effects of acaricides and vaccination on Boophilus cattle-tick populations. *Prev Vet Med* **38**, 47-63.
MacPherson, M. R., Pollock, V. P., Broderick, K. E., Kean, L., O'Connell, F. C., Dow, J. A. and Davies, S. A. (2001). Model organisms: new insights into ion channel and transporter function. L-type calcium channels regulate epithelial fluid transport in Drosophila melanogaster. *Am J Physiol Cell Physiol* **280**, C394-407.
Mans, B. J., Andersen, J. F., Francischetti, I. M. B., Valenzuela, J. G., Schwan, T. G., Pham, V. M., Garfield, M. K., Hammer, C. H. and Ribeiro, J. M. C. (2008a). Comparative sialomics between hard and soft ticks: Implications for the evolution of blood-feeding behavior. *Insect Biochem. Mol. Biol.* **38**, 42-58.
Mans, B. J., Andersen, J. F., Schwan, T. G. and Ribeiro, J. M. C. (2008b). Characterization of anti-hemostatic factors in the argasid, Argas monolakensis: Implications for the evolution of blood-feeding in the soft tick family. *Insect Biochem. Mol. Biol.* **38**, 22-41.
McSwain, J. L., Luo, C., deSilva, G. A., Palmer, M. J., Tucker, J. S., Sauer, J. R. and Essenberg, R. C. (1997). Cloning and sequence of a gene for a homologue of the C subunit of the V-ATPase from the salivary gland of the tick Amblyomma americanum (L). *Insect Mol. Biol.* **6**, 67-76.
Mejri, N., Rutti, B. and Brossard, M. (2002). Immunosuppressive effects of ixodes ricinus tick saliva or salivary gland extracts on innate and acquired immune response of BALB/c mice. *Parasitol Res* **88**, 192-7.
Needham, G., Rosell, R. and Greenwald, L. (1990). Ultrastructure of type-I salivary-gland acini in four species of ticks and the influence of hydration states on the type-I acini ofAmblyomma americanum. *Exp. Appl. Acarol.* **10**, 83-104.
Needham, G. R. and Pannabecker, T. L. (1983). Effects of Octopamine, Chlordimeform, and Demethylchlordimeform on Amine-Controlled Tick Salivary-Glands Isolated from Feeding Amblyomma-Americanum (L). *Pestic. Biochem. Physiol.* **19**, 133-140.
Needham, G. R. and Sauer, J. R. (1975). Control of fluid secretion by isolated salivary glands of the lone star tick. *J. Insect Physiol.* **21**, 1893-8.
Nene, V., Lee, D., Kang'A, S., Skilton, R., Shah, T., De Villiers, E., Mwaura, S., Taylor, D., Quackenbush, J. and Bishop, R. (2004). Genes transcribed in the salivary glands of female Rhipicephalus appendiculatus ticks infected with Theileria parva. *Insect Biochem. Mol. Biol.* **34**, 1117-1128.

Nene, V., Lee, D., Quackenbush, J., Skilton, R., Mwaura, S., Gardner, M. J. and Bishop, R. (2002). AvGI, an index of genes transcribed in the salivary glands of the ixodid tick Amblyomma variegatum. *Int. J. Parasitol.* **32**, 1447-1456.
Pagel Van Zee, J., Geraci, N. S., Guerrero, F. D., Wikel, S. K., Stuart, J. J., Nene, V. M. and Hill, C. A. (2007). Tick genomics: The Ixodes genome project and beyond. *Int. J. Parasitol.* **37**, 1297-1305.
Pannabecker, T. and Needham, G. R. (1985). Effects of Octopamine on Fluid Secretion by Isolated Salivary-Glands of a Feeding Ixodid Tick. *Arch. Insect Biochem. Physiol.* **2**, 217-226.
Pollock, V. P., McGettigan, J., Cabrero, P., Maudlin, I. M., Dow, J. A. and Davies, S. A. (2004). Conservation of capa peptide-induced nitric oxide signalling in Diptera. *J Exp Biol* **207**, 4135-45.
Pollock, V. P., Radford, J. C., Pyne, S., Hasan, G., Dow, J. A. and Davies, S. A. (2003). NorpA and itpr mutants reveal roles for phospholipase C and inositol (1,4,5)- trisphosphate receptor in Drosophila melanogaster renal function. *J Exp Biol* **206**, 901-11.
Ribeiro, J. M. (1987). Role of saliva in blood-feeding by arthropods. *Annu. Rev. Entomol.* **32**, 463-78.
Ribeiro, J. M. (1995). Blood-feeding arthropods: live syringes or invertebrate pharmacologists? *Infect. Agents Dis.* **4**, 143-52.
Ribeiro, J. M. C. (1989). Role of saliva in tick/host interactions. *Exp. Appl. Acarol.* **7**, 15-20.
Ribeiro, J. M. C., Alarcon-Chaidez, F., Francischetti, I. M. B., Mans, B. J., Mather, T. N., Valenzuela, J. G. and Wikel, S. K. (2006). An annotated catalog of salivary gland transcripts from Ixodes scapularis ticks. *Insect Biochem Mol Biol* **36**, 111-129.
Rosario-Cruz, R., Guerrero, F. D., Miller, R. J., Rodriguez-Vivas, R. I., Dominguez-Garcia, D. I., Cornel, A. J., Hernandez-Ortiz, R. and George, J. E. (2005). Roles played by esterase activity and by a sodium channel mutation involved in pyrethroid resistance in populations of Boophilus microplus (Acari: Ixodidae) collected from Yucatan, Mexico. *J Med Entomol* **42**, 1020-5.
Rosay, P., Davies, S. A., Yu, Y., Sozen, M. A., Kaiser, K. and Dow, J. A. (1997). Cell-type specific calcium signalling in a Drosophila epithelium. *J Cell Sci* **110 (Pt 15)**, 1683-92.
Rudolph, D. and Knulle, W. (1974). Site and Mechanism of Water-Vapor Uptake from Atmosphere in Ixodid Ticks. *Nature* **249**, 84-85.
Rutti, B., Schlunegger, B., Kaufman, W. and Aeschlimann, A. (1980). Properties of Na, K-ATPase from the salivary glands of the ixodid tick Amblyomma hebraeum. *Can. J. Zool.* **58**, 1052-9.
Sauer, J. R., Essenberg, R. C. and Bowman, A. S. (2000). Salivary glands in ixodid ticks: control and mechanism of secretion. *J. Insect Physiol.* **46**, 1069-1078.
Sauer, J. R., Mincolla, P. M. and Needham, G. R. (1976). Adrenaline and cyclic AMP stimulated uptake of chloride and fluid secretion by isolated salivary glands of the lone star tick. *Comp. Biochem. Physiol. C* **53**, 63-6.
Schmidt, S. P., Essenberg, R. C. and Sauer, J. R. (1981). Evidence for a D1 dopamine receptor in the salivary glands of Amblyomma americanum (L.). *J. Cyclic Nucleotide Res.* **7**, 375-84.
Schoeler, G. B. and Wikel, S. K. (2001). Modulation of host immunity by haematophagous arthropods. *Ann Trop Med Parasitol* **95**, 755-771.
Shen, A. K., Mead, P. S. and Beard, C. B. (2011). The Lyme Disease Vaccine—A Public Health Perspective. *Clin. Infect. Dis.* **52**, s247-s252.

Šimo, L., Itňan, D. Ž. and Park, Y. (2009a). Two novel neuropeptides in innervation of the salivary glands of the black-legged tick, Ixodes scapularis: Myoinhibitory peptide and SIFamide. *J. Comp. Neurol.* **517**, 551-563.
Šimo, L., Koči, J., Kim, D. and Park, Y. (2014). Invertebrate specific D1-like dopamine receptor in control of salivary glands in the black-legged tick Ixodes scapularis. *J. Comp. Neurol.* **522**, 2038-2052.
Šimo, L., Koči, J. and Park, Y. (2013). Receptors for the neuropeptides, myoinhibitory peptide and SIFamide, in control of the salivary glands of the blacklegged tick Ixodes scapularis. *Insect Biochem. Mol. Biol.* **43**, 376-387.
Šimo, L., Koci, J., Zitnan, D. and Park, Y. (2011). Evidence for D1 dopamine receptor activation by a paracrine signal of dopamine in tick salivary glands. *PLoS One* **6**, e16158.
Šimo, L., Slovák, M., Park, Y. and Žitňan, D. (2009b). Identification of a complex peptidergic neuroendocrine network in the hard tick, Rhipicephalus appendiculatus. *Cell Tissue Res.* **335**, 639-655.
Sonenshine, D. E. (2014). Excretion and Water Balance: Hindgut, Malpighian Tubules, and Coxal Glands. In *Biology of Ticks*, vol. 1, pp. 206-219: Oxford University Press.
Sukumaran, B., Narasimhan, S., Anderson, J. F., DePonte, K., Marcantonio, N., Krishnan, M. N., Fish, D., Telford, S. R., Kantor, F. S. and Fikrig, E. (2006). An Ixodes scapularis protein required for survival of Anaplasma phagocytophilum in tick salivary glands. *J Exp Med* **203**, 1507-17.
Tatchell, R. J. (1967). Salivary Secretion in the Cattle Tick as a Means of Water Elimination. *Nature* **213**, 940-941.
Valenzuela, J. G. (2004). Exploring tick saliva: from biochemistry to 'sialomes' and functional genomics. *Parasitology* **129**.
Valenzuela, J. G., Francischetti, I. M. B., Pham, V. M., Garfield, M. K., Mather, T. N. and Ribeiro, J. M. C. (2002). Exploring the sialome of the tick Ixodes scapularis. *J. Exp. Biol.* **205**, 2843-2864.
Walker, A. R., Fletcher, J. D. and Gill, H. S. (1985). Structural and histochemical changes in the salivary glands of Rhipicephalus appendiculatus during feeding. *Int. J. Parasitol.* **15**, 81-100.
Wikel, S. K. (1999). Tick modulation of host immunity: an important factor in pathogen transmission. *Int. J. Parasitol.* **29**, 851-9.
Wikel, S. K. and Alarcon-Chaidez, F. J. (2001). Progress toward molecular characterization of ectoparasite modulation of host immunity. *Vet Parasitol* **101**, 275-87.
Willadsen, P., Bird, P., Cobon, G. and Hungerford, J. (1995). Commercialisation of a recombinant vaccine against Boophilus microplus. *Parasitology* **110**, S43-S50.
Willadsen, P. and Kemp, D. H. (1988). Vaccination with 'concealed' antigens for tick control. *Parasitol. Today* **4**, 196-198.
Willadsen, P., Riding, G. A., McKenna, R. V., Kemp, D. H., Tellam, R. L., Nielsen, J. N., Lahnstein, J., Cobon, G. S. and Gough, J. M. (1989). Immunologic control of a parasitic arthropod. Identification of a protective antigen from Boophilus microplus. *The Journal of Immunology* **143**, 1346-51.

Chapter 2 - Orchestration of salivary secretion mediated by two different dopamine receptors in the blacklegged tick, *Ixodes scapularis* Say.

Abstract

Salivary secretion is crucial for successful tick feeding, and it is often the mediator of pathogen transmission. Salivation functions to compromise the host immune system and remove excessive water and ions during the ingestion of large blood meals. Control of salivary glands involves autocrine/paracrine dopamine, which is the most potent inducer of tick salivation. Previously, we reported the presence of two dopamine receptors in the salivary glands of the blacklegged tick (*Ixodes scapularis* Say): dopamine receptor (D1) and invertebrate specific D1-like dopamine receptor (InvD1L). Here, we investigated the different physiological roles of the dopamine receptors in the tick salivary secretion by using pharmacological tools that discriminate between the two different receptors. Heterologous expressions followed by reporter assays of the dopamine receptors identified receptor-specific antagonists and agonists. These pharmacological tools were further used to discriminate the physiological role of each receptor by using *in vitro* assays: measuring salivary secretions of isolated salivary glands and monitoring dynamic changes in the size of individual salivary gland acini. Based on the results, we propose that the D1 receptor acts on salivary gland acini epithelial cells for inward fluid transport. InvD1L controls (or modulates) myoepithelial cells in each acinus, which function to pump or gate and facilitate expelling saliva out from the acini to the salivary ducts. We conclude that dopamine acts on the D1 and the InvD1L receptors and leads different physiological actions to orchestrate tick salivary secretion.

Introduction

Ticks are obligatory ectoparasites of many vertebrates and transmit pathogens that cause numerous diseases, including Lyme disease, Rocky Mountain Spotted Fever (RMSF), and Southern Tick-Associated Rash Illness (STARI). Lyme disease transmitted by *Ixodes scapularis* is the most commonly reported vector-born disease in the United States. Ticks are generally attached to the host for a long duration (~ up to 14 days depending on species) for blood meals, unlike other hematophagous insects, such as mosquitoes. Female ticks can normally increase their body weight up to 100 times compared with unfed ticks (Kaufman, 2007). A successful long tick feeding duration, which may be the major reason that they are tremendous disease vectors, requires that the tick be capable of overcoming host defensive responses mainly through salivation.

Tick salivary secretion contains various bioactive components, such as antihaemostatic molecules, anti-inflammatory compounds, and immunomodulators, that compromise the host immune responses (Francischetti et al., 2009; Nuttall et al., 2006; Ribeiro, 1987; Ribeiro, 1989). Salivation also functions to maintain homeostasis by removing excessive water and ions that are processed from large blood meals (Kaufman and Phillips, 1973a; Tatchell, 1967). A pair of salivary glands is located at the anterolateral regions of tick and resemble a cluster of grapes, which consist of three types of acini, types I, II and III. Based on the cellular structure, each type is thought to have different functions: off-host osmoregulation for type I; production and release of bioactive proteins for type II; on-host osmoregulation for type III (Gaede et al., 1997; Rudolph and Knulle, 1974).

In on-host osmoregulation that removes excessive water and wastes during the blood feeding, the majority of water and sodium ions were secreted back into the host via salivary secretion (Kaufman and Phillips, 1973a; Tatchell, 1967). Homogenates of synganglia (tick brain) and dopamine induced fluid secretion in isolated salivary glands (Kaufman, 1976; Kaufman, 1977). Octopamine or cAMP demonstrated low activities on salivary secretion (Kaufman, 1976; Needham and Pannabecker, 1983; Pannabecker and Needham, 1985), whereas acetylcholine, serotonin, and glutamate did not show activity from isolated salivary glands (Kaufman, 1976; Kaufman and Phillips, 1973b).

Earlier studies found that the activity of dopamine on salivary secretion is dependent on extracellular Ca^{2+} (Kaufman, 1976; Kaufman, 1977; Kaufman and Wong, 1983; Needham and

Sauer, 1979). In addition, cyclic AMP (cAMP) was also involved in dopamine-mediated salivary secretion (Hume et al., 1984; Krolak et al., 1983; Schmidt et al., 1981). Recently, we characterised two dopamine receptors: dopamine receptor (D1) and invertebrate-specific D1-like dopamine receptor (InvD1L) in both acini types II and III (Šimo et al., 2014; Šimo et al., 2011). Receptor localisation and downstream coupling in the heterologous expression system suggested that the D1 receptor is likely coupled to cAMP elevation in epithelial cells, and the InvD1L receptor is coupled to Ca^{2+} mobilisation in myoepithelial cells (Šimo et al., 2014; Šimo et al., 2011). Therefore, two different dopamine actions mediated through different acini cell types were proposed, although experimental verifications of the suggested downstream cellular actions and physiological roles of each receptor were not possible because RNA interference targeting those receptors were not practicable in those studies.

In this study, we identified pharmacological agents that distinguish D1 and InvD1L receptors in heterologous receptor expression. The agents discriminating two dopamine receptors successfully revealed different physiological actions in salivary gland acini *in vitro*.

Results

Receptor-specific agonists and antagonists identified in heterologous expressions of D1 and InvD1L

To identify receptor-specific agonists and antagonists of two dopamine receptors, we expressed the receptors in Chinese hamster ovary cell (CHO) for receptor-mediated calcium mobilisation reporter assays as described previously (Šimo et al., 2014; Šimo et al., 2011). Among candidate chemicals that were well known to be active on mammalian D1 receptors, we determined that SKF82958 and apomorphine activated specifically the D1 receptor but not the InvD1L receptor at 10 μM (Fig. 2-1A). SKF82958 and apomorphine activated only the D1 receptor by 80% and 60% of dopamine (10 μM) activity, respectively, while they had no activity on the InvD1L receptor showing 0.02% and 3% of dopamine (10 μM) activity (Fig. 2-1A). Another agonist 6,7-ADTN (10 μM) activated both D1 and InvD1L receptors by 93% and 89% of dopamine activity. We also tested sulfate-conjugated dopamine, dopamine-3-O-sulfate (DA-3S) and dopamine-4-O-sulfate (DA-4S), which were highly abundant in the tick salivary gland in our previous study (Koči et al., 2014). However, both DA-3S and DA-4S did not show any activity on neither the D1 nor the InvD1L receptor in our assay system.

In search of receptor-specific antagonists, which measured the reduction in dopamine activity on the receptor after 15 min pre-incubation with the test compound (10 μM), we identified four antagonists that were specific only to InvD1L receptor: fluphenazine, acepromazine, clozapine, and (+)butaclamol, while (-)butaclamol, sulpiride, and haloperidol had no or low antagonistic activities on either receptor. We also found a common antagonist SCH23390 that showed 77% and 69% antagonism on D1 and InvD1L, respectively (Fig. 2-1B), which was also previously described for dopamine receptors of mosquito and tick (Meyer et al., 2012; Meyer et al., 2011).

Taken together, we identified three groups of pharmacological discriminators: D1-specific agonists, InvD1L-specific antagonists, and a common antagonist. However, there was no InvD1L-specific agonist and D1-specific antagonist among the ligands assessed in this study. In subsequent *in vitro* experiments on isolated salivary glands, we utilised only SKF82958 as D1-specific agonist, fluphenazine as InvD1L-specific antagonist, and SCH23390 as a common antagonist (Fig. 2-1C).

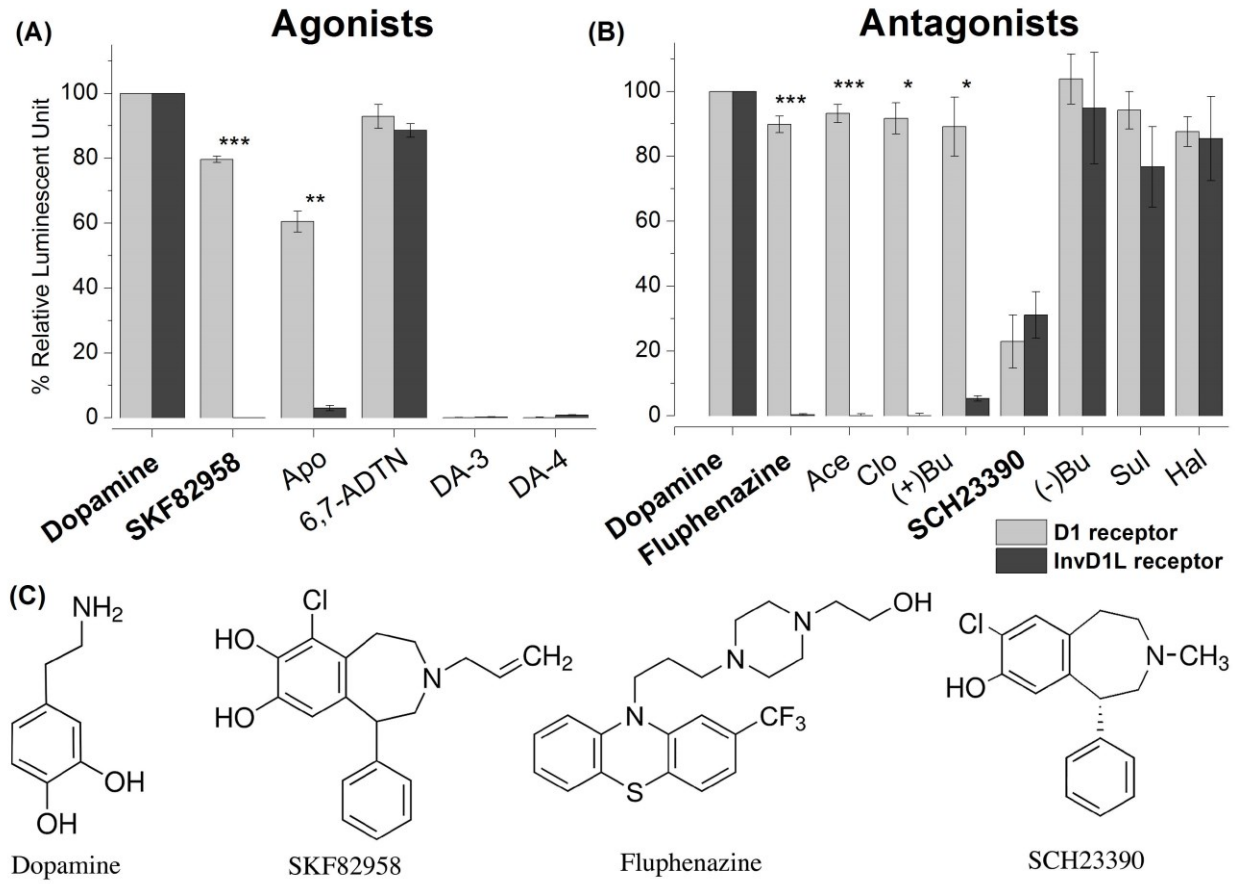

Figure 2-1. Calcium mobilisation assay using aequorin reporter for D1 and InvD1L receptors expressed in Chinese hamster ovary cells (CHO-K1).

The light grey bars represent the D1 receptor results, and the dark grey bars represent the InvD1L receptor results. (A) Agonistic activities of various chemicals (10 μM) on the D1 receptor and InvD1L receptor. The first column represents the full luminescence responses of D1 and InvD1L receptors to 10 μM DA. (B) Antagonistic activities of various chemicals (10 μM) on the D1 and InvD1L receptors. The luminescence responses of D1 and InvD1L receptors to 10 μM DA are shown in the first column, and the responses to 10 μM DA after pre-incubation with different chemicals (10 μM) for 15 min are shown in the remaining columns. The bars in the graphs indicate the averages with s.e.m. for three replicates. (C) Structures of the pharmacological discriminators used in this study: dopamine, SKF82958, fluphenazine and SCH23390. Abbreviations are: Apo, apomorphine; DA-3, dopamine-3-O-sulfate; DA-4, dopamine-4-O-sulfate; Ace, acepromazine; Clo, clozapine; (+)Bu, (+)butaclamol; (-)Bu, (-)butaclamol; Sul, sulpiride; Hal, haloperidol. Asterisks are for statistical significance in the paired t-test, $p < 0.0001$ (***), $p < 0.001$ (**), and $p < 0.01$ (*).

Activities of agonists and antagonists on the secretory activity of isolated salivary glands

To investigate the responses of salivary glands to pharmacological discriminators, we quantified the volumes of secreted saliva from isolated salivary glands by developing the assay method modified from Ramsay's original assay (Fig. 2-2) (Ramsay, 1954). The salivary glands that were pre-incubated with buffer only did not show any secretory activity. Dopamine (1, 10, and 100 μM) induced significant salivary secretion in a dose-dependent manner (Fig. 2-3A,E). The rate of salivary secretion was increased immediately after agonist treatment, peaked at 10 or 15 min, and then gradually decreased until 30 min, which was the end of our observation (Fig. 2-3A-D). The maximal total salivary secretion volume for 30 min was approximately 1.2 μL at 100 μM dopamine (Fig. 2-3E).

SKF82958, a D1-specific agonist activating only the D1 but not the InvD1L receptor, also showed significant, but slightly lower activities than dopamine. At SKF82958 doses of 10 μM and 100 μM, the secretory activity was 44% and 76% of dopamine at the same respective concentrations (Fig. 2-3E,F). The general patterns of secretory activities over time in the post-treatments were similar to the patterns observed in dopamine treatments.

Pre-incubation of the isolated salivary gland with InvD1L-specific antagonist fluphenazine (10 μM) followed by co-incubation of fluphenazine with dopamine or SKF82958 significantly suppressed secretory activity, while the salivary secretion pattern peak at approximately 10 min was similar to agonist treatment alone (Fig. 2-3A-D). We observed approximately 30% reductions at both 1 μM and 10 μM dopamine treatment (Fig. 2-3E). The reduction in SKF82958 treatment was also significant at 10 μM but not at 100 μM (Fig. 2-3F).

Co-incubation of the isolated salivary gland with SCH23390 (10 μM), a common antagonist for both D1 and InvD1L, and dopamine (10 μM) almost completely abolished secretory activity (Fig. 2-4). The antagonistic activity of the SCH23390 was reverted after replacing it with dopamine only (100 μM) without the antagonist (Fig. 2-4).

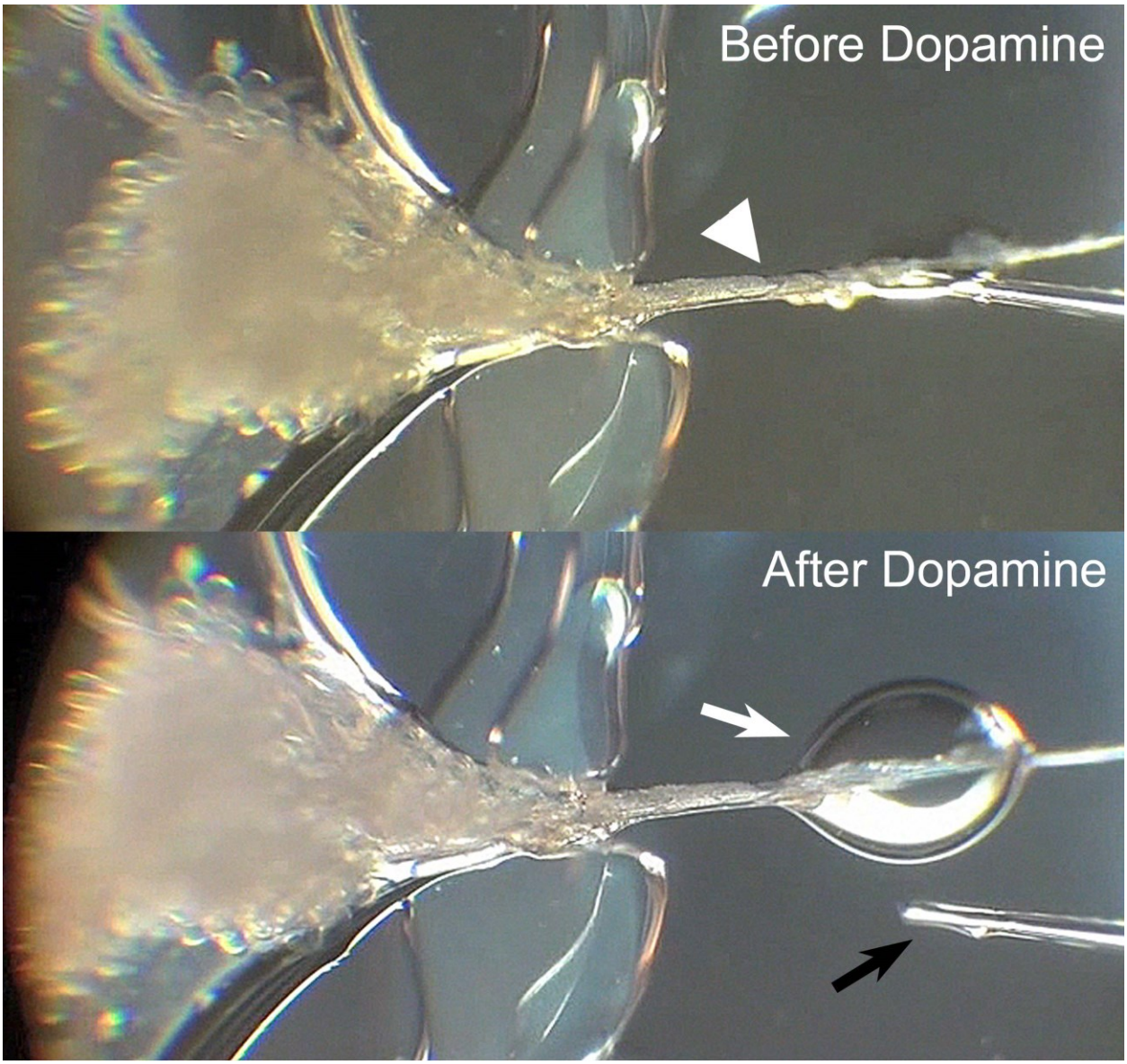

Figure 2-2. Example fluid secretion assay using a whole salivary gland.

A salivary gland preparation is shown before (upper panel) and after dopamine treatment (lower panel). The arrowhead indicates the main salivary gland duct that was pulled out from the Hank's saline reservoir across a narrow vacuum grease dam and attached on the Sylgard plate. The white arrow indicates the drop of saliva that was secreted through the main duct after treatment. The black arrow is the tip of microelectrode that was used for quantifying the secretion volume every 5 min for 30 min.

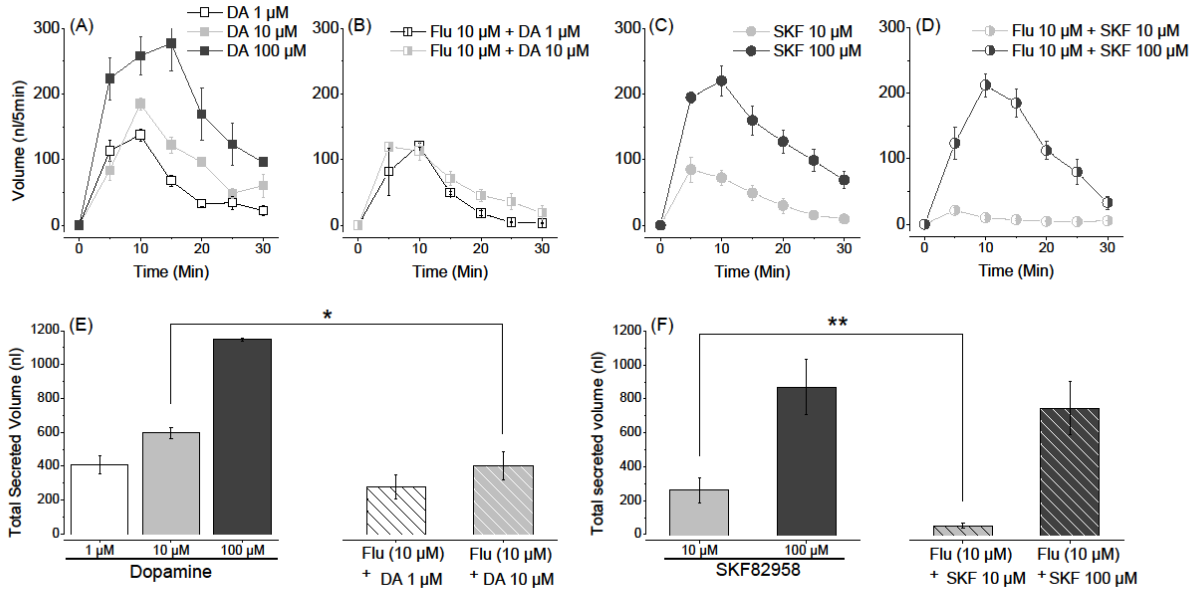

Figure 2-3. Fluid secretion assay using a whole salivary gland with dopamine, D1-specific agonist SKF82958 and InvD1L-specific antagonist fluphenazine.

The salivary secretion pattern over 30 min duration after treatments (A) by different dopamine doses (DA), (B) by 25 min pre-treatment and DA co-incubation with fluphenazine (Flu, 10 µM), (C) by SKF82958 (SKF), and (D) by 25 min pre-treatment and SKF co-incubation with fluphenazine (10 µM). (E) Total volume of secreted saliva by different DA doses (solid bars) and combinatory treatment of DA and Flu (hatched bars), which corresponded to the insets (A) and (B), respectively. (F) Total volume of secreted saliva by different SKF doses (solid bars) and combination of SKF and Flu (hatched bars), which corresponded to the insets (C) and (D), respectively. The bars indicate averages with s.e.m. for more than three replicates. Asterisks indicate statistical significance in a paired t-test, $p < 0.01$ (**) and $p < 0.05$ (*).

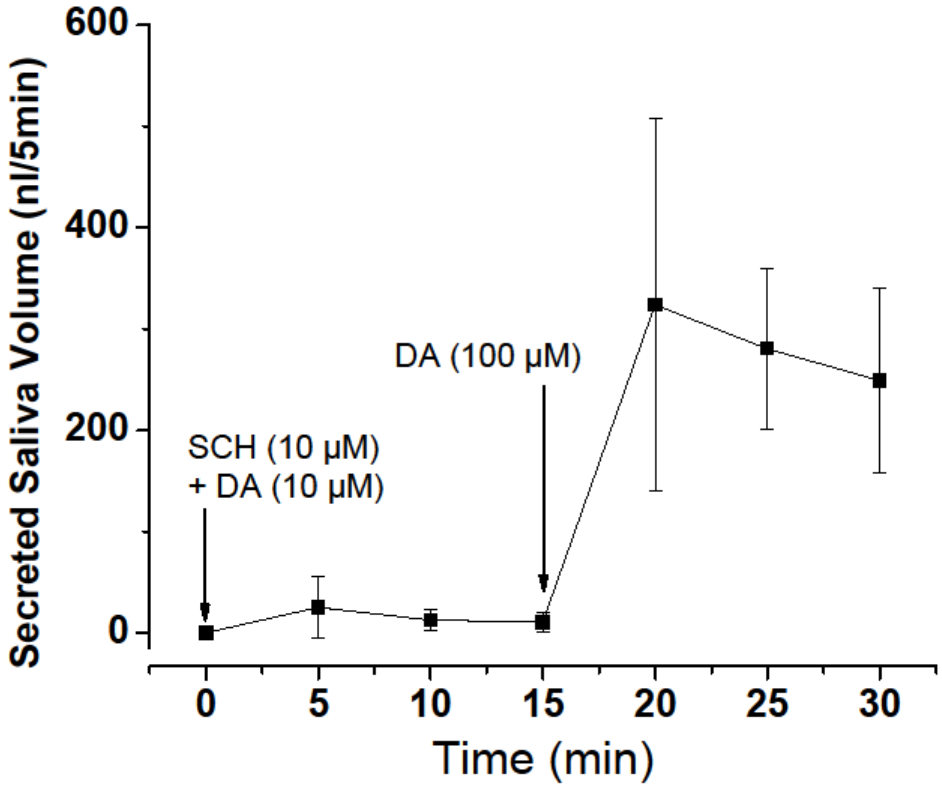

Figure 2-4. Effect of the common antagonist SCH23390 (SCH) on dopamine (DA)-mediated salivary gland fluid secretion.

DA-mediated salivary secretion was abolished by SCH in the first 15 min. Subsequent washing and treatment with DA alone induced significant salivary secretion.

Agonist activity on individual salivary gland acini

Microscopic observation of each acinus after pharmacological agent treatment revealed dynamic changes occurring in each acinus. It was possible to perform multiple experiments for different treatments from a salivary gland by dividing it into several groups containing approximately 10 acini per group. In the initial observations, we found that the acini sizes dynamically changed, especially when they were treated with dopamine. The changes in acini sizes were driven by the changes in luminal acini volumes but not by the changes in sizes of the cells composing the acini (Fig. 2-5A). Therefore, changes in acini sizes were measured and calculated for volume and percent volume change. Based on the volume calculated, each acinus luminal space increased up to approximately 4 nL by dopamine treatment.

Patterns of the changes over time were used to infer physiological changes of the acini: increased and decreased sizes were interpreted as solute influx into the acinar lumen and pumping or gating for saliva discharge through the acinar duct, respectively (Fig. 2-5). The change patterns included rapid or slow reductions in acini sizes, each referred as pumping or gating, respectively, and together as pumping/gating. We set the threshold for counting the pumping/gating category based on the statistics of samples with mock treatments and a rate of reduction higher than 3.5% per minute (see more details in Materials and methods). However, based on our close observations, this method was unavoidable from the false-negative cases, i.e., the cases where true pumping/gating were not counted because the fluid expulsion rate is occasionally masked by equal or higher fluid influx rates, although the positive pumping/gating counts were accurate.

As an example of dynamic changes in acini, dopamine triggered changes in acini sizes (Fig. 2-5A, Appendix A Movie 1) and volume (Fig. 2-5B). Typical pumping is shown by rapid reduction of the acini size that appeared, such as a squeezing muscular contraction of the acini (Appendix B Movie 2). In some cases, slow reduction in size occurred over a relatively long duration. This case was considered to be gating because subtle movements of the acinar duct valve in concurrence with slow volume reduction were observed in some cases (Appendix C Movie 3).

The maximum sizes of the acini that were activated by dopamine at the four different doses (100 nM – 100 μM) demonstrated a typical dose-response of size increase up to 1 μM but slight reductions at the higher concentrations 10 and 100 μM (Fig. 2-6A). Similarly, the D1

specific agonist SKF82958 also showed significant activities for the increased acini size at all doses but with slightly lower activities than dopamine. Similar to the dopamine treatments, the higher doses induced stronger responses up to 10 μM, but the highest dose 100 μM showed a slightly reduced degree of response. The pumping/gating frequency was highest in the 1μM dopamine treatment (42%) but was progressively reduced in the higher dopamine doses (Fig. 2-6C). In the SKF82958 treatments, pumping/gating was much less frequent than that of dopamine with a maximum count of 18% of acini at the 10 μM dose (Fig. 2-6D).

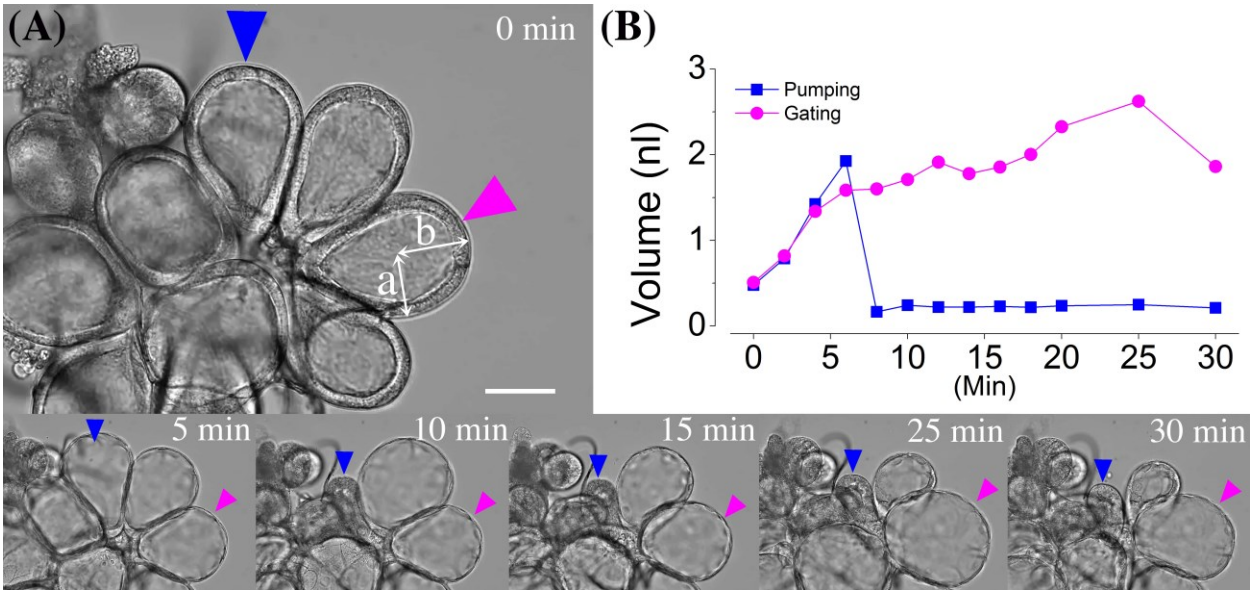

Figure 2-5. Dynamic responses of individual salivary gland acini to dopamine (DA) treatment.

(A) An example indicating the changes of salivary glands acini recorded by a video camera with 200x magnification for 30 min after 10 μM dopamine treatment. Dotted lines and arrowheads indicate two randomly selected acini for measuring the volume change. Those colours for dotted lines and arrowheads correspond to the line colours in (B). (B) Each line indicates changes in individual acini volume to dopamine treatment for 30 min. Blue and purple lines are indicating the example of pumping and gating, respectively. Scale bar = 50 μm.

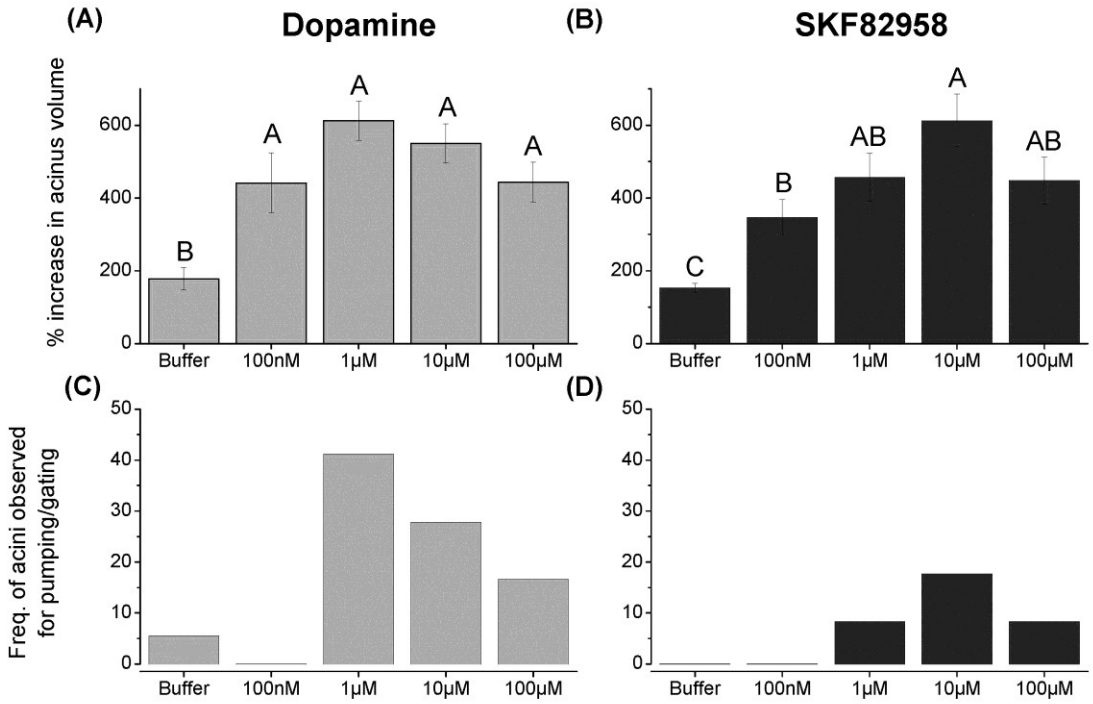

Figure 2-6. Dynamic responses of individual acini to dopamine receptor agonists.

(A) Percent increase in the acini volume calculated for the maximum size reached within 30 min after dopamine treatment. (B) Percent increase in the acini volume after SKF82958 treatment. (C, D) Frequencies of acini observed for pumping/gating in each treatment. The data in (A, B) are averaged with the s.e.m. for at least three biological replicates. The data in (C, D) are for frequencies in observations of more than 18 acini for each data point. The data were analysed by ANOVA-Tukey-Kramer HSD (p=0.05). Hank's saline (buffer) indicated mock treatment.

Effects of antagonists on agonist-mediated individual salivary gland acini

The activities of dopamine or SKF82958 for increased acini volume were completely abolished by SCH23390, the common antagonist of both D1 and InvD1L (Fig. 2-7A). Consequently, the acini that were pre-treated with SCH23390 did not show any pumping/gating activity (Fig. 2-7B).

Pre-treatments of acini with InvD1L-specific antagonist fluphenazine followed by dopamine or SKF82958 treatments did not significantly reduce the maximum acini sizes (Fig. 2-8A). However, reduced frequencies of pumping/gating by the pre-treatments were apparent in both dopamine and SKF82958 treatments (Fig. 2-8B). The frequency of dopamine-induced pumping/gating was reduced from 28% to 17% by fluphenazine pre-treatment. Pre-treatment eliminated SKF82958 treatment-mediated pumping/gating (18% to 0%) (Fig. 2-8B).

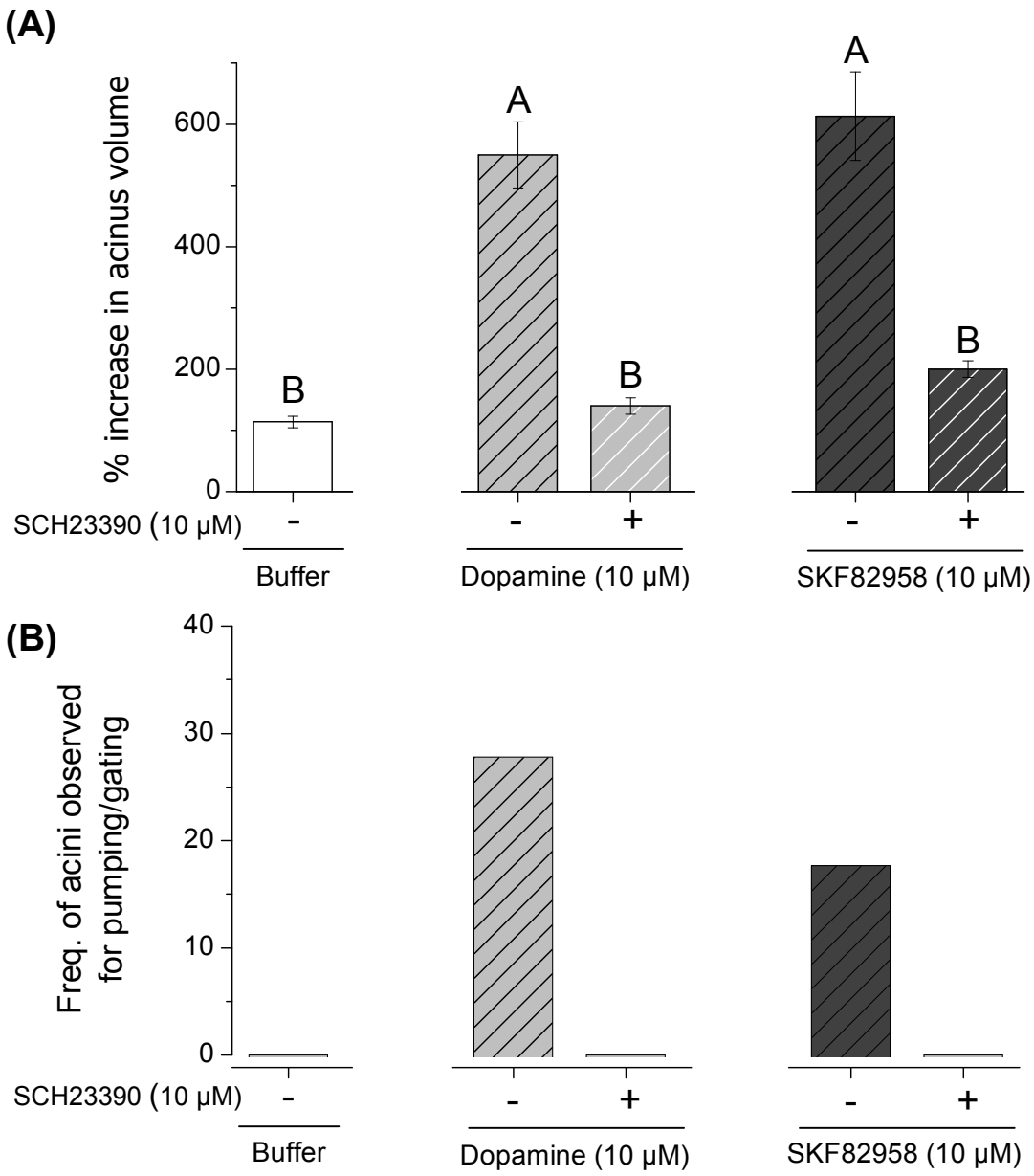

Figure 2-7. Effects of common dopamine receptor antagonist SCH23390 (SCH) on dopamine- or SKF82958-mediated salivary gland acini dynamics.

(A) Percent increase in the acini volume after various combinatory treatments. (B) Frequencies of acini observed for pumping/gating in each treatment. The data in (A) are the average with the s.e.m. for at least three biological replicates. The data in (B) are frequencies in observations of more than 6 acini for each data point. The data were analysed by ANOVA-Tukey-Kramer HSD (p=0.05).

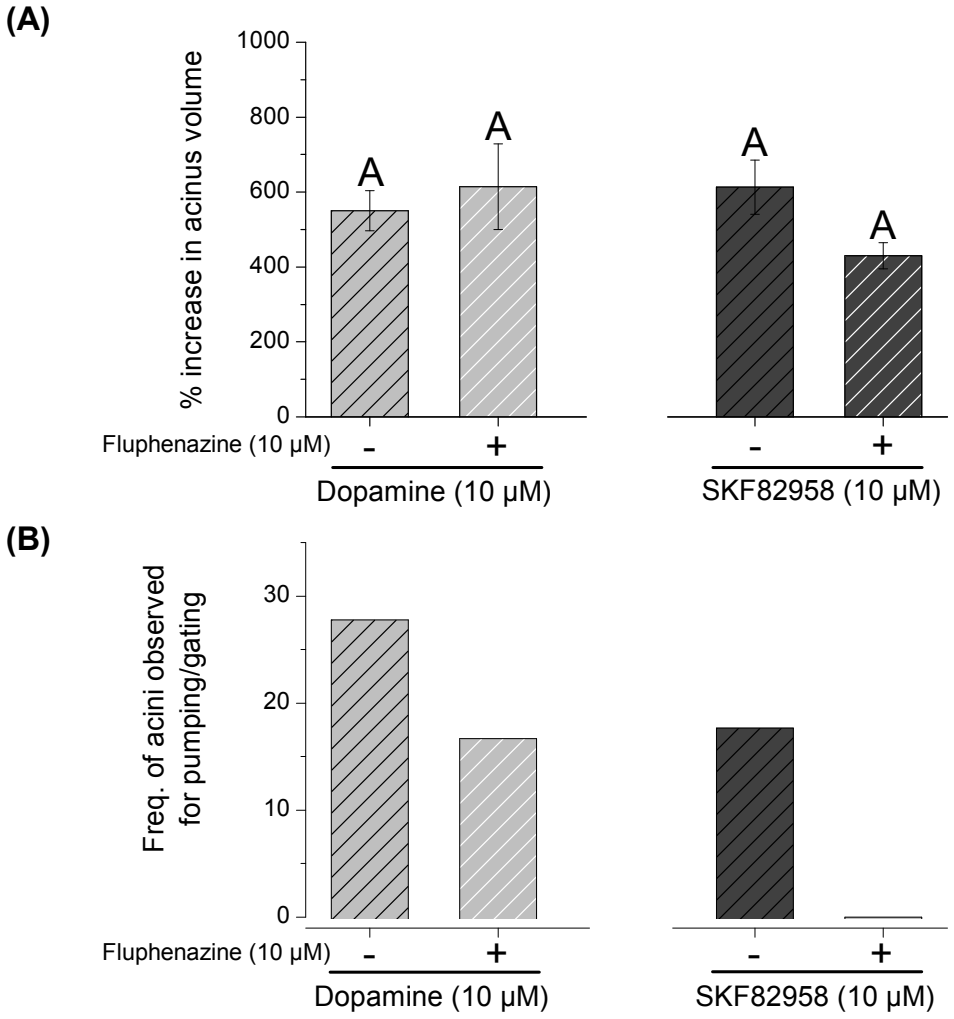

Figure 2-8. Effects of InvD1L-specific blocker fluphenazine (Flu) on dopamine- or SKF82958-mediated salivary gland acini dynamics.

(A) Percent increase in acini volume after various combinatory treatments. (B) Frequencies of acini observed for pumping/gating in each treatment. The data in (A) are the averages with s.e.m. for at least three biological replicates. The data in (B) are frequencies in observations of more than 18 acini for each data point. The data were analysed by ANOVA-Tukey-Kramer HSD (p=0.05).

Discussion

In dopamine-mediated osmoregulatory salivary secretion by the tick, we determined that two combinatory physiological actions occur in the type III salivary gland acini: inward fluid transport and release of the luminal content. Dopamine treatment immediately activated fluid influx as indicated by increased luminal volume (Fig. 2-5). In contrast to the description made in *Ixodes ricinus*, where increased luminal size accommodated the fluid influx without increased acini size (Bowman and Sauer, 2004), we observed rapid acini expansion up to approximately 5 times because of increased luminal volume (Fig. 2-5 and Movie 1). Visually detectable levels of fluid efflux through the acinar duct in this study found mainly two main categories of efflux patterns in different acini: acini with slowly reduced sizes over time (gating) and acini with rapid collapse for expelling fluid (pumping). In rare occasions, we observed subtle movements of acinar valve flaps in the gating acini (Movie 3). On the other hand, the pumping acini, when it occurred in the intermediate size before the acini was fully expanded, appeared to be driven by a squeezing contraction of the acini (Movie 2). These were difficult to distinguish when the acini were fully expanded because rapid size reduction could be partly caused by high internal pressure. Summing up the observations, two components in the salivary secretion are epithelial cell fluid transport for solute influx and myoepithelial cell contraction for generating internal pressure with opening the valve allowing saliva efflux through the acinar duct. The full salivary secretion rate required both processes based on the experiment using pharmacological tools (Fig. 2-3 and see next paragraph). Observation of the salivary glands in real time provided physiological events that were involved in salivary secretion, although we do not know whether the observed levels of acini expansion occur in an *in vivo* system that is enclosed in the rigid body wall.

Use of receptor-specific pharmacological tools in this study suggests that the downstream physiological events are mediated through different dopamine receptors D1 and InvD1L, which were previously characterised in the tick salivary glands (Šimo et al., 2014; Šimo et al., 2011). The results of this study support the function of D1 for solute influx and InvD1L for pumping/gating in type III acini. The most pronounced result was demonstrated in the acini that were treated with the combination of D1-specific agonist SKF82958 and InvD1L-specific antagonist fluphenazine abolishing the pumping/gating with normal acini size increase (Fig. 2-8) and significantly diminishing fluid secretion by whole salivary glands (Fig. 2-3F). Treatment

with dopamine and fluphenazine in combination and SKF82958 alone, however, reduced but did not completely abolish the pumping/gating frequencies and fluid secretion , although fluphenazine and SKF82958 clearly distinguished recombinant receptors in the heterologous system at the 10 μM dose. This leaky activity in suppression of pumping/gating suggests the presence of other signalling pathways that interact with dopamine signalling for pumping/gating. Such candidates could be the neuropeptides myoinhibitory peptide (MIP) and SIFamide, which were found in the neural projections reaching the basal region of acini (Šimo et al., 2009; Šimo et al., 2013). Alternatively, an unidentified signalling system acting through the octopamine receptor, which is likely cross-activated by dopamine, could have also been involved in this process.

Previous studies in dopamine signalling pathways (Hume et al., 1984; Sauer et al., 2000; Schmidt et al., 1981) and in characterising the D1 and InvD1L receptors in tick salivary glands (Šimo et al., 2014; Šimo et al., 2011), and this study are all well congruent and provide further insight into the mechanisms of tick salivary gland control. Dopamine activates crucial Ca^{2+} (Kaufman, 1976; Needham and Sauer, 1979) and cAMP (Hume et al., 1984) downstream signalling pathways in tick salivary secretion. Heterologous receptor expression determined that D1 has higher dopamine sensitivity and was mainly coupled to cAMP elevation, while InvD1L was coupled to Ca^{2+} elevation with lower dopamine sensitivity (Šimo et al., 2014; Šimo et al., 2011). Immunohistochemistry revealed that the D1 is located in the acini epithelial cells and the InvD1L is located in axonal projections reaching to the basal region of acini and in another distinguished projections further extended to the apical region of acini (Šimo et al., 2014; Šimo et al., 2011). These characteristics of D1 and InvD1L suggest that an initial low dose of dopamine activates D1 in epithelial cells leading the cAMP-mediated fluid transport. Then, high dopamine doses acting on the InvD1L trigger (or modulate) Ca^{2+}-mediated myoepithelial cell contraction and/or acinar valve flap for saliva efflux through the salivary duct.

While this study focused on dopamine actions in the type III acini, the roles of the two different dopamine receptors in type II acini are thought to be similar. Although type II acini function mainly for secretion of the protein components of saliva, they also contain epithelial cell types with similar immunoreactive patterns for D1 and InvD1L receptors. Visual investigation of fluid flow through type II acini was not possible due to lack of dopamine-induced acinar expansion as in acini type III. Employing additional experimental tools, such as

electrophysiology, will be required to understand the physiological mechanism underlying dopamine and their receptors in type II acini.

The autocrine/paracrine dopamine (Koči et al., 2014) and the downstream systems built in the salivary glands are also likely interacting with neural commands. The neural projections reaching to the basal region of acini containing MIP/SIFamide are also positive with InvD1L antibodies (Šimo et al., 2014). The co-localisation suggests that dopamine action includes modulation of MIP/SIFamide neuronal secretory activities at axon terminals. Candidate functions of MIP and SIFamide were previously suggested as controls of acinar valves, myoepithelial cells, and dopamine secretion, based on the anatomy of the axon terminal in acini (Šimo et al., 2009; Šimo et al., 2013). Therefore, we conclude that osmoregulatory salivary secretion in ticks involves the orchestration of interactions of multiple components for dynamic controls.

Materials and methods

Functional expression and pharmacological assays of two dopamine receptors: D1 and InvD1L

The full open reading frame (ORF) for each D1 and InvD1L were inserted into the pcDNA 3.1 (+) expression vector (Invitrogen, Carlsbad, CA, USA). Expression plasmids were prepared for high purity and concentrations (>1 μg/μl) and were then sequenced. Functional GPCR expression was performed based on a previous description with modifications (Jiang et al., 2013; Park et al., 2003; Šimo et al., 2014; Šimo et al., 2011). A one-to-one mixture of the receptor-containing plasmid and the codon-optimised human apoaequorin-containing plasmid (Vernon and Printen, 2002) were used for transfections of Chinese Hamster Ovary (CHO) cells by using *TransIT*®- LT1 (Mirus, Madison, WI, USA). Approximately 24-48 hours after the transfection, cells were harvested with trypsin-EDTA (Gibco, Grand Island, NY, USA) and resuspended in 3 ml DMEM/F12 media with 0.1% bovine serum albumin (BSA) (Amresco, Solon, OH, USA). Coelenterazine h (final concentration 5 μM; AAT Bioquest, Sunnyvale, CA, USA) was added into the resuspended cells. After a 3-hour incubation, cells were additionally incubated for 30 minutes followed by adding 27 ml DMEM/F12 media, including 0.1% bovine serum albumin

(BSA) (Amresco, Solon, OH, USA). For the agonist assay, various dopamine agonists (final concentration 10 μM) were prepared in a 96-well plate, upon which transfected cells (~ 15,000 cells in 50 μL) were applied. For the antagonist assay, the cells were pre-incubated with various dopamine antagonists (final concentration 10 μM) for 15 minutes, followed by 10 μM dopamine treatment. Luminescence, the indicator of calcium mobilisation, was monitored for 20 seconds (100 ms exposure in every 100 ms) immediately following the application of either transfected cells (for the agonist assay) or dopamine (for the antagonist assay). Luminescence values were integrated over time for 20 seconds and normalised to the largest positive control response and to the negative control background values.

Chemicals

The following chemicals were used for the agonist and antagonist assays. Dopamine agonists included SKF82958, 6,7-ADTN, apomorphine (Sigma, Saint Louis, MO, USA), dopamine-3-O-sulfate, and dopamine-4-O-sulfate (RTI international, Research Triangle Park, NC, USA). Dopamine antagonists included acepromazine, fluphenazine, clozapine, sulpiride, haloperidol, SCH23390, (+)butaclamol, and (-)butaclamol (Sigma, Saint Louis, MO, USA).

Tick and salivary gland preparation

The blacklegged tick *I. scapularis* was purchased from the Tick Rearing Center at Oklahoma State University (Stillwater, OK, USA). Partially engorged female ticks (weighing 12-19 mg, 4-5 days blood-fed) were prepared from an artificial feeding system that was modified from the method developed by (Krober and Guerin, 2007). Tick feeding chambers were maintained at 37°C with a 16:8 photoperiod (Krober and Guerin, 2007). The defibrinated bovine blood (Cedarlane, Burlington, NC, USA) contained 10 μM Gentamycin solution (Sigma, Saint Louis, MO, USA) and 100 μM ATP (Sigma, Saint Louis, MO, USA), and we replaced blood meals every 12 hours. Salivary glands of partially engorged female ticks were dissected and pre-incubated in Hank's saline (Sigma, Saint Louis, MO, USA). For microscopic video recording of individual acini, whole salivary glands were cut into small pieces, each containing approximately 10 acini per group. For the *in vitro* fluid secretion assay, whole salivary glands were examined following pre-incubation in Hank's saline for 1 hr.

in vitro fluid secretion assays

A modified Ramsay's assay (Ramsay, 1954) was established for tick salivary glands that have much shorter ducts than other insect Malpighian tubules. Salivary glands were placed in a droplet (30 µl) of Hank's saline on a 60 mm X 15 mm petri dish coated with Sylgard® (World Precision Instrument, Inc., Sarasota, FL, USA) after pre-incubation of isolated intact salivary glands in Hank's saline for an hour. The main duct was pulled out from the Hank's saline droplet crossing over a narrow dam (0.5 – 1 mm) made of high vacuum grease (Dow Corning Corporation, Midland, MI, USA) and immobilised on the Sylgard® petri dish surface. Heavy mineral oil (Fisher Scientific, Fair Lawn, NJ, USA) covered both the Hank's saline and the main salivary gland duct to collect secreted saliva (Fig. 2-2A). To establish basal levels of excretion induced by Hank's saline, measurements were taken in the first 5 minutes after preparation of the fluid secretion assay. A micro-injector (Nanoliter 2000, World Precision Instrument, Inc., Sarasota, FL, USA) controlled by a micro-syringe pump controller (Micro4, World Precision Instrument, Inc., Sarasota, FL, USA) was used for withdrawing the secretion formed at the tip of the main duct in the heavy mineral oil, and the volume withdrawn was recorded in every 5 min for 30 min. For the agonist assay, we measured secreted saliva for 30 min after drug treatment. For the antagonist assay, salivary glands were pre-incubated in antagonist for 25 min, and then agonists were administered to salivary glands in the presence of the antagonists (Fig. 2-2B).

Measurement of the individual type III acini responses to pharmacological treatments

The size changes occurring in type III acini after treatment with pharmacological agents were video recorded. The video record was replayed for plotting volume changes over time (for approximately 30 min) every 2 min. The acinus volume was calculated by the equation for an ellipsoid volume: Volume $= \frac{4\pi}{3} a^2 b$, where a and b are outer radiuses demonstrated in Fig. 2-5A. For an unbiased observation, we randomly pre-selected two individual type III acini on the focal plane of the microscope, measured the changes and calculated acini volumes. Increased acini size was generally interpreted as inward fluid transport, while reduced size demonstrated two

different patterns: pumping and gating. For statistical analysis of acini pumping/gating frequencies, we established thresholds for volume reduction over time. The thresholds were determined by the percent volume reductions that were observed in the mock treatments ($p < 0.01$). Acini-defined pumping/gating revealed more than 3.15% volume reduction per minute from the maximum to the lowest in the 30 min observation. Thereby, the formula for the threshold of pumping/gating was: $\left\{ \left(\frac{V_{max} - V_{min}}{V_{min}} \right) \Big/ (T_{min} - T_{max}) \right\} * 100 < -3.15\ (\%)$, where V is volume and T is time.

For the antagonist assay, salivary glands were pre-incubated in antagonist for 25 min followed by administration of agonist to salivary glands in the presence of antagonists.

List of symbols and abbreviations

Ace	acepromazine
Apo	apomorphine
(-)Bu	(-)butaclamol
(+)Bu	(+)butaclamol
cAMP	cyclic AMP
CHO	Chinese hamster ovary
Clo	clozapine
D1	dopamine receptor
DA	dopamine
DA-3	dopamine-3-O-sulfate
DA-4	dopamine-4-O-sulfate
DMEM	Dulbecco's Modified Eagle Medium
EDTA	Ethylenediaminetetraacetic acid
Flu	fluphenazine
GPCRs	G-protein coupled receptors
Hal	haloperidol
InvD1L	Invertebrate specific D1-like dopamine receptor
max	maximum
min	minimum
MIP	myoinhibitory peptide
ORF	open reading frame
π	pi
SCH	SCH23390
SKF	SKF82958
Sul	sulpiride

References

Bowman, A. S. and Sauer, J. R. (2004). Tick salivary glands: function, physiology and future. *Parasitology* **129**, S67-S81.

Francischetti, I. M., Sa-Nunes, A., Mans, B. J., Santos, I. M. and Ribeiro, J. M. (2009). The role of saliva in tick feeding. *Front. Biosci.* **14**, 2051-88.

Gaede, K., Kn, Uuml and Lle, W. (1997). On the mechanism of water vapour sorption from unsaturated atmospheres by ticks. *J. Exp. Biol.* **200**, 1491-8.

Hume, M. E., Essenberg, R. C., McNew, R. W., Bantle, J. A. and Sauer, J. R. (1984). Adenosine-3',5'-monophosphate in salivary glands of unfed and feeding female lone star ticks, Amblyomma americanum (L.). *Comp. Biochem. Physiol.* **79**, 47-50.

Jiang, H., Lkhagva, A., Daubnerová, I., Chae, H.-S., Šimo, L., Jung, S.-H., Yoon, Y.-K., Lee, N.-R., Seong, J. Y., Žitňan, D. et al. (2013). Natalisin, a tachykinin-like signaling system, regulates sexual activity and fecundity in insects. *Proc. Natl. Acad. Sci.* **110**, E3526-E3534.

Kaufman, W. R. (1976). The influence of various factors on fluid secretion by in vitro salivary glands of ixodid Ticks. *J. Exp. Biol.* **64**, 727-742.

Kaufman, W. R. (1977). The influence of adrenergic agonists and their antagonists on isolated salivary glands of ixodid ticks. *Eur. J. Pharmacol.* **45**, 61-8.

Kaufman, W. R. (2007). Gluttony and sex in female ixodid ticks: How do they compare to other blood-sucking arthropods? *J. Insect Physiol.* **53**, 264-273.

Kaufman, W. R. and Phillips, J. E. (1973a). Ion and Water-Balance in Ixodid Tick Dermacentor-Andersoni .1. Routes of Ion and Water Excretion. *J. Exp. Biol.* **58**, 523-536.

Kaufman, W. R. and Phillips, J. E. (1973b). Ion and Water-Balance in Ixodid Tick Dermacentor-Andersoni .2. Mechanism and Control of Salivary Secretion. *J. Exp. Biol.* **58**, 537-547.

Kaufman, W. R. and Wong, D. L. (1983). Evidence for multiple receptors mediating fluid secretion in salivary glands of ticks. *Eur. J. Pharmacol.* **87**, 43-52.

Koči, J., Šimo, L. and Park, Y. (2014). Autocrine/paracrine dopamine in the salivary glands of the blacklegged tick Ixodes scapularis. *J. Insect Physiol.*

Krober, T. and Guerin, P. (2007). The tick blood meal: from a living animal or from a silicone membrane? *ALTEX* **24**, 39-41.

Krolak, J. M., Ownby, C. L., Barker, D. M. and Sauer, J. R. (1983). Immunohistochemical localization of adenosine 3':5'-cyclic monophosphate in female ixodid tick Amblyomma americanum (L.) salivary glands. *J. Parasitol.* **69**, 152-7.

Meyer, J. M., Ejendal, K. F., Avramova, L. V., Garland-Kuntz, E. E., Giraldo-Calderon, G. I., Brust, T. F., Watts, V. J. and Hill, C. A. (2012). A "genome-to-lead" approach for insecticide discovery: pharmacological characterization and screening of Aedes aegypti D(1)-like dopamine receptors. *PLoS Negl. Trop. Dis.* **6**, e1478.

Meyer, J. M., Ejendal, K. F., Watts, V. J. and Hill, C. A. (2011). Molecular and pharmacological characterization of two D(1)-like dopamine receptors in the Lyme disease vector, Ixodes scapularis. *Insect Biochem. Mol. Biol.* **41**, 563-71.

Needham, G. R. and Pannabecker, T. L. (1983). Effects of Octopamine, Chlordimeform, and Demethylchlordimeform on Amine-Controlled Tick Salivary-Glands Isolated from Feeding Amblyomma-Americanum (L). *Pestic. Biochem. Physiol.* **19**, 133-140.

Needham, G. R. and Sauer, J. R. (1979). Involvement of calcium and cyclic AMP in controlling ixodid tick salivary fluid secretion. *J. Parasitol.* **65**, 531-42.
Nuttall, P. A., Trimnell, A. R., Kazimirova, M. and Labuda, M. (2006). Exposed and concealed antigens as vaccine targets for controlling ticks and tick-borne diseases. *Parasite Immunol.* **28**, 155-63.
Pannabecker, T. and Needham, G. R. (1985). Effects of Octopamine on Fluid Secretion by Isolated Salivary-Glands of a Feeding Ixodid Tick. *Arch. Insect Biochem. Physiol.* **2**, 217-226.
Park, Y., Kim, Y. J., Dupriez, V. and Adams, M. E. (2003). Two subtypes of ecdysis-triggering hormone receptor in Drosophila melanogaster. *J. Biol. Chem.* **278**, 17710-5.
Ramsay, J. A. (1954). Active Transport of Water by the Malpighian Tubules of the Stick Insect, Dixippus Morosus (Orthoptera, Phasmidae). *J. Exp. Biol.* **31**, 104-113.
Ribeiro, J. M. (1987). Role of saliva in blood-feeding by arthropods. *Annu. Rev. Entomol.* **32**, 463-78.
Ribeiro, J. M. (1989). Role of saliva in tick/host interactions. *Exp. Appl. Acarol.* **7**, 15-20.
Rudolph, D. and Knulle, W. (1974). Site and Mechanism of Water-Vapor Uptake from Atmosphere in Ixodid Ticks. *Nature* **249**, 84-85.
Sauer, J. R., Essenberg, R. C. and Bowman, A. S. (2000). Salivary glands in ixodid ticks: control and mechanism of secretion. *J. Insect Physiol.* **46**, 1069-1078.
Schmidt, S. P., Essenberg, R. C. and Sauer, J. R. (1981). Evidence for a D1 dopamine receptor in the salivary glands of Amblyomma americanum (L.). *J. Cyclic Nucleotide Res.* **7**, 375-84.
Šimo, L., Itňan, D. Ž. and Park, Y. (2009). Two novel neuropeptides in innervation of the salivary glands of the black-legged tick, Ixodes scapularis: Myoinhibitory peptide and SIFamide. *J. Comp. Neurol.* **517**, 551-563.
Šimo, L., Koči, J., Kim, D. and Park, Y. (2014). Invertebrate specific D1-like dopamine receptor in control of salivary glands in the black-legged tick Ixodes scapularis. *J. Comp. Neurol.* **522**, 2038-2052.
Šimo, L., Koči, J. and Park, Y. (2013). Receptors for the neuropeptides, myoinhibitory peptide and SIFamide, in control of the salivary glands of the blacklegged tick Ixodes scapularis. *Insect Biochem. Mol. Biol.* **43**, 376-387.
Šimo, L., Koci, J., Zitnan, D. and Park, Y. (2011). Evidence for D1 dopamine receptor activation by a paracrine signal of dopamine in tick salivary glands. *PLoS One* **6**, e16158.
Tatchell, R. J. (1967). Salivary Secretion in the Cattle Tick as a Means of Water Elimination. *Nature* **213**, 940-941.
Vernon, W. I. and Printen, J. A. (2002). Assay for intracellular calcium using a codon-optimized aequorin. *BioTechniques* **33**, 730.

Chapter 3 - Multiple functions of Na/K-ATPase in dopamine-induced salivation of the Blacklegged tick, *Ixodes scapularis*

Abstract

Tick salivation during blood-feeding is crucial for successful tick feeding, which includes excretory water, ions, and bioactive components for compromising the hosts' immune responses. Control of salivary secretion involves autocrine dopamine activating two dopamine receptors: D1 and Invertebrate-specific D1-like dopamine receptors. In this study, we investigated Na/K-ATPase as an important component in the epithelial physiology. Immunoreactivity for Na/K-ATPase revealed basal infolding of lamellate cells in type-I, abluminal interstitial (epithelial) cells in type-II, and labyrinth-like infolding structures opening towards the lumen in type-III acini. A high dose of ouabain, a Na/K-ATPase specific blocker, abolished dopamine-induced salivary secretion via suppressing the influx of fluid in type III acini. A mild dose of ouabain resulted in a slightly reduced volume of highly hyperosmolar secretion, suggesting an additional ouabain action is for inhibition of ion resorptive function of Na/K-ATPase in type I acini. Dopamine/ouabain were not involved in activation of protein secretion, while basal constitutive level of protein was found in the dopamine-induced saliva. We propose that the dopamine-dependent primary saliva formation, mediated by Na/K-ATPase in type III and type II acini, is followed by a dopamine-independent resorptive function of Na/K-ATPase in type I acini located in the proximal end of the salivary duct.

Introduction

Ticks are hematophagous arthropod vectors that transmit various disease-causing pathogens to both humans and animals throughout the world. Across the United States, the most commonly reported vector-borne disease is Lyme disease, transmitted by the blacklegged tick, *Ixodes scapularis Say*. Ticks can feed on their host for up to two weeks without detachment and increase their body weight considerably (i.e., up to 100 times(Kaufman, 2007)). The salivary glands (SG) of ticks perform crucial functions during this long term feeding. The salivary secretion at the early stage of feeding is thought to contain various bioactive components, compromising the hosts' immune responses(Francischetti et al., 2009; Nuttall et al., 2006; Ribeiro, 1987; Ribeiro, 1989) for the successful establishment of the feeding-site. Inadvertently, the compromised immune state at the feeding lesion provides a means for opportunistic pathogens to be transmitted to the host via the saliva and the SG. Another important function of the tick SG is the excretion of excess ions and water for maintaining homeostasis when large amounts of blood are ingested. Off-host, ticks secrete salty saliva, which allows them to capture atmospheric water molecules(Gaede and Knülle, 1997; Rudolph and Knulle, 1974) and prevent desiccation.

The multiple roles of the SG are likely attributed to the different types of acini comprising the SG. There are at least three different types of acini, organizing the SG into grape-like clusters, and the ultrastructure of each type of SG acini suggests their roles in female ticks (Coons et al., 1994; Coons and Roshdy, 1973; Fawcett et al., 1981a; Fawcett et al., 1981b; Gaede and Knülle, 1997; Krolak et al., 1982). A small number of type I acini are attached to the main duct, which are thought to be essential for water absorption in the off-host stage. Type II acini are attached to secondary and tertiary ducts and their granular cell types indicate their function for the secretion of bioactive proteins. A large number of type III acini are attached to the tertiary ducts and are likely important for the excretion of water and solutes.

Mechanisms controlling tick salivary secretion have long been studied and a number of candidate signaling molecules have been identified; dopamine, pilocarpine, prostaglandin E_2, and two different neuropeptides, myoinhibitory peptide (MIP) and SIFamide(Bowman et al., 1996; Bowman et al., 1997; Kaufman, 1978; Sauer et al., 2000; Šimo et al., 2013). Among various pharmacological reagents that have been studied in tick salivary secretion, dopamine has been

shown to be the most potent direct signaling molecule for triggering tick salivation(Kaufman, 1976; Kaufman, 1977; Kaufman and Phillips, 1973a; Kaufman and Phillips, 1973b; Kaufman and Phillips, 1973c; Needham and Pannabecker, 1983; Tatchell, 1967), while pilocarpine (a muscarinic cholinergic receptor agonist) is thought to be indirectly acting through the synganglion (brain)(Kaufman and Phillips, 1973b; Needham and Sauer, 1975). Dopamine produced from the SG(Kaufman and Wong, 1983; Koči et al., 2014) exhibits autocrine functions via two distinct dopamine receptors, D1 dopamine receptor (D1) and Invertebrate-specific D1-like dopamine receptor (InvD1L), producing independent physiological actions; influx of water and solutes in type III acini and partially in type II acini, and contraction of myoepithelial cells in types II and III acini for expelling the contents out from the acini(Šimo et al., 2014; Šimo et al., 2011), respectively.

The mechanisms of dopamine's downstream involvement in water and solute transport through epithelial types of cells in SG acini are not well understood, while the involvement of Na/K-ATPase has been suggested based on ouabain's (Na/K-ATPase antagonist) ability to abolish dopamine-induced salivary secretion(Kaufman and Phillips, 1973c; McSwain et al., 1997; Rutti et al., 1980). Consequently, silencing of the Na/K-ATPase gene via RNA interference demonstrated the importance of Na/K-ATPase to tick blood feeding, as it directly affected ticks' oviposition and their successful feeding(Karim et al., 2008). An ultrastructural study visualized rich Na/K-ATPase-like reactions by using a phosphatase cytochemical method in acini type I(Needham et al., 1990).

In this study, we revisited these findings to investigate the roles of Na/K-ATPase in tick salivary secretion. The effects of ouabain on ion compositions and protein secretion in dopamine-induced salivation were examined. We provide evidence supporting the presence of opposing physiological roles of Na/K-ATPase for the absorptive and the excretory functions of acini types I and III, respectively.

Results and Discussion

Molecular characterization of Na/K-ATPase: two alternatively spliced isoforms, expression patterns, and immunolocalization in the salivary glands

Computational annotation of the gene encoding Na/K-ATPase (ISCW002538) was found in Vectorbase (https://www.vectorbase.org). The gene spans a 37,229bp long genomic region, consisting of three contigs in the assembled genome sequence; ABJB010911356, ABJB010845527, and ABJB010956121. However, the ISCW002538 prediction lacked a 5' terminal region, including the untranslated region (UTR) and the start codon. After manual annotation, followed by confirmation via reverse transcriptase (RT)-PCR, we identified an additional 5' exon (exon 1 in Fig. 3-1A) linked to the second exon, which is also corrected for 9 bp shorter than the previous ISCW002538 prediction (exon 2 in Fig. 3-1A). We also identified an alternatively spliced exon, exon 16 (Fig. 3-1A), which encodes 31 amino acid residues that are homologous to exon 17 (Fig. 3-1B). Based on RT-PCR results using exon specific primers for exons 16 and 17, we found that these exons are utilized in a mutually alternative manner. Transcripts containing exon 17 appear to be more abundant in the salivary glands, as is evidenced by relative band strengths in the electrophoresis of RT-PCR products (see Appendix D Fig. S1). In addition, exon 18 is 136 bp longer in the 5' direction than is currently stated in the ISCW002538 prediction. The corrected sequence for Na/K-ATPase was submitted to GenBank with the accession number KU560919 and KU56020. Na/K-ATPase transcript levels were investigated in the SG of females from different feeding stages via quantitative real time RT-PCR (qRT-PCR), revealing a dramatic increase at the onset of feeding, reaching its peak (23-fold increase from the day 1 feeding) at day 4 of feeding, approximately two days before the rapid engorgement phase (Fig. 3-1C). Phylogenetic analysis using the neighbor joining method showed that the single copy Na/K-ATPases in arthropods are all clustered in a monophyletic group (Fig. 3-1D).

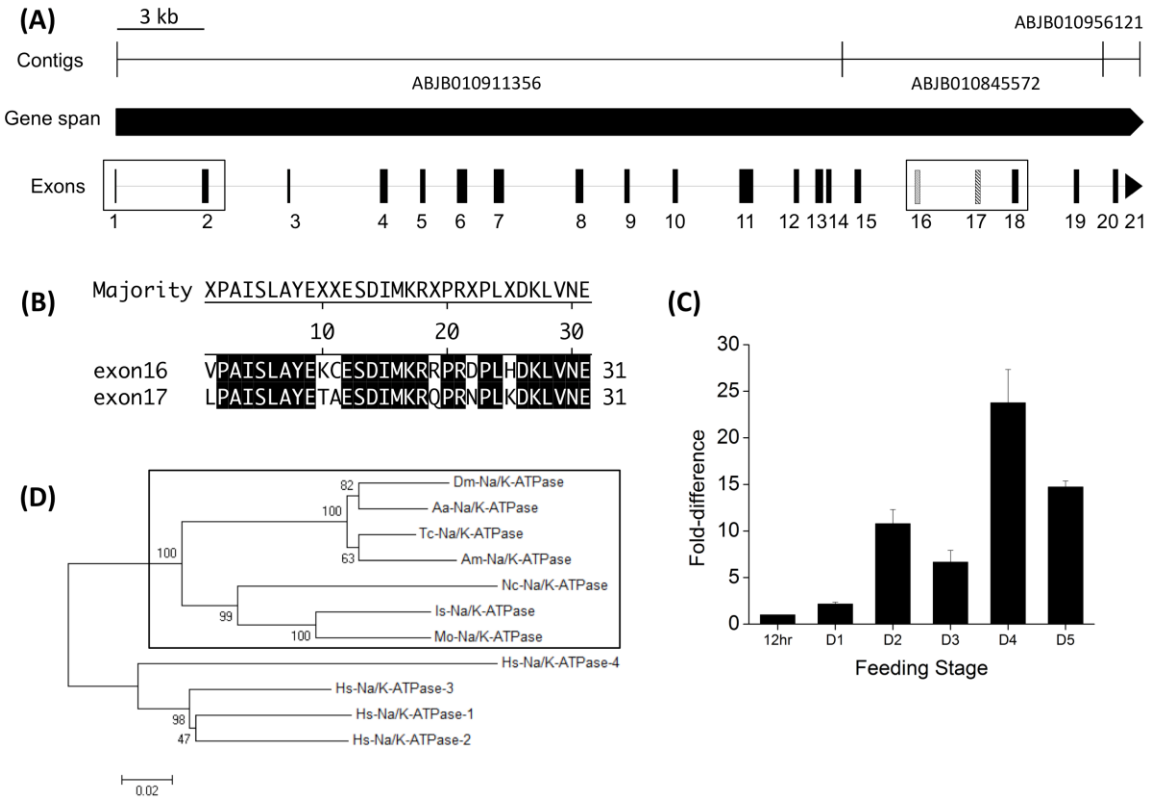

Figure 3-1. Gene structure, phylogeny, and expression profiles of *I. scapularis* Na/K-ATPase.

(A) Gene structure of Na/K-ATPase (ISCW002538) including 21 exons. The two boxes indicate corrected regions of the ISCW002538 as determined by manual annotation and experimental confirmation in the present study. The region of exon 1 and exon 2 (exon1 of ISCW002538) is in the first box. The two mutually alternative exons, exons 16 and 17 are in the second box. (B) Amino acid sequence alignment of exon16 and exon17. Black shades indicate identical amino acid residues. (C) Stage-specific expression profile of Na/K-ATPase, from 12 hrs to 5-days after the onset of feeding. (D) Phylogenetic relationship of Na/K-ATPase including *I. scapularis* Na/K-ATPase. The phylogenetic tree was built using the Neighbor-joining method. The numbers at nodes represent percentage support from 1,000 bootstrap replicates. GenBank Accession numbers: *Metaseiulus occidentali* (XP_003737553.1), *Neoseiulus cucumeris* (AGQ56700.1), *Drosophila melanogaster* (AAF55825.3), *Tribolium castaneum* (XP_008196418.1), *Apis mellifera* (XP_006564225.1), *Aedes aegypti* (XP_001662217.1), and four genes of *Homo sapiens* (NP_000692.2, NP_000693.1, NP_689509.1, and NP_653300.2).

In order to localize Na/K-ATPase in tick SG, a mouse monoclonal antibody (a5) for Na/K-ATPase was utilized. Na/K-ATPase immunoreactivity was present in all three different types of acini (Fig. 3-2A): lamellate cells in type I (Fig. 3-2B), abluminally located epithelial cells (interstitial cells(Fawcett et al., 1981a)) resembling a web-like structure in between granular cells in type II (Fig. 3-2C&E), and epithelial cells (f-cells(Fawcett et al., 1981a)) in type III (Fig. 3-2D&F).

In type I acini (Fig. 3-2B), immunoreactivity reveals a vertical pattern toward the basolateral surface, which agrees with a previous ultrastructural study using a phosphatase cytochemical method for visualization of Na/K-ATPase localization(Needham et al., 1990). The ultrastructural study described that the subcellular location of the staining was on the extensive infolding membrane from the basolateral surface of lamellate cell(Needham et al., 1990). The immunoreactive epithelial cells containing small nuclei in type II acini were located in between granular cells, distinguished by large nuclei, and were also referred to as abluminal interstitial cells(Fawcett et al., 1981a) (Fig. 3-2E). In type III, the staining pattern in the epithelial cells was found broadly toward the periphery of each epithelial cell. This subcellular region is likely the place where extensive membrane folding forms a labyrinth, opening towards the lumen, as previously described in the ultrastructure(Fawcett et al., 1981a) (Fig. 3-2F).

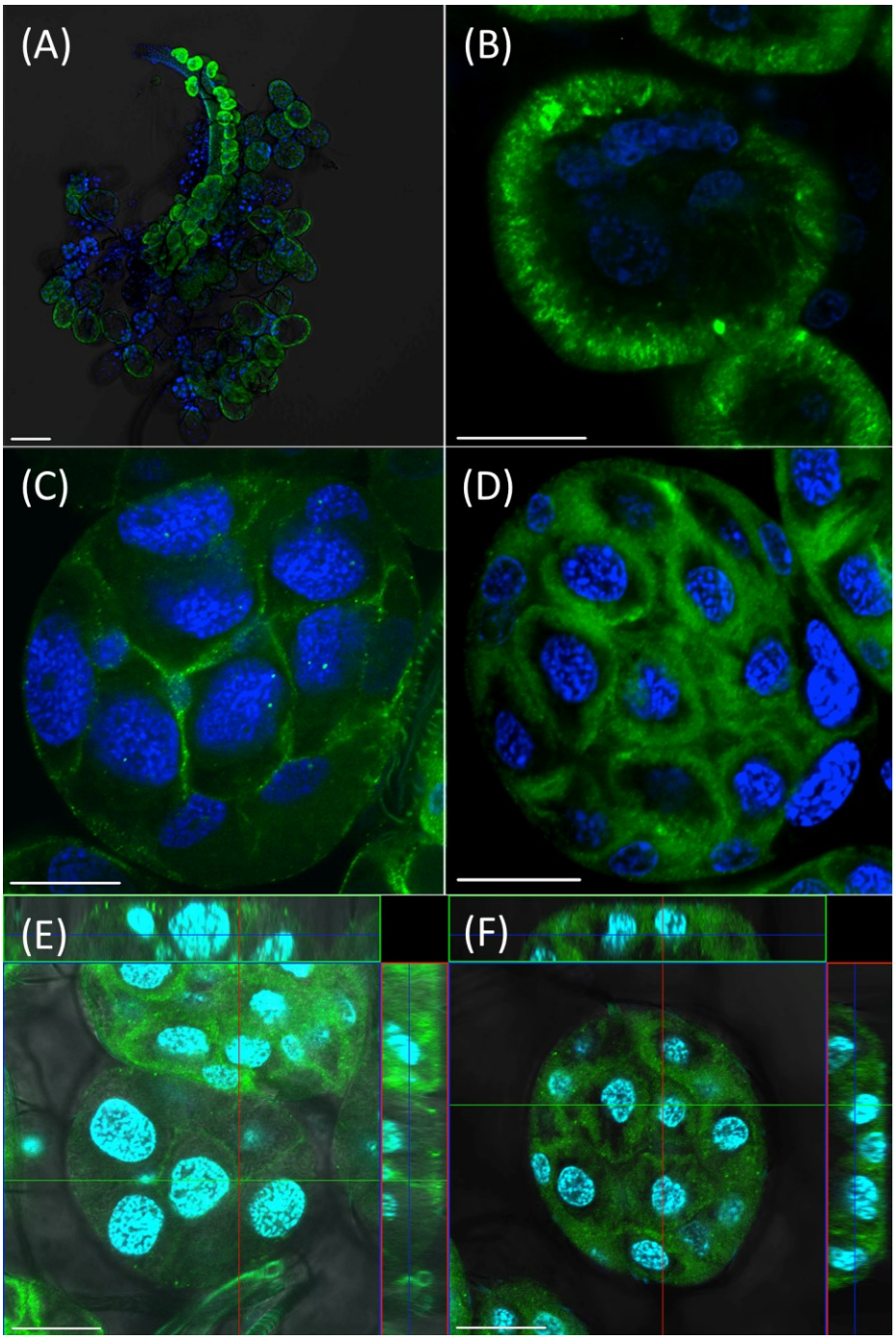

Figure 3-2. Na/K-ATPase immunoreactivity from three types of salivary gland acini (partially engorged female ticks).

(A) Overview of salivary glands at low magnification. (B) Type I acini. (C and E) Type II acini. (D and F) Type III acini. (E and F) Orthoview of type II and type III acini. Positive staining (green) was detected on the epithelial cells of all types of acini from the salivary glands. The blue color shows nuclei stained with DAPI. Scale bars are for 100 µm (A) and 20 µm (B-F).

Inhibitory effect of ouabain on dopamine-induced salivary excretion

A Modified Ramsay's assay(Ramsay, 1954), measuring the amount of salivary secretion from isolated salivary glands, was performed to understand the overall impact of ouabain, a Na/K-ATPase inhibitor, on salivary gland physiology. In general, the rate of dopamine-induced salivary secretion rapidly increased in volume for up to 10 minutes, and then gradually decreased up until 30 minutes, marking the end of observation (Fig. 3-3A). Co-incubations of isolated salivary glands in ouabain and dopamine (10 μmol l^{-1}) were performed using two doses of ouabain (1 and 10 μmol l^{-1}). Ouabain at 1 μmol l^{-1} induced salivary secretion similar to that in the dopamine-only treatment, although the secreted volume was slightly lower than in the dopamine-only treatment. However, the 10 μmol l^{-1} ouabain treatment almost completely inhibited dopamine-induced salivary secretion after 10 minutes (Fig. 3-3A&B). The total volume of secreted saliva after 30 minutes was 1.38 μL (dopamine only), 1.02 μL (1 μmol l^{-1} ouabain with 10 μmol l^{-1} dopamine), and 0.14 μL (10 μmol l^{-1} ouabain with 10 μmol l^{-1} dopamine) (Fig. 3-3C).

Next, we employed an assay method using microscopic observation of individual acini following dopamine treatments in order to understand the roles of Na/K-ATPase(Kim et al., 2014). As previously reported, dopamine (10 μmol l^{-1}) triggers an influx of water/solutes into type III acini, which is evidenced by increasing luminal volume. Additionally, dopamine also induced acini pumping/gating for the discharging of saliva via the acinar duct, as described in a previous study(Kim et al., 2014). Using a fixed dose of dopamine (10 μmol l^{-1}), we tested the effects of ouabain treatments on luminar volume, from 10 nmol l^{-1} to 100 μmol l^{-1}, at 10-fold intervals. Ouabain showed dose-dependent suppression of dopamine induced inward fluid transport (Fig. 3-4A). The percentage volume change of each acinus' lumen (i.e. water-solute influx) was decreased with increasing doses of ouabain up to 1 μmol l^{-1} (Fig. 3-4A). At ouabain levels above 10 μmol l^{-1}, acini dynamics were completely abolished (Fig. 3-4A&B). Additionally, lower doses of ouabain (1 μmol l^{-1}) not only partially inhibited dopamine-induced inward fluid transport (53% of dopamine only treatment), but also inhibited pumping/gating (53% of dopamine only treatment) (Fig. 3-4).

Although earlier studies reported the inhibitory effect of ouabain on catecholamine-induced tick salivary secretion, and also on ATPase activity in the salivary glands(Kaufman et al., 1976; Kaufman and Phillips, 1973c; Qureshi et al., 1991; Rutti et al., 1980), the current study further

elucidates the mechanism by showing that the observed inhibitory activity is directly impacting water/solute influx into the lumen of acini. Additionally, reduced pumping/gating is a likely a consequence of the lack of this influx. Co-existence of Na/K-ATPase and D1 dopamine receptor in the epithelial cells of type II and III acini (this study and Simo et al(Šimo et al., 2011), respectively) suggests that the target of the D1 receptor-mediated intracellular signaling for salivary secretion includes Na/K-ATPase.

Dopamine-induced salivary secretion is orchestrated by two distinct physiological mechanisms: water/solute influx into the lumen via D1 dopamine receptor (D1) and discharging the fluid by pumping/gating via invertebrate-specific D1-like dopamine receptor (InvD1L)(Kim et al., 2014). This study demonstrated that dopamine-induced water/solute influx was completely inhibited by a Na/K-ATPase blocker (ouabain) at levels above 10 μmol l^{-1} (Fig. 3-4A). In addition, inhibition of inward fluid transport in the type III acini by the Na/K-ATPase blocker resulted in reductions of dopamine-induced secretion from isolated salivary glands (Fig. 3-3).

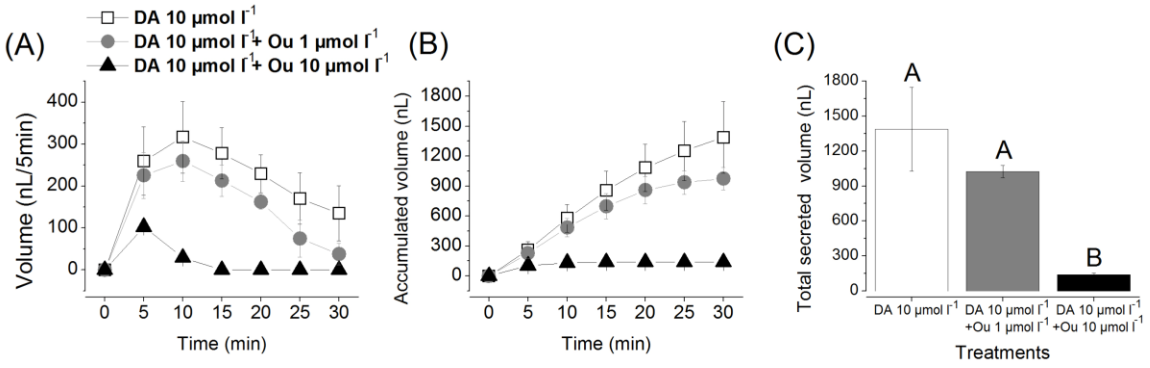

Figure 3-3. Secretory activities of isolated salivary glands by dopamine and ouabain treatments.

(A) The salivary secretion pattern observed over a 30-minute time period following treatments of dopamine (10 µmol l^{-1}) alone (empty box) and dopamine 10 µmol $l^{-1}$with two distinct ouabain (Ou) doses (1 and 10 µmol l^{-1}, grey circle and black triangle, respectively). (B) Accumulated saliva volume over a 30-minute time period after treatments. (C) Total volume of secreted saliva in 30 minutes for each treatment (dopamine, empty column; ouabain 1µmol l^{-1}, grey column; ouabain 10µmol l-1, black column). The bars indicate averages with standard deviations of three replicates. The data were analyzed by an ANOVA-Tukey-Kramer HSD test (p=0.05).

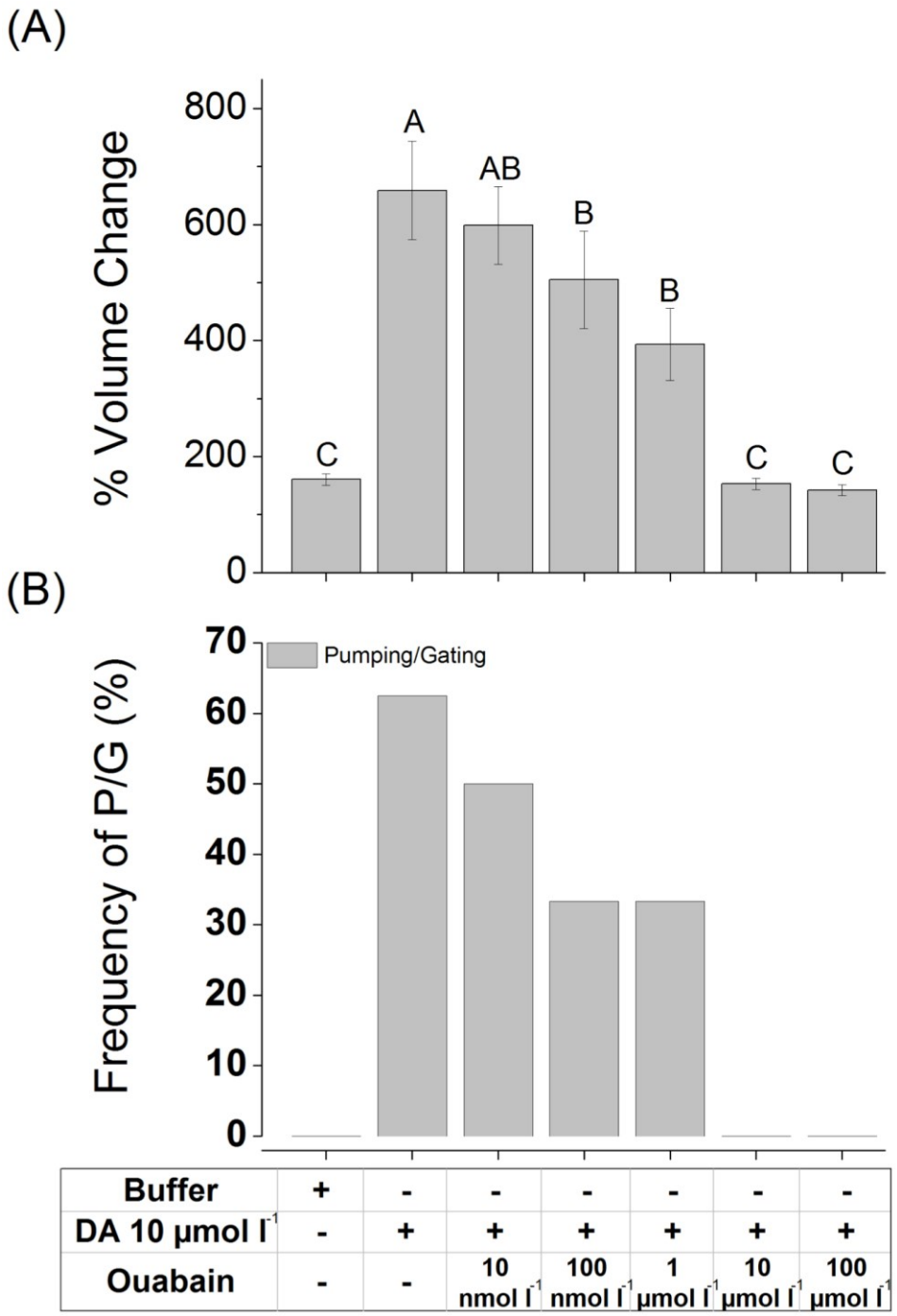

Figure 3-4. Effect of ouabain on dopamine-mediated fluid influx in type III acini.

(A) Percentage increase in acinar volume after various combinatory treatments. (B) Frequencies of acini observed for pumping/gating in each treatment. The data in A are the averages with standard error of mean for at least three biological replicates. The data in B are frequencies in observations of more than six acini for each data point. The data were analyzed by an ANOVA-Tukey-Kramer HSD test (p=0.05).

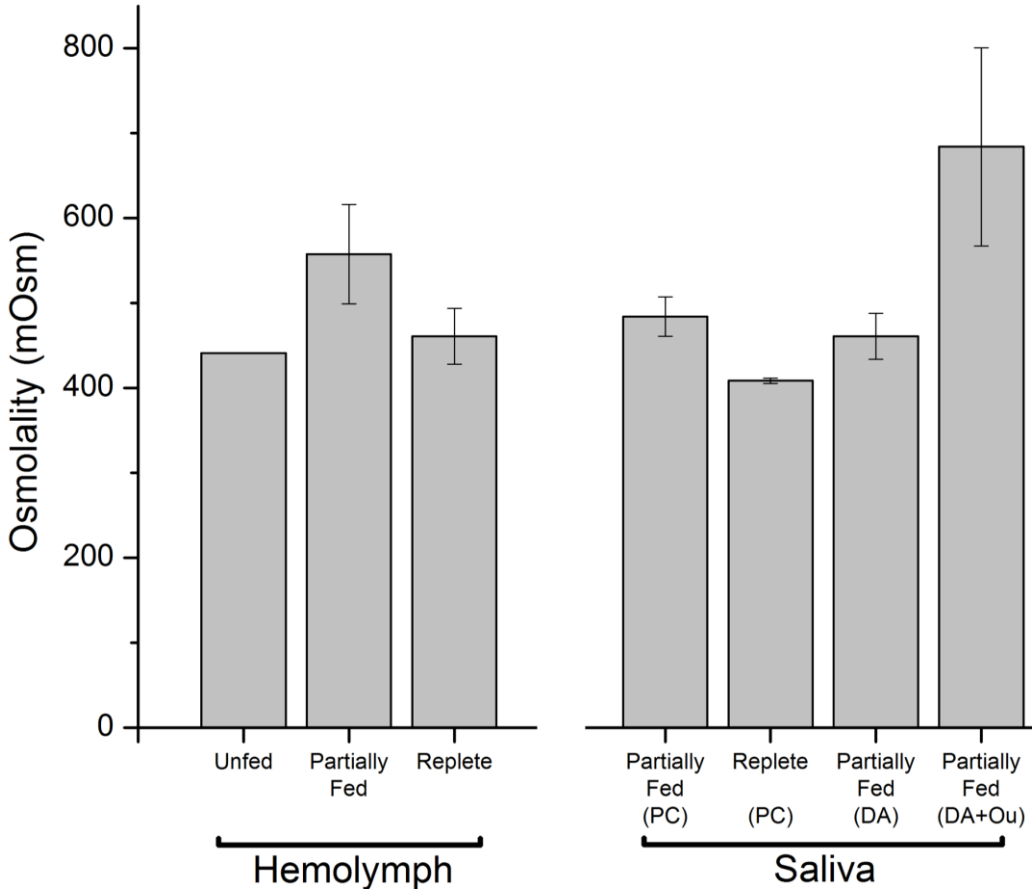

Figure 3-5. Osmolarities of hemolymph and saliva secreted by pilocarpine or dopamine treated ticks.

Hemolymph was collected from three different feeding stages: unfed, partially-fed, and replete. For the collection of saliva, 2 µl of pilocarpine was injected into ticks (partially fed and replete ticks). Saliva collected from dopamine only and dopamine with ouabain were from isolated salivary glands in via the modified Ramsay's assay. DA: dopamine (10 µmol l^{-1}), Ou: ouabain (1 µmol l^{-1}), and PC: pilocarpine (10 mg ml^{-1}).

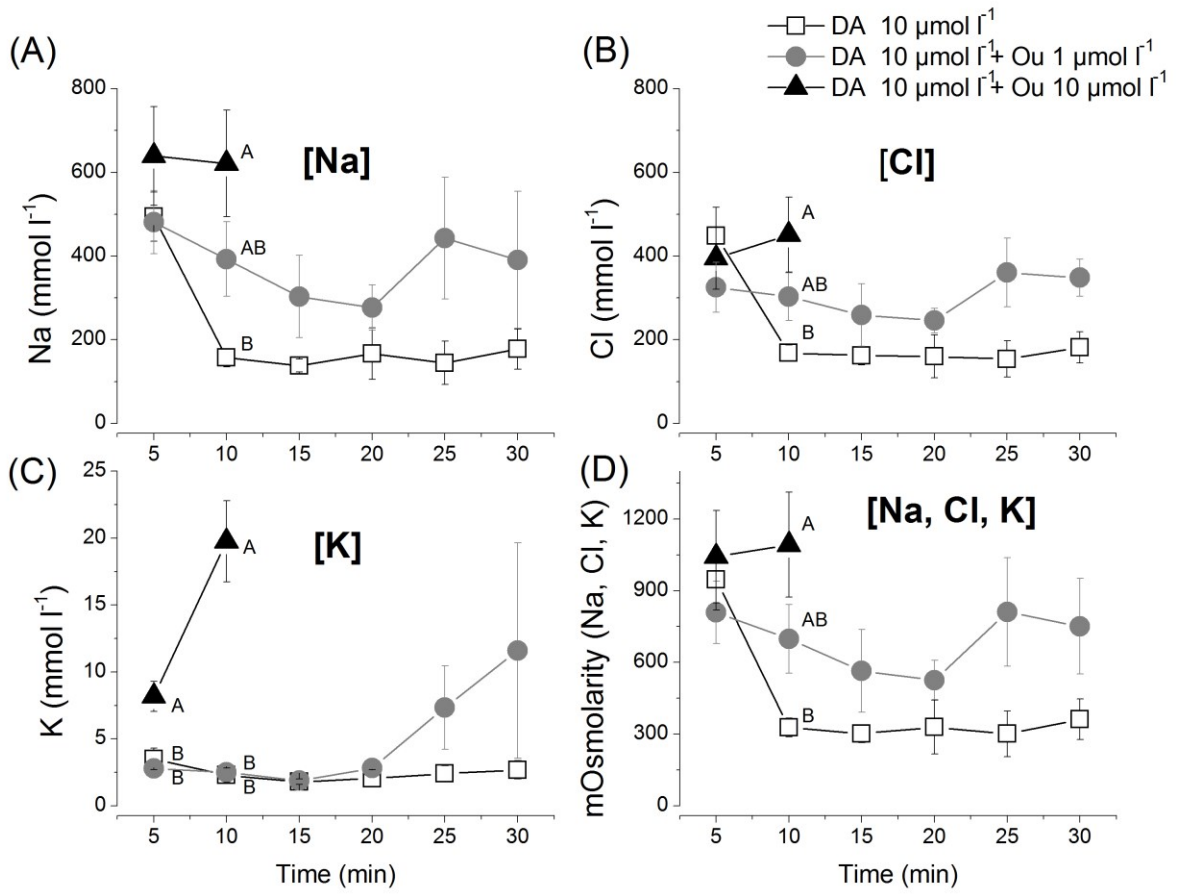

Figure 3-6. Ion composition and osmotic concentration of secreted saliva from isolated salivary glands.

(A-C) The major three ions' (Na^+, Cl^-, K^+) secretion patterns over a 30-minute time period following treatments: dopamine (DA) 10 µmol l^{-1} alone (empty box) and dopamine 10 µmol $l^{-1}$with distinct ouabain (Ou) doses (1 and 10 µmol l^{-1}, grey circle and black triangle). (D) The pattern of total osmotic concentration of three major ions (Na^+, Cl^-, and K^+) in the saliva secreted over a 30 minute time period. SEM/EDS was used to analyze each ion concentration from each time point. Standard curves for each ion (Na^+, Cl^-, and K^+) were generated with NaCl and KCl (see Appendix G Fig. S4). The data were analyzed by an ANOVA-Tukey-Kramer HSD test (p=0.05).

Hyperosmolar dopamine-induced salivary secretion by ouabain

We were interested in the effects of dopamine/ouabain on ion concentrations of the salivary secretion. A pre-treatment baseline was established by measuring the osmotic pressures of hemolymph and saliva in adult *I. scapularis* females. Hemolymph osmotic pressures were 441, 557±82, and 461±46 mOsm (±S.D.) for unfed, partially fed (11-21 mg tick weight after 4 to 5-days feeding), and replete stages, respectively (Fig. 3-5). These values are approximately within the range of the hemolymph osmotic pressure observed in other tick species: 350-400 mOsm in partially fed and replete *I. ricinus*(Campbell et al., 2010), 375-527 mOsm in partially fed *Dermacentor andersoni*(Kaufman and Phillips, 1973a), 360-441 mOsm in unfed and partially fed *Amblyomma americanum (Hsu and Sauer, 1975; Needham et al., 1990)*, and 341.7 mOsm in unfed *Amblyomma variagatum*(Gaede and Knülle, 1997).

The dopamine/pilocarpine-induced salivary secretion from the partially fed *I. scapularis* female SG was determined to be 461-484 mOsm, hyposmotic when compared to the hemolymph osmotic pressure 557 mOsm from the same stage (Fig. 3-5). Saliva collected from the partially fed female injected with 2 µl of pilocarpine (10 mg ml^{-1} in Hank's saline) was 484±40 mOsm (Fig. 3-5). Saliva collected via Ramsay's assay (see section 2) from isolated salivary glands in Hank's saline (~380 mOsm), treated with dopamine, was 461±38 mOsm (Fig. 3-5). For both *in vivo* injections and *in vitro* treatments of isolated SG, saliva was collected for 30 mins following treatment. The hyposmolar salivary secretion in *I. scapularis* was similar to that of partially fed *D. andersoni* (Kaufman and Phillips, 1973a). However, a different pattern was described in a study of partially fed *I. ricinus,* which showed hyperosmolar secretion in the feeding stage(Campbell et al., 2010). In off-host ticks, hyperosmolar salivary secretions have been shown in *A. americanum*(Sauer and Hair, 1986). We speculate that the duration of saliva collection in different experiments may have caused this discrepancy, because we found that early secretion (the first 5 min) after dopamine-only treatment contains highly hyperosmotic saliva (~946 mOsm) (Fig. 3-6D). Therefore, experiments using the saliva collected immediately after the induction of secretion (by pilocarpine or dopamine) may have found hyperosmolar (~<10min) secretion, whereas collection over a longer duration has resulted in hyposmolar saliva.

Salivary secretions collected every 5 mins during the course of the modified Ramsey's assay were subjected to measurement of their ion compositions. The initial analysis of saliva using

scanning electron microscopy/energy dispersive X-ray spectroscopy (SEM-EDS) identified three major ions: Na^+, Cl^-, and K^+. Sodium rich saliva has been described in a number of tick species, including *A. americanum*(Hsu and Sauer, 1975) and *D. andersoni*(Kaufman and Phillips, 1973a). When analyzing changes in the osmotic pressure and ion composition of saliva over the 30 min duration following dopamine treatment, an interesting observation was that the dopamine only treatment induced high osmolar salivary secretion (946 mOsm) in the first 5 min, but lowered afterward. The saliva secreted in the first 5 min might primarily consist of saliva that is already contained within the salivary ducts and the acini lumen at equilibrium and is expelled as a result of a dopamine-induced influx of water/solutes into the acini. Therefore, the saliva at the equilibrium state is likely highly hyperosmolar, but becomes diluted by the subsequent influx of hyposmotic saliva resulting from dopamine treatment.

Ouabain treatments resulting in hyperosmolar dopamine-induced salivary secretion were surprising. The one μmol l^{-1} ouabain treatment showed a mild inhibitory activity on the total volume of salivary secretion (Fig. 3-3C), but resulted in a highly increased osmotic pressure of 684±202 mOsm for the 30 min (1.5-fold of dopamine alone 461±38 mOsm) (Fig. 3-5). In the 30 mins following the combined treatment of dopamine and ouabain, the concentrations of the three major ions, Na^+, Cl^-, and K^+ were all increased in the saliva compared to that of the dopamine-only treatment (Fig. 3-6). Na^+ and Cl^- concentrations were coupled for their fluctuating pattern, while K^+ exhibited an increase in the last 10 min of the 30 min observation period. At a higher dose of ouabain, 10 μmol l^{-1}, which resulted in a very low level of dopamine-induced salivary secretion (Fig. 3-3), saliva collection was possible only for the first two 5 min intervals. These samples were highly rich in Na^+ and Cl^-. The K^+ concentration went up to 19.6 μmol l^{-1} (8.5-fold more than the 2.3 μmol l^{-1} in the dopamine-only treatment at the same time interval) (Fig. 3-6).

The hyperosmotic dopamine-induced salivary secretion from the ouabain treatment provided an opportunity to understand the roles of Na/K-ATPase in salivary secretion. Current results suggest two opposite physiological roles of Na/K-ATPase: ion and water influx into the lumen of type III (and likely also in type II) acini forming the primary saliva, as was shown by the volume increase in type III acini in section 2, and the reabsorption present in type I acini located in the proximal region of the main duct (see more about the reabsorptive function of type I acini in

section 5). Although the experimental results fit well in the general outline of the model, there are a number of questions arising.

The dramatic increases in ion concentrations, accompanied by a slight reduction in dopamine-induced salivary secretion volume, like those noted in the 1 μmol l^{-1} ouabain treatment, demands further explanation for the mechanism disrupting the balance between ion/water secretion and resorption. If similar levels of inhibition for Na/K-ATPase occurred in both type I and type III acini, the saliva should have similar ionic concentrations to that of the saliva induced by dopamine alone. A possible explanation for the disrupted ion balance could be that the Na/K-ATPases in type I acini vs. those in type III acini exhibit differing sensitivities to ouabain. Thus, at the lower dose, the resorption function of type I acini was inhibited, while partial secretory function of type III acini remained for the production of the hyperosmolar primary salivary secretion. Both secretion and resorption functions were almost completely blocked by the higher dose (10 μmol l^{-1}) of ouabain. The different ouabain sensitivities could be attributed to possible differences in accessibility of the targets by ouabain (note the different localizations of immunoreactivity in Fig. 3-2), either due to different cellular subunit composition, or to the possibility that different isoforms of Na/K-ATPase possess different posttranslational modifications.

Finally, what could be the contribution of Na/K-ATPase to the dopamine-mediated hyposmotic salivary secretion? Based on the fact that the higher dose (10 μmol l^{-1}) of ouabain almost completely abolished salivary secretion, the ouabain sensitive Na/K-ATPase must be the major component in dopamine's downstream physiology. The saliva present in the SG prior to dopamine treatment appeared to already be highly hyperosmotic, as inferred from the high osmolarity of saliva secreted in the first 5 min following dopamine treatment (Fig. 3-6). In this case, activation of Na/K-ATPase to form electrochemical gradients may not be necessary for fluid transport across epithelial cell layers, unless Na/K-ATPase is only functioning for the production of a local osmotic gradient in a subcellular region, such as the labyrinth-like structure present in the epithelial cells. Although significant direct contributions of Na/K-ATPase on the electrochemical gradient may occur, based on the high K^+ concentrations in the 10 μmol l^{-1} ouabain treatment, Na/K-ATPase might be involved in dopamine-mediated activation of water channels (aquaporins) as a parallel mechanism in the downstream dopamine pathway, which is also inhibited by ouabain. Changes in ionic strengths, whether directly or indirectly mediated by

Na/K-ATPase activity in the microdomain, would affect aquaporin activity, just as changes in pH have been shown to control aquoaporin(Tournaire-Roux et al., 2003). Regulation of pH in subcellular organelles by Na/K-ATPase has also been reported(Cain et al., 1989).

Na/K-ATPase located in the infolding of apical membranes of epithelial cells in type III acini does not appear to be a common phenomenon, while Na/K-ATPase localization in the basolateral regions for resorptive systems (type I acini) is well documented for the epithelial cells of the mammalian kidney(Giebisch, 1998). In mammalian retinal pigment epithelium cells, apically located Na/K-ATPase is known to be important for pH control by coupling with $Na^+/HCO3^-$ (Strauss, 2005). In addition, the model for insect salivary glands (American cockroach) includes apical Na/K-ATPase in an acinar cell(Just and Walz, 1994), named the p-cell (peripheral cell), functioning for primary saliva production(Hille and Walz, 2008).

The electrochemical gradient formed by the efflux of $3Na^+$ towards the lumen and the counter flow of $2K^+$ in type III acini must be coupled with other machineries for the epithelial physiology: extrusion of K^+ and basolateral influx of Na^+ in the epithelial cells, and the luminal influx of Cl^- and water through transcellular and paracellular routes. Similarly, the resorption function of Na/K-ATPase located on the basolateral infolding of type I acini is likely associated with similar types of machinery, but for the opposite directional flows.

It is worth noting a major difference between Na/K-ATPases in type I and type III acini; the former seems to be dopamine-independent, while the latter is controlled by dopamine. Indeed, a previous study for the localization of dopamine receptors D1 and InvD1L did not find immunoreactivity in the type I acini(Šimo et al., 2014; Šimo et al., 2011), supporting the possibility of dopamine-independent Na/K-ATPase actions.

No activity of dopamine/ouabain for increased amount of protein in the saliva

We expanded our scope to examine the effects of dopamine and ouabain on the secretion of proteins in the saliva. We have established a fluorescent dye-based method for protein quantification from 2 nL samples collected from the modified Ramsay's assay. In order to avoid the potential problem of directly using crude saliva, which may contain unknown components, obscuring the quantification method, we initially calibrated the quantification by comparing the results to those obtained from an Agilent 2200 TapeStation that requires a 2 µL sample of saliva. Samples used for the calibration consisted of saliva collected following the injection of

pilocarpine (10 mg ml^{-1}) and dopamine (10 μmol l^{-1}) into partially fed females (5-days after the onset of feeding, ~ 21mg in the weight). Saliva samples were pooled from two individuals, totaling six pools that were tested both in the Agilent 2200 TapeStation and in the fluorescent dye-based method, and the calibration was made.

In examination of the 5 min interval salivary secretions obtained from the modified Ramsey's assay, we did not find any indication of increased protein secretion from either treatment, dopamine-only or the combination of dopamine and ouabain (1 μmol l^{-1}). Basal protein secretion levels of ~300 μg mL^{-1} protein per 5 min were observed over the 30 min observation period and, like the case of ion concentration, the saliva secreted in the first 5 min contained high amounts of protein (483 μg mL^{-1} and 844 μg mL^{-1}, respectively) (Fig. 3-7), which is likely the salivary contents present in the salivary gland prior to dopamine-induced salivation. Therefore, we conclude that neither dopamine nor ouabain affected the basal protein secretion level up to 30 mins after the pharmacological treatments. Our result did not support the earlier model proposed by Sauer's group(Sauer et al., 2000). In this model, they proposed a sequential activation of dopamine for basolateral secretion of prostaglandin E_2 (PGE_2), which is then responsible for triggering the secretion of salivary proteins, including anticoagulant components(Qian et al., 1998; Sauer et al., 2000; Yuan et al., 2000). Based on this model, increased protein secretion is expected to coincide with increased saliva volume (10 and 15 min after dopamine treatment), which was not observed in our study. We were also unable to find any visible responses of salivary gland acini to PGE_2 (100 μmol l^{-1}) treatment, including vesicular dynamics of type II granular cells (Kim and Park, unpublished data). Further investigation is needed to test the possibility that the dopamine signaling pathway is responsible for maintaining basal levels (~300 μg mL^{-1} $5min^{-1}$) of protein secretion.

Over the course of this study, the results from Agilent 2200 TapeStation analyses of small sample volumes for accurate protein quantification, and the accompanying band patterns in the mini capillary tube, provided an interesting observation unexpectedly. First, we found that the protein amounts of pilocarpine vs. dopamine inductions were not significantly different on the Agilent 2200 TapeStation, supporting that the muscarinic acetylcholine synapse in the central nervous system and SG autocrine dopamine are in the same pathway(Reuben Kaufman, 2010). Second, we found high variations among samples (pools of two individuals) in the protein band patterns of the saliva from approximately similar feeding stages of the same batch of ticks

(Appendix F Fig. S3). A previous study with *R. appendiculatus* also found high variations in the protein band patterns by pooling multiple groups of five individuals (Wang et al., 2001). Future work pushing the sensitivity limit down to the individual level by using advanced techniques may make it possible to shed light on the roles of salivary contributions at the individual level in "feeding aggregation" behavior of ticks.

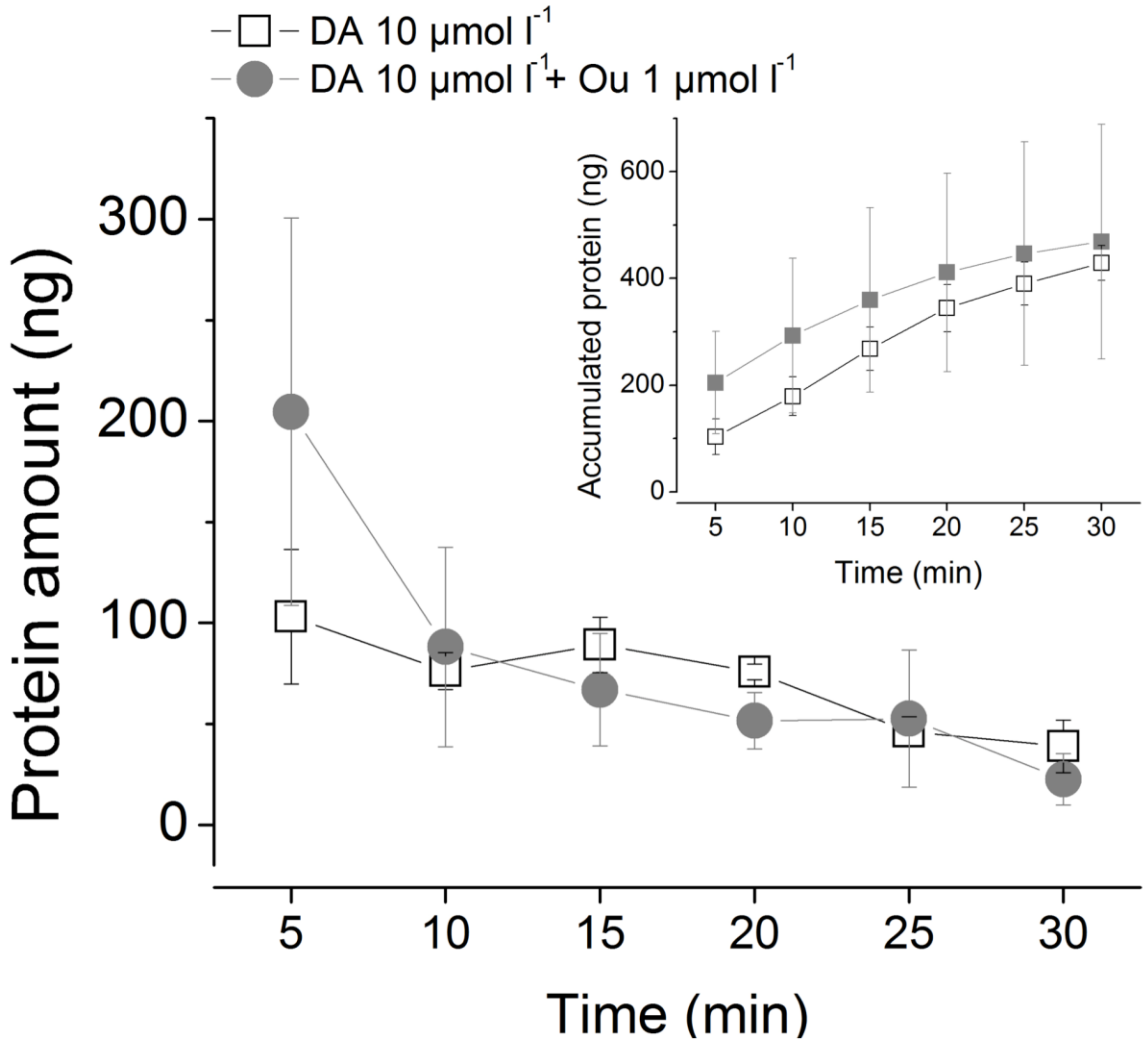

Figure 3-7. Protein quantification of secreted saliva.

Protein secretion over a 30-minute time period following treatments: dopamine (10 µmol l^{-1}) alone (empty box) and dopamine (10 µmol l^{-1}) with ouabain (1 µmol l^{-1}) (grey circle). Inset graph, accumulated protein amounts over 30 minutes after treatments. Values were plotted after conversion by applying value ratio between CBQCA analysis and TapeStation analysis.

Absorptive function of the type I acini

Since the combined treatments of ouabain and dopamine exhibited an increased ion concentration, suggesting the resorptive function of type I acini for ions and water (see section 3), we designed an experiment to test whether type I acini might also have an absorptive function. We employed an assay using dehydrated off-host ticks to identify the route of water absorption. Dehydrated ticks were fed with water containing Rhodamine123 (1 μmol l^{-1}) using a capillary tube on the chelicera. We found that type I acini were the only site where Rhodamine123 was taken up (3/5 individuals) in the salivary glands (Fig. 3-8), while some individuals accumulated Rhodamine123 in both the salivary glands and midgut (2/5) (Fig. 3-8C and see Appendix I Fig. S6). Accumulation of Rhodamine123, which is a commonly used tracer dye for visualizing membrane transport(Forster et al., 2012; Perrière et al., 2007), in the cells of type I acini only indicates the presence of an absorptive function in those cells. This result obtained in unfed ticks is likely applicable to the feeding stage for the resorptive function of type I salivary acini.

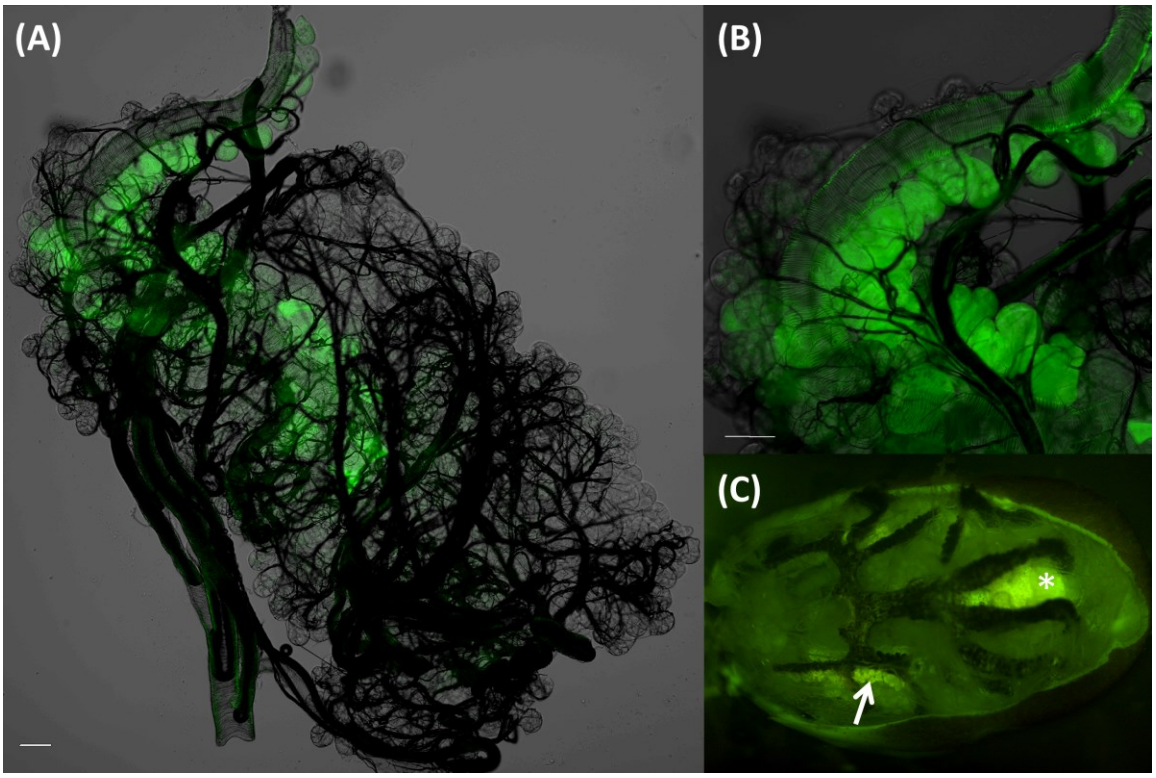

Figure 3-8. Absorptive function of type I acini shown by absorption of Rhodamine 123.

Ticks were dissected to trace the fluorescence after the desiccated tick was offered a drop of water containing Rhodamine 123 (1 mmol l^{-1}) for ~5 hr, (A) Intact salivary glands of unfed tick. (B) Magnified view of type I acini. (C) Overview of fluorescence from whole unfed tick body after the tergum was removed. Arrow in (C) indicates the salivary glands. Asterisk indicates hindgut and rectal sac that is autofluorescent (See Appendix I Fig. S6). Scale bars equal 50 µm.

Conclusion

This study revealed a number of unique features of tick salivary glands, although the current knowledge is far from complete in terms of elucidating the model for epithelial physiology. New discoveries and questions predicated by this study are summarized below.

- The formation of primary saliva in type III and likely also in type II acini is followed by resorption of ions and water in the proximally located type I acini. Filtering functions of excretory organs and the formation of primary excretion, followed by resorption, are commonly found in other arthropods' salivary glands (Gupta and Hall, 1983; Hille and Walz, 2008; Lang and Walz, 2001) and Malpighian tubules(Beyenbach, 1995; O'Donnell and Maddrell, 1995) (kidney of arthropods).
- A major downstream physiology in the dopamine-mediated salivary secretion pathway is the action of Na/K-ATPase in the epithelial cells of type III (and likely also in type II) acini for sodium-rich primary saliva formation, while Na/K-ATPase in type I acini is dopamine-independent for its resorptive function.
- The locations of Na/K-ATPase expression, revealed via immunohistochemistry, indicate that the Na/K-ATPase in type I acini is located in the basolateral infoldings, implying its likely role in Na^+ resorption according to the epithelial model. However, the Na/K-ATPase in type III acini is located in the apical labyrinth-like infolding, implying a Na^+ secretion function. These differing functions of Na/K-ATPase at different locations are similar to the proposed model for salivary secretion of cockroaches(Hille and Walz, 2008). The observed localizations and functions (i.e., hyposmotic salivary secretion) in this study suggest that Na/K-ATPase functions, not only for local electrochemical gradient formation, but also potentially for the activation of the water channel, aquaporin.
- Evidence for an absorptive function of type I acini, which has been suspected in previous studies, is provided via the fluorescent dye experiment in this study. This finding may offer a potential route for the delivery of acaricidal agents into off-host ticks.

Materials and Methods

Ticks and salivary glands

Blacklegged ticks (*Ixodes scapularis*) were purchased from the Tick Rearing Center at Oklahoma State University. Partially engorged female ticks (the weight 12-21 mg, 4-5 days blood fed) were prepared using a modified artificial feeding system (Kröber and Guerin, 2007). Salivary glands were isolated from partially engorged female ticks and pre-incubated in Hank's saline buffer for 1hr. Isolated salivary glands were then examined for the responses of either an individual acinus or whole salivary glands. For immunolocalization, salivary glands were immediately fixed after dissection.

Molecular cloning, manual annotation, and confirmation of isoforms

The sequence data for Na/K-ATPase, ISCW002538, was downloaded from Vectorbase(Giraldo-Calderón et al., 2015) (https://www.vectorbase.org). We made manual annotations by correcting the ISCW002538 sequence based on its homology with other arthropod Na/K-ATPases and determining the translation initiation site prediction via GeneFinder (www.softberry.com). For experimental verification of the mRNA sequence, cDNA was synthesized from total RNA extracted from two pairs of salivary glands of partially fed female ticks using Direct-zol™ RNA miniprep with TRI-Reagent® (Zymo). Salivary gland total RNA (500 ng) served as the template for cDNA synthesis via SuperScript® III Reverse Transcriptase (Invitrogen). Using New England Biolabs (NEB) *Taq* DNA polymerase with ThermolPol® buffer (NEB), RT-PCR was performed to amplify the 5' terminal end of Na/K-ATPase, including the 5' UTR, exon1, exon2, and isoforms -a and –b via different PCR conditions, depending on the regions of the Na/K-ATPase transcript. All primers are provided in table 1. PCR reactions were conducted in 25 µL volumes, including 10X NEB ThermoPol buffer, 0.1 µM each dNTPs, and 0.4 µM of each primer. PCR programs were as follows: for 5' terminal of Na/K-ATPase (95°C for 30 sec, 30 cycles: 95°C for 30 sec, 61°C for 30 sec, 68°C for 90 sec, with a final extension of 5 min at 68°C); for nested PCR of the 5' terminal of Na/K-ATPase (95°C for 30 sec, 35 cycles: 95°C for 30 sec, 60°C for 30 sec, 68°C for 30 sec, with a final extension for 5 min at 68°C); for isoforms -a and –b (95°C for 30 sec, 35 cycles: 95°C for

30 sec, 58°C for 30 sec, 68° for 30 sec, with a final extension of 5 min at 68°C). For amplification of the region from exon15 to exon19, a high fidelity enzyme, PrimeSTAR® HS DNA polymerase (TAKARA), was used. PCR products were subsequently purified and cloned into the pGEM®-T Easy vector (Promega) and sequenced.

In order to distinguish between isoform-a and isoform-b, PCR products of each isoform were digested with a specific restriction enzyme (BstXI), which digested only isoform-b but not isoform-a (see Appendix D Fig. S1). After restriction enzyme digestion, products were run on a 1% agarose gel for confirmation.

Table 3-1. Primer information

Purpose for primers	Primers (5' to 3')
5' terminal forward primer	CTTGAGGTGGCGGTGCAG
5' terminal reverse primer	GATGGCATACTGTGGAACCATG
5' terminal nested forward primer	GACGCAGCCCTAGTGCGTG
5' terminal nested reverse primer	CAATCCACAGTAGTAAGGAGAAC
Exon15-19 specific forward primer	CTGGAATATACCTGCCATAC
Exon15-19 specific reverse primer	GTATGGCAGGTATATTCCAG
Isoform-a specific reverse primer	TCAGCGGGTTCCGGGGCTGA
Isoform-b specific reverse primer	GAAGGGGATCGCGCGGTCTT
qPCR-Na/K-ATPase forward primer	AGACATGCTGCCTGCTATTTC
qPCR-Na/K-ATPase reverse primer	CGTTCACCAGTTTGTCCTTC
qPCR-RPS4 forward primer	GGTGAAGAAGATTGTCAAGCAGAG
qPCR-RPS4 reverse primer	TGAAGCCAGCAGGGTAGTTTG

Phylogenetic analysis

Using MEGA6[61], a phylogenetic tree was constructed using the neighbor joining method, with 1000 bootstrap replicates (Figure 1D). The deduced amino acid sequence of *I. scapularis* Na/K-ATPase were analyzed via multiple sequence alignment with other Na/K-ATPase genes of,

not only *Homo sapiens,* but also other arthropods: *Metaseiulus occidentali*, *Neoseiulus cucumeris*, *Drosophila melanogaster*, *Tribolium castaneum*, *Apis mellifera*, and *Aedes aegypti*.

Quantitative RT-PCR

To obtain a stage-specific expression profile of the Na/K-ATPase transcript, total RNA was extracted from three pairs of salivary glands of ticks at each of six different feeding stages (12 hrs, 1 day, 2 days, 3 days, 4 days, and 5 days after feeding) via Direct-zol™ RNA miniprep with TRI-Reagent® (Zymo). Subsequently, the salivary gland total RNAs (500ng) served as templates for cDNA synthesis using SuperScript® III Reverse Transcriptase (Invitrogen). qRT-PCR experiments were performed using SYBR Select Master Mix (Applied Biosystems) in a CFX Connect (Bio-Rad) thermal cycler on a 96-well plate with optical sealing tape. All reactions were carried out in duplicate, in 10 µl volumes. Na/K-ATPase quantification was performed using primers targeting a 98-bp fragment of the Na/K-ATPase transcript (F: 5'-AGACATGCTGCCTGCTATTTC-3'; R: 5'CGTTCACCAGTTTGTCCTTC-3'), while a 174-bp fragment (Primers: F: 5'-GGTGAAGAAGATTGTCAAGCAGAG-3'; R: 5'-TGAAGCCAGCAGGGTAGTTTG-3') of the *I. scapularis* gene, Ribosomal Protein S4 (RPS4, GenBank Accession No. DQ066214), served as an internal reference gene(Koči et al., 2013). Quantification of Na/K-ATPase expression levels was calculated via the ΔΔCt method. Transcript levels are expressed as the fold difference, relative to the expression levels exhibited by salivary glands from the 12 hr time point, where error bars represent the experimental variation among technical replicates.

Immunolocalization of Na/K-ATPase

To localize *I. scapularis* Na/K-ATPase, a mouse monoclonal antibody (a5) against chicken Na/K-ATPase(Takeyasu et al., 1988) was purchased from the Developmental Studies Hybridoma Bank at the University of Iowa, IA, USA. Partially engorged female ticks were dissected in Hank's saline buffer and then fixed in Bouin's solution (37% formaldehyde and saturated solution of picric acid 1:3) at 4°C for 2 days. Fixed salivary glands were washed with PBS containing 1% Triton X-100 (PBST). After incubation with 5% normal goat serum (Jackson ImmunoResearch) for 20 minutes, the tissue was incubated with the a5 antibody at 4°C for 2

days. Following primary antibody incubation, tissues were washed with PBST and subsequently incubated with a goat-anti-mouse IgG antibody, conjugated with Alexa Fluor 488 (Molecular Probes), overnight at 4°C. Tissues were then washed with PBST, incubated in 300 nM 4',6'-diamino-2-phenylindole (DAPI, Sigma) for 5 minutes, and then mounted in glycerol. Images were captured with a confocal microscope (Zeiss LSM 700).

Assay measuring the responses of individual type III acinus

All details were described in a previous study(Kim et al., 2014). Briefly, dissected salivary glands were pre-incubated in Hank's saline buffer for ~1 hr. Pharmacological agents were then applied into either individual acini. Dynamic changes of acini were video recorded and analyzed by measuring the radius of individual acini. The acini volume change and frequency of pumping/gating were analyzed every 2 minutes for a total of 30 mins.

Modified Ramsay's assay and collection of salivary secretion

Secreted saliva from isolated intact salivary glands was collected and quantified via Nanoliter2000 (WPI) every 5 mins for 30 mins. Secreted saliva was spotted into a layer of heavy mineral oil on a slide glass and stored at -80°C for the further analysis. Dopamine (Sigma) and ouabain (LC Laboratory) were purchased and used for pharmacological assays.

Protein quantification of secreted saliva

To quantify protein amounts in secreted saliva, a modified CBQCA protein quantification method (Invitrogen) was established, due to the limited volume of secreted saliva, which was at the tens of nanoliter level for each sampling point. A Nanoliter2000 (WPI) was used to spot drops of both protein standards (bovine serum albumin, BSA) and secreted saliva onto a slide glass, which was covered by heavy mineral oil to prevent evaporation. Next, the same volume of reaction mixture (0.1M sodium borate (2): KCN (1): CBQCA (2)) was added into the saliva drops. Following a 1-hour incubation of reactions in the dark, images of each nanoliter drop were captured using a CoolSnap ES2 CCD camera (Photometrics). Two factors were used for the calibration of protein amounts: Serial dilutions of BSA (0, 0.5, 1, 2, and 4 mg ml^{-1}; see Appendix E Fig. S2) and tick saliva from a partially fed tick whose secretion was induced by

pilocarpine or dopamine. A protein standard curve was obtained from the tested concentrations of BSA. Since the tick saliva contains non-protein components, causing over estimation of protein amounts in the tick saliva, we corrected the estimated quantity using the quantity measured in the Agilent 2200 TapeStation (Agilent Technologies, see Appendix F Fig. S3). Therefore, the protein quantification method measured only the concentration of proteins larger than 10 kDa.

Measurement of major ions (Na^+, Cl^-, and K^+) in secreted saliva

Secreted saliva was analyzed to obtain elemental composition and concentrations via scanning electron microscopy (SEM)/energy-dispersive X-ray spectroscopy (EDS) with a silicon drift detector (SDD), which allowed us to overcome the limitation of small volumes of saliva. Using a Nanoliter2000 (WPI) 2 nl of saliva was spotted onto the silicon wafer grid substrate (Pelcotec^{TM}) (see Appendix H Fig S5), which was dried and kept at room temperature until analysis. A Nova NanoSEM 430 (FEI Company) equipped with EDS (Oxford Instruments) was used to image and analyze each dried saliva spot, and INCA software version 4.15 (Oxford Instruments) provided elemental values as weight percentages and atomic percentages. The value of the substrate silicon was used as an internal control or background. To get a standard curve for each element (Na^+, Cl^-, and K^+), NaCl (Fisher Scientific) and KCl (Fisher Scientific) were spotted onto the silicon substrate with differing concentrations: NaCl (10, 50, 100, 200, 400, 600 and 800 mmol l^{-1}) and KCl (2, 4, 8, 16, 32, 64, and 100 mmol l^{-1}). The standard curves for each ion were generated based on atomic % values of each concentration (see Appendix G Fig S4 and Appendix H Fig. S5). The osmotic concentrations of secreted saliva were also measured by osmometer (5100B Vapor pressure osmometer, Wescor, Inc.). The differences in the rates of osmotic concentrations between SEM/EDS and osmometer were applied to convert the finalized values for ion osmotic concentrations (Fig. 3-6).

Rhodamine123 and water ingestion into dehydrated unfed female ticks

In order to dehydrate unfed female ticks, unfed ticks were placed in an incubator with 25% relative humidity (RH) for 12 hours. Rhodamine123 (Sigma) 1 mmol l^{-1} or water filled 1µL micropipettes (Drummond) were then placed onto the mouthparts (chelicera) of dehydrated

unfed female ticks. Ticks were then placed into rehydration conditions (RH 98%) for 5 hours. After ingestion of Rhodamine123 or water, salivary glands were dissected, fixed in 4% formaldehyde at room temperature for 1 hour, washed in PBST (1% Triton X-100), and imaged on a confocal microscope (Zeiss LSM 700).

References

Beyenbach, K. W. (1995). Mechanism and regulation of electrolyte transport in Malpighian tubules. *J. Insect Physiol.* **41**, 197-207.

Bowman, A. S., Dillwith, J. W. and Sauer, J. R. (1996). Tick salivary prostaglandins: Presence, origin and significance. *Parasitol. Today* **12**, 388-96.

Bowman, A. S., Gengler, C. L., Surdick, M. R., Zhu, K., Essenberg, R. C., Sauer, J. R. and Dillwith, J. W. (1997). A novel phospholipase A2 activity in saliva of the lone star tick, Amblyomma americanum (L.). *Exp. Parasitol.* **87**, 121-32.

Cain, C. C., Sipe, D. M. and Murphy, R. F. (1989). Regulation of endocytic pH by the Na+,K+-ATPase in living cells. *Proc. Natl. Acad. Sci. U. S. A.* **86**, 544-548.

Campbell, E. M., Burdin, M., Hoppler, S. and Bowman, A. S. (2010). Role of an aquaporin in the sheep tick Ixodes ricinus: Assessment as a potential control target. *Int. J. Parasitol.* **40**, 15-23.

Coons, L. B., Lessman, C. A., Ward, M. W., Berg, R. H. and Lamoreaux, W. J. (1994). Evidence of a myoepithelial cell in tick salivary glands. *Int. J. Parasitol.* **24**, 551-62.

Coons, L. B. and Roshdy, M. A. (1973). Fine Structure of the Salivary Glands of Unfed Male Dermacentor variabilis (Say) (Ixodoidea: Ixodidae). *J. Parasitol.* **59**, 900-912.

Fawcett, D. W., Doxsey, S. and Büscher, G. (1981a). Salivary gland of the tick vector (R. appendiculatus) of East Coast fever. I. Ultrastructure of the type III acinus. *Tissue Cell* **13**, 209-230.

Fawcett, D. W., Doxsey, S. and Büscher, G. (1981b). Salivary gland of the tick vector (R. appendiculatus) of East Coast fever. II. Cellular basis for fluid secretion in the type III acinus. *Tissue Cell* **13**, 231-253.

Forster, S., Thumser, A. E., Hood, S. R. and Plant, N. (2012). Characterization of Rhodamine-123 as a Tracer Dye for Use In *In vitro* Drug Transport Assays. *PLoS One* **7**, e33253.

Francischetti, I. M., Sa-Nunes, A., Mans, B. J., Santos, I. M. and Ribeiro, J. M. (2009). The role of saliva in tick feeding. *Front. Biosci.* **14**, 2051-88.

Gaede, K. and Knülle, W. (1997). On the mechanism of water vapour sorption from unsaturated atmospheres by ticks. *J. Exp. Biol.* **200**, 1491-8.

Giebisch, G. (1998). Renal potassium transport: mechanisms and regulation. *Am. J. Physiol. Renal Physiol.* **274**, F817-F833.

Giraldo-Calderón, G. I., Emrich, S. J., MacCallum, R. M., Maslen, G., Dialynas, E., Topalis, P., Ho, N., Gesing, S., Consortium, t. V., Madey, G. et al. (2015). VectorBase: an updated bioinformatics resource for invertebrate vectors and other organisms related with human diseases. *Nucleic Acids Res.* **43**, D707-D713.

Gupta, B. L. and Hall, T. A. (1983). Ionic distribution in dopamine-stimulated NaCl fluid-secreting cockroach salivary glands. *Am. J. Physiol.* **244**, R176-86.

Hille, C. and Walz, B. (2008). Characterisation of neurotransmitter-induced electrolyte transport in cockroach salivary glands by intracellular Ca2+, Na+ and pH measurements in duct cells. *J. Exp. Biol.* **211**, 568-576.

Hsu, M. H. and Sauer, J. R. (1975). Ion and water balance in the feeding lone star tick. *Comp. Biochem. Physiol. A Comp. Physiol.* **52**, 269-76.

Just, F. and Walz, B. (1994). Immunocytochemical localization of Na+/K+-ATPase and V-H+-ATPase in the salivary glands of the cockroach, Periplaneta americana. *Cell Tissue Res.* **278**, 161-170.
Karim, S., Kenny, B., Troiano, E. and Mather, T. (2008). RNAi-mediated gene silencing in tick synganglia: A proof of concept study. *BMC Biotechnol.* **8**, 30.
Kaufman, W. R. (1976). The influence of various factors on fluid secretion by in vitro salivary glands of ixodid Ticks. *J. Exp. Biol.* **64**, 727-742.
Kaufman, W. R. (1977). The influence of adrenergic agonists and their antagonists on isolated salivary glands of ixodid ticks. *Eur. J. Pharmacol.* **45**, 61-8.
Kaufman, W. R. (1978). Actions of some transmitters and their antagonists on salivary secretion in a tick. *Am. J. Physiol.* **235**, R76-81.
Kaufman, W. R. (2007). Gluttony and sex in female ixodid ticks: How do they compare to other blood-sucking arthropods? *J. Insect Physiol.* **53**, 264-273.
Kaufman, W. R., Diehl, P. A. and Aeschlimann, A. A. (1976). Na, K-ATPase in the salivary gland of the ixodid tick Amblyomma hebraeum (Koch) and its relation to the process of fluid secretion. *Experientia* **32**, 986-7.
Kaufman, W. R. and Phillips, J. E. (1973a). Ion and Water-Balance in Ixodid Tick Dermacentor-Andersoni .1. Routes of Ion and Water Excretion. *J. Exp. Biol.* **58**, 523-536.
Kaufman, W. R. and Phillips, J. E. (1973b). Ion and Water-Balance in Ixodid Tick Dermacentor-Andersoni .2. Mechanism and Control of Salivary Secretion. *J. Exp. Biol.* **58**, 537-547.
Kaufman, W. R. and Phillips, J. E. (1973c). Ion and Water-Balance in Ixodid Tick Dermacentor-Andersoni .3. Influence of Monovalent Ions and Osmotic Pressure on Salivary Secretion. *J. Exp. Biol.* **58**, 549-564.
Kaufman, W. R. and Wong, D. L. (1983). Evidence for multiple receptors mediating fluid secretion in salivary glands of ticks. *Eur. J. Pharmacol.* **87**, 43-52.
Kim, D., Šimo, L. and Park, Y. (2014). Orchestration of salivary secretion mediated by two different dopamine receptors in the blacklegged tick Ixodes scapularis. *J. Exp. Biol.* **217**, 3656-3663.
Koči, J., Šimo, L. and Park, Y. (2013). Validation of Internal Reference Genes for Real-Time Quantitative Polymerase Chain Reaction Studies in the Tick, Ixodes scapularis (Acari: Ixodidae). *J. Med. Entomol.* **50**, 79-84.
Koči, J., Šimo, L. and Park, Y. (2014). Autocrine/paracrine dopamine in the salivary glands of the blacklegged tick Ixodes scapularis. *J. Insect Physiol.*
Kröber, T. and Guerin, P. (2007). The tick blood meal: from a living animal or from a silicone membrane? *ALTEX* **24**, 39-41.
Krolak, J. M., Ownby, C. L. and Sauer, J. R. (1982). Alveolar structure of salivary glands of the lone star tick, Amblyomma americanum (L.): unfed females. *J. Parasitol.* **68**, 61-82.
Lang, I. and Walz, B. (2001). Dopamine-induced epithelial K+ and Na+ movements in the salivary ducts of Periplaneta americana. *J. Insect Physiol.* **47**, 465-474.
McSwain, J. L., Luo, C., deSilva, G. A., Palmer, M. J., Tucker, J. S., Sauer, J. R. and Essenberg, R. C. (1997). Cloning and sequence of a gene for a homologue of the C subunit of the V-ATPase from the salivary gland of the tick Amblyomma americanum (L). *Insect Mol. Biol.* **6**, 67-76.

Needham, G., Rosell, R. and Greenwald, L. (1990). Ultrastructure of type-I salivary-gland acini in four species of ticks and the influence of hydration states on the type-I acini ofAmblyomma americanum. *Exp. Appl. Acarol.* **10**, 83-104.
Needham, G. R. and Pannabecker, T. L. (1983). Effects of Octopamine, Chlordimeform, and Demethylchlordimeform on Amine-Controlled Tick Salivary-Glands Isolated from Feeding Amblyomma-Americanum (L). *Pestic. Biochem. Physiol.* **19**, 133-140.
Needham, G. R. and Sauer, J. R. (1975). Control of fluid secretion by isolated salivary glands of the lone star tick. *J. Insect Physiol.* **21**, 1893-8.
Nuttall, P. A., Trimnell, A. R., Kazimirova, M. and Labuda, M. (2006). Exposed and concealed antigens as vaccine targets for controlling ticks and tick-borne diseases. *Parasite Immunol.* **28**, 155-63.
O'Donnell, M. J. and Maddrell, S. H. (1995). Fluid reabsorption and ion transport by the lower Malpighian tubules of adult female Drosophila. *J. Exp. Biol.* **198**, 1647-53.
Perrière, N., Yousif, S., Cazaubon, S., Chaverot, N., Bourasset, F., Cisternino, S., Declèves, X., Hori, S., Terasaki, T., Deli, M. et al. (2007). A functional in vitro model of rat blood–brain barrier for molecular analysis of efflux transporters. *Brain Res.* **1150**, 1-13.
Qian, Y., Yuan, J., Essenberg, R. C., Bowman, A. S., Shook, A. L., Dillwith, J. W. and Sauer, J. R. (1998). Prostaglandin E2 in the salivary glands of the female tick, Amblyomma americanum (L.): calcium mobilization and exocytosis. *Insect Biochem. Mol. Biol.* **28**, 221-8.
Qureshi, A. E., Roddy, C. W., Mumma, R. A., Essenberg, R. C. and Sauer, J. R. (1991). Cyclic AMP and calcium modulated ATPase activity in the salivary glands of the lone star tick Amblyomma americanum (L.). *Insect Biochem.* **21**, 399-405.
Ramsay, J. A. (1954). Active Transport of Water by the Malpighian Tubules of the Stick Insect, Dixippus Morosus (Orthoptera, Phasmidae). *J. Exp. Biol.* **31**, 104-113.
Reuben Kaufman, W. (2010). Ticks: Physiological aspects with implications for pathogen transmission. *Ticks Tick Borne Dis.* **1**, 11-22.
Ribeiro, J. M. (1987). Role of saliva in blood-feeding by arthropods. *Annu. Rev. Entomol.* **32**, 463-78.
Ribeiro, J. M. (1989). Role of saliva in tick/host interactions. *Exp. Appl. Acarol.* **7**, 15-20.
Rudolph, D. and Knulle, W. (1974). Site and mechanism of water vapour uptake from the atmosphere in ixodid ticks. *Nature* **249**, 84-85.
Rutti, B., Schlunegger, B., Kaufman, W. and Aeschlimann, A. (1980). Properties of Na, K-ATPase from the salivary glands of the ixodid tick Amblyomma hebraeum. *Can. J. Zool.* **58**, 1052-9.
Sauer, J. R., Essenberg, R. C. and Bowman, A. S. (2000). Salivary glands in ixodid ticks: control and mechanism of secretion. *J. Insect Physiol.* **46**, 1069-1078.
Sauer, J. R. and Hair, J. A. (1986). Morphology, physiology, and behavioral biology of ticks: Ellis Horwood limited.
Šimo, L., Koči, J., Kim, D. and Park, Y. (2014). Invertebrate specific D1-like dopamine receptor in control of salivary glands in the black-legged tick Ixodes scapularis. *J. Comp. Neurol.* **522**, 2038-2052.
Šimo, L., Koči, J. and Park, Y. (2013). Receptors for the neuropeptides, myoinhibitory peptide and SIFamide, in control of the salivary glands of the blacklegged tick Ixodes scapularis. *Insect Biochem. Mol. Biol.* **43**, 376-387.
Šimo, L., Koci, J., Zitnan, D. and Park, Y. (2011). Evidence for D1 dopamine receptor activation by a paracrine signal of dopamine in tick salivary glands. *PLoS One* **6**, e16158.

Strauss, O. (2005). The Retinal Pigment Epithelium in Visual Function. *Physiol. Rev.* **85**, 845-881.
Takeyasu, K., Tamkun, M. M., Renaud, K. J. and Fambrough, D. M. (1988). Ouabain-sensitive (Na+ + K+)-ATPase activity expressed in mouse L cells by transfection with DNA encoding the alpha-subunit of an avian sodium pump. *J Biol Chem* **263**, 4347-54.
Tatchell, R. J. (1967). Salivary Secretion in the Cattle Tick as a Means of Water Elimination. *Nature* **213**, 940-941.
Tournaire-Roux, C., Sutka, M., Javot, H., Gout, E., Gerbeau, P., Luu, D.-T., Bligny, R. and Maurel, C. (2003). Cytosolic pH regulates root water transport during anoxic stress through gating of aquaporins. *Nature* **425**, 393-397.
Wang, H., Kaufman, W. R., Cui, W. W. and Nuttall, P. A. (2001). Molecular individuality and adaptation of the tick Rhipicephalus appendiculatus in changed feeding environments. *Med. Vet. Entomol.* **15**, 403-412.
Yuan, J., Bowman, A. S., Aljamali, M., Payne, M. R., Tucker, J. S., Dillwith, J. W., Essenberg, R. C. and Sauer, J. R. (2000). Prostaglandin E(2)-stimulated secretion of protein in the salivary glands of the lone star tick via a phosphoinositide signaling pathway. *Insect Biochem. Mol. Biol.* **30**, 1099-106.

Chapter 4 - Transcriptome of the lone star tick, *Amblyomma americanum*, revealing molecular interactions between the vector and the pathogen, *Ehrlichia chaffeensis*

Abstract

The lone star tick, *Amblyomma americanum*, is an obligatory ectoparasite of many vertebrates and the primary vector of *Erhlichia chaffeensis*, the causative agent of human monocytic ehrlichiosis. This study aimed to investigate the comparative transcripts of *A. americanum* underlying the processes of pathogen acquisition and of immunity towards the pathogen. Differential expressions (DE) of the transcripts in six different libraries were compared: adult females or males at the transmissive feeding stage following nymphal infestation by feeding on *Erhlichia*-infected white-tailed deer (infected female and male, If and Im), those that are *Erhlichia*-free (uninfected females or males, Uf and Um), and those that were not exposed to the pathogen (non-exposed females or males, NEf and NEm). Trinity assembly pipeline produced 140,574 transcripts from trimmed and filtered raw sequence reads (about 117M reads). The Gold-transcript set of the transcriptome data was established in order to minimize noise by retaining only transcripts homologous to official peptide sets of *Ixodes scapularis* and *A. americanum* ESTs, and transcripts covered with high enough frequency from the raw data. Comparison of the gene ontology (GO) term enrichment data for the six groups tested here revealed an upregulation of genes for defense responses against the pathogen and for the supply of intracellular Ca^{++} for pathogen proliferation in the pathogen-exposed ticks. Analyses of DE, focused on functional subcategories including immune, sialome, neuropeptides, and GPCRs, revealed that *E. chaffeensis*-exposed ticks exhibited an upregulation of transcripts involved in the IMD pathway, antimicrobial peptides, lysozyme, kunitz, insulin-like peptide, and bursicon receptor, while transcripts for metalloprotease were down regulated in general. This study found that ticks exhibit enhanced expression of genes responsible for defense against *E. chaffeensis*, while the pathogen may also modulate tick gene expression in order to facilitate invasion of tick cells and increase the likelihood of future transmission into mammalian hosts.

Introduction

The lone star tick, *Amblyomma americanum*, is the primary vector of the pathogen *Ehrlichia chaffeensis,* the causative agent of human monocytic ehrlichiosis. This species of tick has a large geographic distribution, spanning nearly the entire eastern half of the United States. *A. americanum* is also known to transmit southern tick-associated rash illness (STARI) (Anderson et al., 1993; James et al., 2001). The processes of pathogen acquisition and transmission in ticks have been recognized as important areas of study, which aim to develop and provide potential tool(s) for the disruption of pathogen transmission, such as a transmission blocking vaccine (Richardson et al., 1993).

Ticks acquire *E. chaffeensis*, a Rickettsiales bacteria, during larval and nymphal feedings on infected vertebrate reservoirs, such as white-tailed deer, and later transmit the pathogens to other vertebrate hosts, including humans, during subsequent feedings (Ewing et al., 1995). Although *A. americanum* is the major vector of *E. chaffeensis*, vegetation ticks (host-seeking unfed ticks) in nature exhibit infection rates by *E. chaffeensis* as low as 1% (Anderson et al., 1993), indicating that tick acquisition of the pathogen may be a limiting step for the prevalence of the pathogen. Successful invasion of the pathogen into the vector requires the establishment of the pathogen in the midgut, before travelling to the salivary glands, where it is transmissible during subsequent blood feedings of the tick. During this process, an arms race ensues between the pathogen and the tick, materializing in complex ways. Pathogens must cross at least two cellular barriers, including the midgut epithelia and salivary gland cell layers, while simultaneously circumventing the tick's innate immune system. Thus, the pathogen may manipulate the endogenous physiological and cellular machinery of ticks in order to facilitate the invasion, while it also copes with the tick immune systems. In addition, the pathogen takes advantage of the bioactive components present in the tick's saliva to facilitate its successful transmission and invasion into the vertebrate host upon tick feeding (Francischetti et al., 2009).

Upon infection, the tick's immune system is activated, presumably to suppress the pathogen population to below harmful levels. For example, *Ixodes scapularis* has demonstrated induced expression of 5.3 kDa-antimicrobial peptides via JAK/STAT pathway in the salivary glands in an effort to stave off a potential infection of *Anaplasma phagocytophilum* (Sultana et al., 2010). Additionally, *I. scapularis* nymph and ISE6 cells exhibited differential ferritin expression against infections of *A. phagocytophilum* and *A. marginale* (Zivkovic et al., 2009).

Meanwhile, the obligatory intracellular parasite, rickettsia, must invade and form intracellular inclusions in tick cells in order to multiply themselves before being released into extracellular compartments; e.g. travelling from midgut cells to the hemolymph or from salivary gland cells to the saliva (Ayllón et al., 2013; Dedonder et al., 2012; Liu et al., 2011). *A. phagocytophilum* modulates the transcription of tick genes encoding fodrin and voltage-dependent anion selective channel in the salivary glands and midgut, inhibiting the host's apoptosis-mediated defense system (Ayllón et al., 2013). These processes may utilize host cellular pathways: endosome-mediated cellularization, iron and calcium-dependent proliferation, and cytoskeleton-dependent spreading as preciously described in vertebrate hosts (Alves et al., 2014).

In this study, we aimed to understand the differences in tick gene expression resulting from exposure to the pathogen, in order to understand the interactions between the vector *A. americanum* and the pathogen *E. chaffeensis*. Comparisons of gene expression were made among males and females from groups of adult ticks that have not been exposed to the pathogen (NE) and that have either remained uninfected (U) or become infected (I) following nymphal acquisition feeding. Females and males of each group were used for RNA sequencing to compare the differential gene expression. A search was conducted for differences in gene expression between U and I, while NE served as the baseline for comparisons. The study yielded a number of *A. americanum* genes involved in the immune response against *E. chaffeensis,* as well as several genes whose expression are putatively modulated by *E. chaffeensis* for subverting the tick defense system. Large numbers of the genes involved in the immune system, in pathogen proliferation, and the secretion of salivary proteins were captured in the study.

Materials and Methods

Preparation of ticks: Pathogen non-exposed ticks, Uninfected ticks, and Infected ticks

For preparations of uninfected and pathogen infected adult ticks, nymphs were inoculated onto a white-tailed deer, which was already infected by *E. chaffeensis*. The ticks, after molting into adults, were then inoculated onto a naïve white-tailed deer, and allowed to feed for seven days, at which point, the partially engorged females and males were collected. Individual ticks were cut along the longitudinal midline, and one half was analyzed via pathogen specific PCR diagnosis to assess whether the ticks were infected or uninfected by *E. chaffeensis*. The remaining half of each tick was used for RNAseq (see below). For preparation of pathogen-free ticks (non-exposed), adult female and male *A. americanum* ticks, purchased from the tick rearing center at Oklahoma State University, were fed on a naïve rabbit for seven days. Therefore, three categories of samples are compared here: Non-exposed females/males (NEf/NEm) that were fed on a naïve rabbit as control groups, infected females/males (If/Im) that were exposed to pathogen and became infected, and uninfected females/males (Uf/Um) that were exposed to pathogen but not infected.

Preparation of RNA and libraries

Total RNA was extracted from a pool of three individual ticks from each group (NEf, NEm, If, Im, Uf, and Um) using Direct-zol™ RNA miniprep (Zymo research, Irvine, CA, USA) following manufacturer's protocol. The qualities and quantities of total RNAs were analyzed by Bioanalyzer 2100 (Agilent Technologies, Inc. Santa Clara, CA, USA) and NanoDrop (Thermo Scientific, Wilmington, DE, USA), respectively. At the integrated genomic facility (IGF) at Kansas State University, six different libraries were generated with group-specific tagging from 1 µg of each total RNA using the TruSeq RNA Library Preparation Kit v2 (Illumina, Inc., San Diego, CA, USA), following the manufacturer's protocol.

Illumina sequencing and bioinformatics

For each of the six libraries tagged by different adapters, one hundred cycles of single direction sequencing were performed in the Illumina HiSeq 2500 (Illumina, Inc., San Diego, CA, USA) at the genome sequencing facility at the University of Kansas Medical Center (KUMC). The 208,878,905 total raw sequence reads included the following: NEf = 28,403,332 reads, NEm = 39,445,131 reads, If = 35,850,648 reads, Im = 35,128,945 reads, Uf = 33,107,132 reads, and Um = 36,943,717 reads. FastQC (Andrews) in Galaxy (Blankenberg et al., 2010; Giardine et al., 2005; Goecks et al., 2010) was used for trimming and filtering the sequence reads with the following parameters: Sequence trimming- 5'/3', window size 3, step size 1, and quality score (>=30), Sequence filtering- minimum size (>40nt), minimum quality (>=30), and maximum number of bases allowed outside of quality range 5. After trimming and filtering, de novo assembler Trinity (Grabherr et al., 2011) produced 140,574 transcripts (contigs) from the 117,528,041 cleaned sequence reads.

1) Differential expressions and Gene ontology (GO) term enrichment analyses

RSEM (RNA-seq by expectation-maximization) (Li and Dewey, 2011) estimated transcript abundances by aligning each library to the Trinity assembly, which in turn provided FPKM (fragments per kilobase transcript length per million fragments mapped) values for transcripts. EdgeR (Empirical analysis of digital gene expression data in R)(Robinson et al., 2010) was used for analysis of differential expressions among groups. DE transcripts were filtered for significance in EdgeR to establish the FDR (false discovery rate) <0.001 & fold change (FC) >4x. The transcripts with significant levels of DE in pairwise comparisons of libraries were used for the generation of a heatmap and for clustering analysis. Heatmaps were produced by Java Treeview (Saldanha, 2004) after clustering transcripts by Cluster 3.0 (de Hoon et al., 2004). Clustering was performed for the data following normalization of the data to the transcript expression levels in Non-exposed ticks (NEf and NEm). GO-term enrichment tests of the DE transcripts against GO-terms of gold-transcript set (GTS) were made by Fisher's exact test for p-value (<0.01) in Blast2GO program (Gotz et al., 2008).

2) Post-assembly quality control and processing for gold-transcript set (GTS)

The quality of the Trinity assembly was evaluated and further processed to build the gold-transcript set (GTS). No significant redundancies of the assembled transcripts were identified during self-blast searches of the GTS, although GTS contained 12,670 isotigs that are isoforms counted for alternative splicings. As is typical of transcriptomes assembled using short reads, instances of independent contigs covering different regions of the same gene, separated by gaps, were often found. There were no significant contaminations of the data by transposable elements or mitochondrial sequences, while *E. chaffeensis* contaminations (6 out of 140,574 transcripts, 0.00004% at E < 1E-100 in blastn search) were found and removed from the assembly. In order to build the GTS, the Trinity assembly was filtered for sequences homologous to *A. americanum* ESTs (tblastn, E-value < 1e-100) obtained from the NCBI database, and to *Ixodes scapularis* peptides (blastx, E-value < 1e-30) obtained from Vectorbase (Giraldo-Calderón et al., 2015). At last, we removed any sequences with FPKM < 1 and lacking homology to any *A. americanum* ESTs or *I. scapularis* peptides with the stringency described above.

3) DE in subsets of genes for immune-related, tick sialome, neuropeptides, and GPCRs

To investigate differential expressions of tick transcripts in response to *E. chaffeensis* infection, subsets of the GTS were separately analysed: immune-related (Gulia-Nuss et al., 2016), tick sialome(Ribeiro et al., 2006), neuropeptides (Gulia-Nuss et al., 2016), and GPCRs(Gulia-Nuss et al., 2016). The genes were identified by homology searches against subsets of genes previously described for *I. scapularis,* as cited above. The best hits yielded through tblastn searches (e-value < 1e-10) of the GTS were subsequently back-blasted to *I. scapularis* genes. Then, only putative orthologies, the best hits in the reciprocal blast, of each gene were selected. In the case of the sialome set, since large numbers of paralogy occur due to recent gene expansions, the results from tblastn searches (e-value < 1e-10) of the GST were directly used. DE transcripts were extracted for FPKM > 1 and >10-fold difference. In order to remove artifacts generated by different isoforms, DE were selected only for isoforms with similar expression patterns.

Results and discussion

The assembly of the Illumina sequences, representing six different groups of ticks (non-exposed female/male, infected female/male, and un-infected female/male), was analyzed for three main purposes: 1) Establishing a Gold transcript set (GTS) of transcriptome data to minimize noise in the analyses. 2) Genomic level of differential expressions (DE) categorized by gene ontology (GO) term enrichment analyses for comparisons between male and female and among NE, I, and U groups. 3) The DE focused to the subcategories of genes relevant to the immune pathway, sialome, neuropeptides, and GPCRs.

Sequence analyses for a Gold-transcript set (GTS), and annotation:

A total 208,878,905 raw reads were produced by Illumina 2500 after one hundred cycles of single direction sequencing for six different tagged libraries. The De novo assembler Trinity produced 140,574 transcripts after trimming and filtering the raw data based upon sequence quality (>=30) and length (>=40nt). The assembled transcripts were then subjected to blast searches against the *I. scapularis* official peptide set from the annotated genome sequence and against *A. americanum* ESTs (21,438 sequences), while also being filtered against *Ehrlichia* and *A. americanum* mitochondrial sequences, which were present in very low numbers in the data. The GTS was then established by selection of transcripts showing for sufficient enough frequency (FPKM>1) or for highly similar sequences with *I. scapularis* peptides or *A. americanum* ESTs regardless of the frequency (Fig. 4-1). Manual assessment of the final GTS (61,802 transcripts) for a number of transcripts indicated the presence of typical problems characteristic of transcriptome assembly, independent pieces of transcripts covering different regions of what has been putatively determined to be the same gene. We found that the redundancy of the transcripts by putative allelic contigs were undetectable or rare, while splicing isoforms occurred at a frequency of about 20% in the GTS (12,670 out of 61,802 transcripts). Annotation of 61,802 transcripts in Blast2GO yielded the following statistics (Fig. 4-2): 36,475 (59%) transcripts were blasted without significant hits at e-value (1e-3), 13,807 (22.3%) transcripts were annotated by Blast2GO, 7,320 (11.8%) transcripts were mapped with GO (gene ontology), 4,174 (6.8%) transcripts were with blast hits, and 26 (0.04%) transcripts were with InterProScan without significant blast hits. GO distribution showed 20% (12,145), 14% (8,536)

and 16% (9,725 transcripts) of GTS were annotated in molecular functions (MF), biological process (BP), and cellular components (CC), respectively. The results of blast hits in the non-redundant (nr) database showed that *I. scapularis* was the species with the most frequent blast hits (Fig. 4-2). This GTS, established by the above highly stringent criteria to be of reliable quality, was further used for DE analyses.

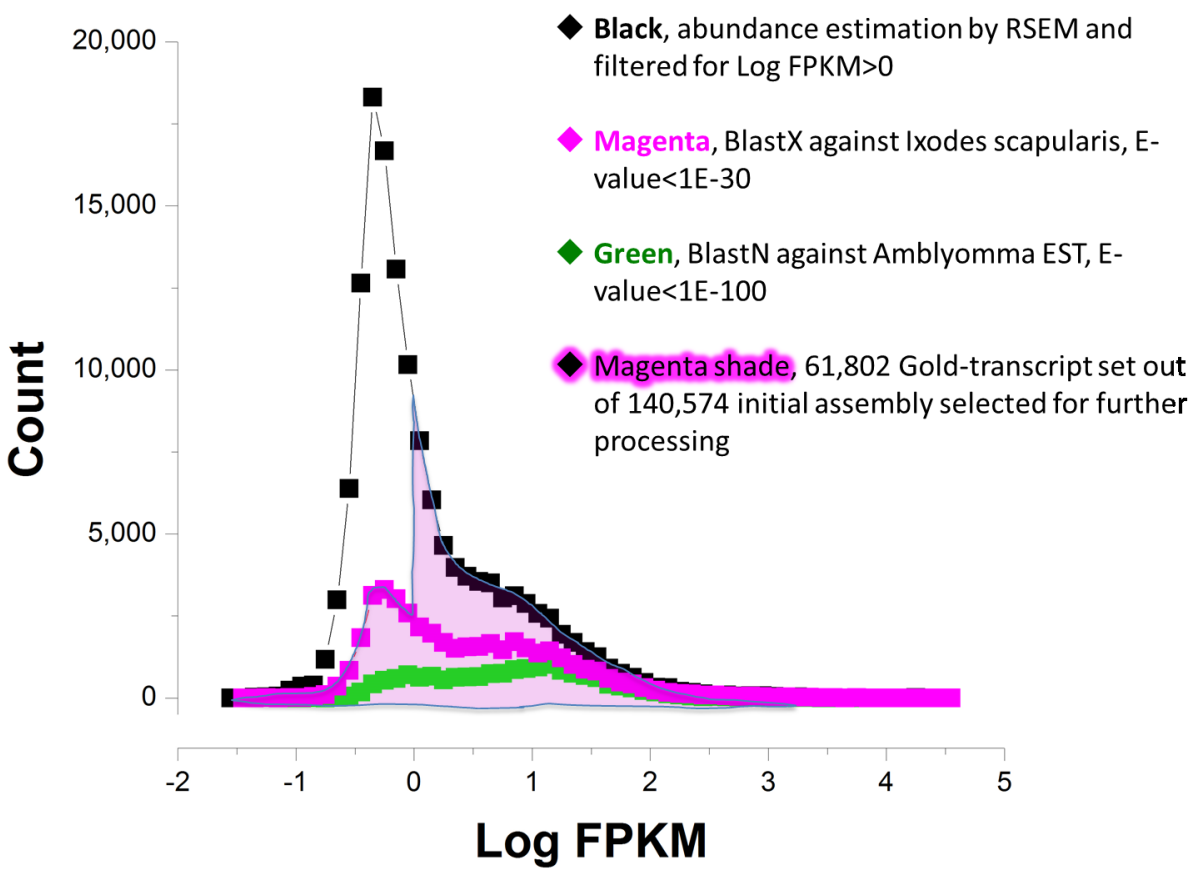

Figure 4-1. Histogram showing FPKM (Fragments per Kilobase of transcripts per Million fragments) of the assemblies and their similarities to to *I. scapularis* official gene set and *A. americanum* EST providing the criteria for forming the Gold-transcript set (GTS).

Among the assembly (140,571 transcripts), the GTS (61,802 transcripts) was selected for Log (FPKM)>0 and significant blast hits.

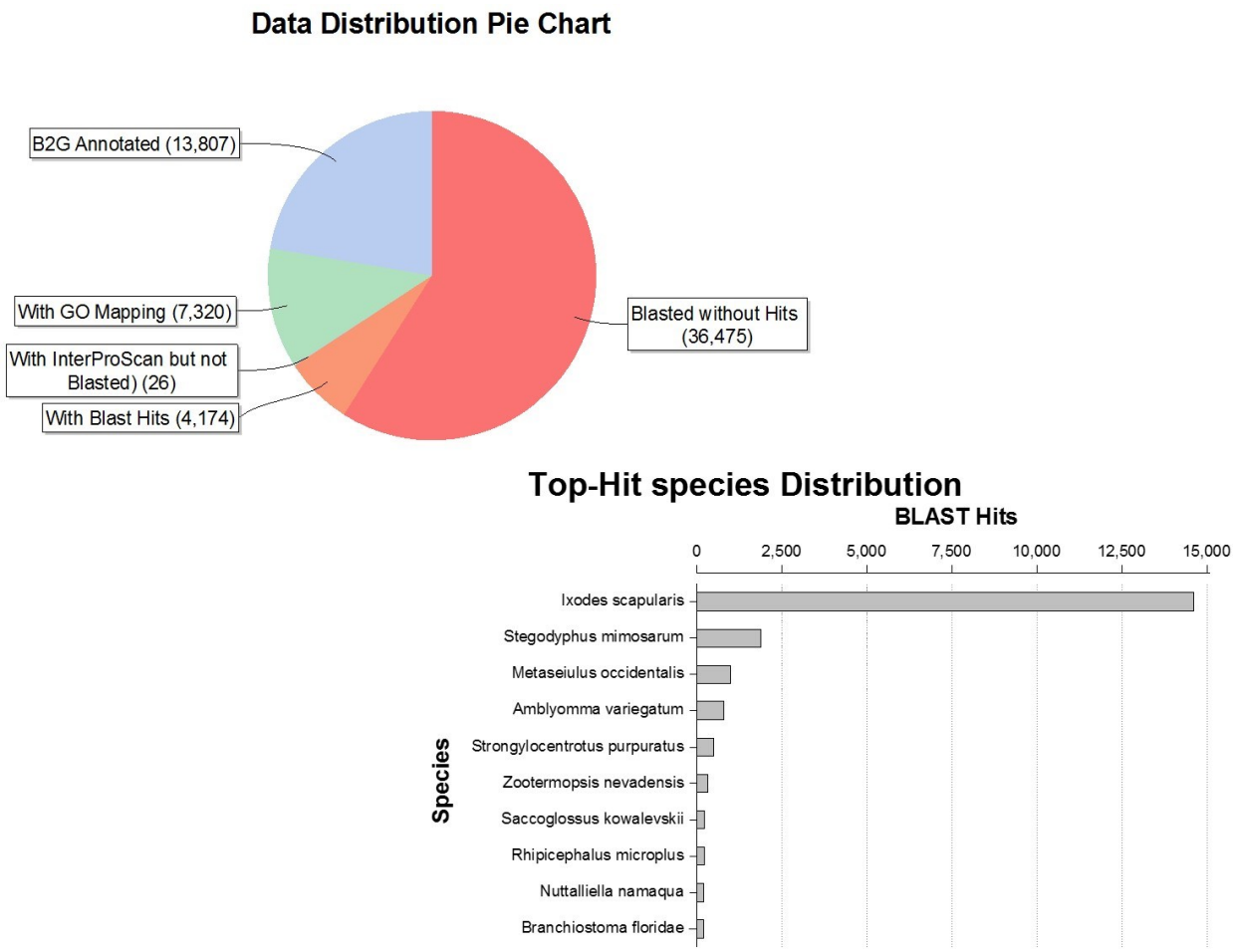

Figure 4-2. Statistics of annotations for Gold-transcript set (GTS; 61,802 transcripts) in Blast2GO.

Pie chart described proportional distribution for the result of different categories of Blast2GO annotation. Bar chart showed the numbers of blast hits from top 10 species.

Analysis of differential expressions (DE) between males and females:

The number of DE transcripts in all combinatorial pairwise comparisons were in the range of 156 to 839 transcripts for FDR (false discovery rate) <0.001 indicating 0.1% false positive and fold change (FC) >4x (Fig. 4-3 and 4). Since the major categories of the DE transcripts were found to be significantly different from NE, in both NEf and NEm, the frequencies of NE were used as the normalization to assess the differences of I and U. For low expressions in I and U compared to the NE, three clusters are present: low-low (LL) for low in both I and U, low-normal (LN) for low in I and normal in U, and normal-low (NL) for normal in I and low in U. High (H) expressions of I and U compared to the NE were also clustered in a similar fashion with clusters representing HH, HN, and NH (Fig. 4-3 and 4). About 6% (range 4.5 to 10.8% and 1.5 to 9.7% for L and H, respectively) of transcripts from each cluster were found to be common in both males and females, as they are shown in overlapping regions of the Venn diagrams (Fig. 4-3 and 4).

The GO-term enrichment analyses, for each cluster against GTS with p-value (<0.01) in Fisher's exact test using Blast2GO, revealed a number of interesting GO-terms relevant to pathogen-vector interactions, which are on the top of the Venn diagrams in Fig. 4-3 and 4. It is worth noting that large numbers of GO terms in immune-related, cytoskeletal, and ion transport functions were captured in these searches. Specifically, the enriched GO-terms "negative regulation of defense response" was found 19% in LN cluster, and "defense response" was found 24% in HN in male cluster, both commonly supporting upregulation of immune system in the pathogen-exposed ticks. "Ca^{++} ion transport", regulating the intracellular Ca^{++} concentration that is required in *Ehrlichia* proliferation (Alves et al., 2014), was also found in HN and NH in female clusters, suggesting that *Ehrlichia* modulates the set of genes necessary for supplying Ca^{++} for *Ehrlichia* proliferation. However, "Cl^- transport" was found in both HH and in LN in female clusters, indicating different subsets of transcripts in this GO-term, with Cl^- transport being regulated in two different ways during pathogen exposure.

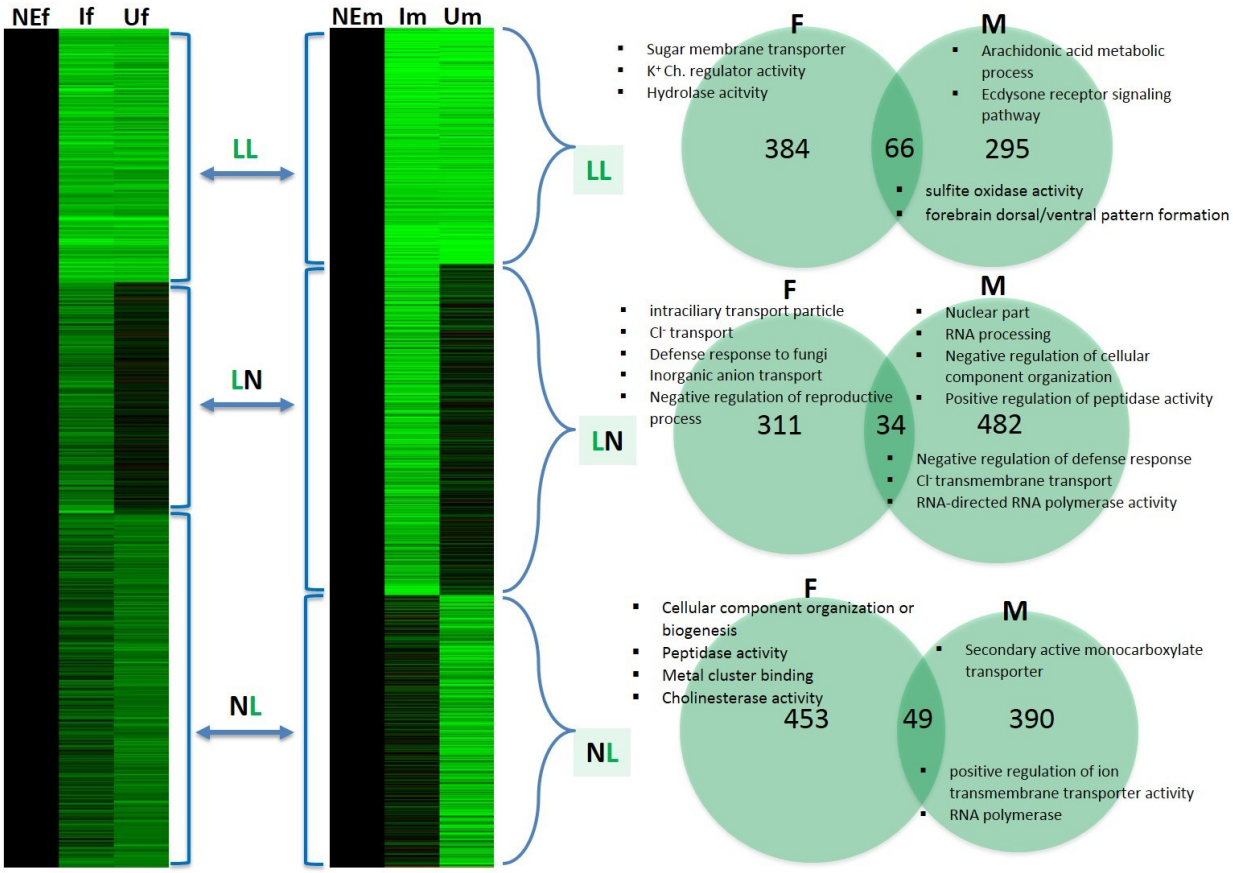

Figure 4-3. Clusters with the transcripts that were downregulated in pathogen-exposed female and male.

GO-term enrichment analyses for each cluster was performed for p-value (<0.01) in Fisher's exact test. Numbers in Venn diagram indicated transcripts for differential expressions (FDR <0.001 & fold differences >4x). Representative GO-terms are on the top of the Venn diagram.

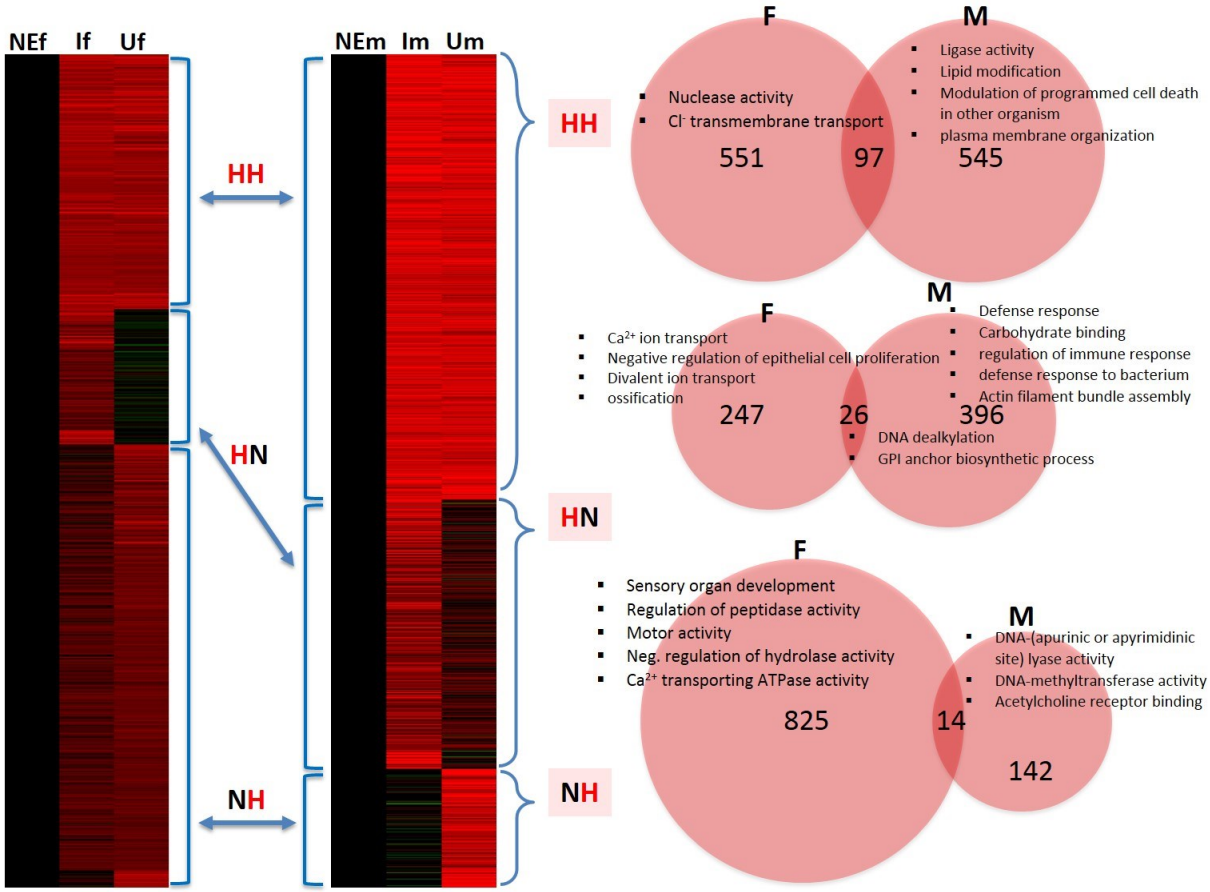

Figure 4-4. Clusters with the transcripts that were downregulated in pathogen-exposed female and male.

GO-term enrichment analyses for each cluster was performed for p-value (<0.01) in Fisher's exact test. Numbers in Venn diagram indicated transcripts for differential expressions (FDR <0.001 & fold changes >4x). Representative GO-terms are on the top of the Venn diagram.

Analysis of DE among non-exposed female (NEf), infected female (If), and uninfected female (Uf)

In addition to the analyses of the entire transcriptome, we performed in-depth analyses of the focused sets of transcripts. The categories of transcripts selected for further analyses were the genes involved in: immune pathways, tick sialome, neuropeptides, and GPCRs. Differential expressions of transcripts among NEf, If, and Uf were categorized based on the gene sets previously published for *I. scapularis* (Gulia-Nuss et al., 2016; Ribeiro et al., 2006) by performing blast searches (e-value < 1e-10) of GTS against the *I. scapularis* database and retaining the best hits (Appendix J Table 1-4). We obtained a number of interesting transcripts showing DE depending on pathogen exposure.

1) Comparison of immune-related genes (Fig. 4-5): The vectorial capacity of ticks may be associated with an optimal level of immune response that allows for pathogen transmission, while concurrently suppressing the pathogen population below levels that would be detrimental to the fitness of the tick itself. A previous study in *I. scapularis* has identified a set of immune-related 88 genes in 14 groups (or pathways)(Gulia-Nuss et al., 2016). Based on the immune-related gene set, our initial homology search identified 703 transcripts (1.1%) from the GTS showing immune related transcripts. Among these, 19 DE transcripts, having FPKM >1 and fold change (FC) > 10x, were captured in NEf, If, and Uf comparisons (Fig. 4-5). DE transcripts were identified as putative orthologies based on the best hits in reciprocal blast. Among the immune-related genes showing DE, most transcripts were captured with high expressions in If and Uf compared to the NEf. Seven transcripts involved in the IMD pathway were all moderately up-regulated in both If and Uf (Fig. 4-5), while two transcripts, including the toll receptor, in the toll pathway were also found to be upregulated. The most significantly up-regulated transcript was the hebraein-like antimicrobial protein, showing 43 and 27 fold higher expressions in If and Uf, respectively, compared to the NEf. Hebraein, a histidine-rich antimicrobial peptide (AMP), was originally characterized from the hemolymph of *A. hebraeum*, and showed antimicrobial activity against gram-negative bacteria (Lai et al., 2004). In addition, transcripts in the Jak/Stat pathway and Fibrinogen-related protein were up-regulated, while some transcripts of Jak/Stat pathway were down-regulated. Interestingly, lysozyme, a gene known for

serving as a defensive mechanism in insects (Shelby et al., 1998), was down regulated in If, but not in Uf. Down regulation of lysozyme transcript may be a consequence of tick cells being manipulated by the intracellular *Ehrlichia* pathogen. Also, DUOX, a gene known for the production of reactive oxygen species as a defensive mechanism against infectious microbes (Ha et al., 2009), was up regulated in Uf, but not in If. Up regulation of DUOX in Uf may be indicative of a defense mechanism that has successfully suppressed pathogen invasion. Overall, a large number of the transcripts in the IMD pathway were upregulated in response to the gram-negative bacteria, *E. chaffensis*, while other transcripts in the toll and JAK/STAT pathways also exhibited changes in expression levels. A limitation for transcriptomic analysis would not capture the post-translational modifications, which occurred for the proteins related to immune pathway.

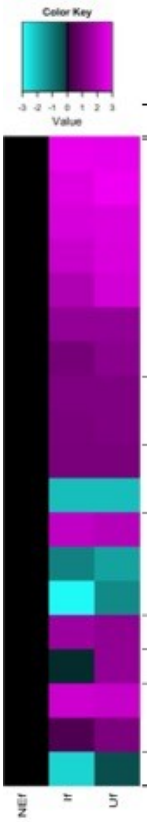

				FPKM		
Pathway	ISCW	GTSid	Sequence Description (immune pathway gene)	NEf	If	Uf
IMD	ISCW002130	c54076_g1_i2	traf2 and nck interacting kinase (IKK beta)	0.00	5.52	5.27
	ISCW010694	c57427_g1_i2	inhibitor of apoptosis protein 1 and 2 (IAP2)	0.00	4.14	6.84
	ISCW015192	c57738_g5_i2	hypothetical protein (POSH)	0.00	3.17	3.49
	ISCW008954	c21018_g1_i1	homeobox protein (Caudal)	0.00	1.91	3.29
	ISCW015192	c54997_g1_i4	hypothetical protein (POSH)	0.00	0.77	2.64
	ISCW003529	c50315_g1_i2	protein kinase (IKK gamma)	0.06	1.96	2.07
	ISCW002130	c50872_g1_i4	camp-dependent protein kinase (IKK beta)	0.15	1.64	3.65
Toll	ISCW020989	c8741_g1_i2	Protein Slit Isoform (Toll)	0.13	1.99	2.05
	ISCW022740	c52114_g2_i1	leucine-rich repeat-containing protein 4b-like (Toll)	0.18	2.27	2.65
RNAi	ISCW009472	c57536_g2_i2	dead box atp-dependent rna helicase (Rm62)	1.45	15.95	16.55
	ISCW011768	c41146_g1_i1	translation initiation factor (Argonaute)	1.12	0.00	0.00
JAK/STAT	ISCW016699	c53723_g1_i2	tyrosine protein kinase receptor tie-1 (JAK receptor)	0.00	1.53	1.01
	ISCW016158	c43035_g1_i1	hepatocyte growth factor receptor-like (JAK)	5.92	0.42	0.12
	ISCW016158	c32331_g1_i1	hepatocyte growth factor receptor (JAK)	8.12	0.00	0.43
AMPs	ISCW002113	c39223_g1_i1	hebreain-like protein (AMP)	4.79	206.21	129.87
Duox	ISCW007865	c53890_g2_i1	peroxidasin homolog (Duox)	0.19	0.16	6.02
Fibrinogen-related	ISCW024686	c55010_g1_i2	FREP partial (Fibrinogen-related protein)	0.00	2.14	1.82
	ISCW013746	c57901_g1_i2	Ixoderin (Fibrinogen-related protein)	0.13	0.31	1.81
Lysozymes	ISCW001645	c30864_g1_i1	Lysozyme (Lysozyme)	2.37	0.00	1.20

Figure 4-5. Differential expressions of the transcripts in immune related pathway.

Heatmap indicated the level of differential expressions of transcripts, which described as either magenta (up-regulation) or cyan (down-regulation). The values of color key indicated fold changes as log10. More details of the methods are in the text.

2) Comparison of sialome-related genes (Fig. 4-6 & 7): Tick saliva containing bioactive molecules facilitates tick feeding by inhibiting mammalian host defensive mechanisms: hemostatic, inflammation, and immune systems (Francischetti et al., 2009b), and also includes the components facilitating pathogen transmission (Ramamoorthi et al., 2005). A previous study in *I. scapularis* has described the gene set for the sialome, 459 genes in 27 groups (Ribeiro et al., 2006). Based on that sialome gene set, our initial homology search identified 507 transcripts (0.8%) from the GTS showing sialome related genes. Among these, 55 DE transcripts were captured in the same fashion with DE transcripts of immune-related in pairwise comparisons among NEf, If and Uf (Fig. 4-6 and 7). The major groups of DE were found in Kunitz domain-containing proteins (named "Kunitz" hereafter), 9&7-kDa families of peptides (named as "9&7 families" hereafter), other putative antiprotease polypeptide (named as "other antiprotease" hereafter), metalloprotease, other enzymes, other unknown function (named as "unknown" hereafter) and lipocalin. Since different subsets in each group of sialome-related genes were up- or down-regulated, it is difficult to predict the functional implications.

A number of transcripts in Kunitz, 9&7 families, other antiprotease, and other enzymes were significantly up regulated from pathogen-exposed females (Fig. 4-6). In the Kunitz group, all DE transcripts were expressed higher in Uf than in If. Kunitz domain containing proteins are normally known to provide anticoagulant activity in saliva in order to facilitate blood feeding. In addition, bacteriostatic properties of Kunitz-type proteins in the tick midgut have been reported in *Dermacentor variabilis* (Ceraul et al., 2008). Upregulation within the Kunitz group in Uf could be indicative of similar defensive bacteriostatic properties against *E. chaffeensis* invasion. Most transcripts in 9&7 families, other antiprotease, and other enzymes were expressed either at higher levels in If than Uf or similarly in both. We speculate that *E. chaffeensis* might induce upregulation of these transcripts and consequently facilitate its transmission into the host. Upregulation of transcripts in other antiproteases, such as serpin, might increase activities inhibiting blood clotting and activation of the complement system in the host, which then promotes pathogen transmission, while upregulation of other enzymes, including serine carboxypeptidase, might facilitate blood digestion in the tick midgut (Motobu et al., 2007).

Large numbers of transcripts in metalloprotease, lipocalin, and unknown were significantly down regulated from pathogen exposed female ticks (Fig. 4-7). Lipocalin functions in anti-inflammatory activities by scavenging histamine and serotonin in mammalian hosts

(Mans and Ribeiro, 2008; Mans et al., 2008). Interestingly, five out of the total seven DE transcripts were down-regulated. These transcripts are clustered in the phylogenetic tree constructed using their amino acid sequences (Fig. 4-8). Upregulated transcripts were also clustered, with the exception of one. The fact that the genes within the lipocalin group exhibit similar patterns of expression suggests that they might share cis- or trans- gene regulatory factors and therefore are regulated in a similar manner (either up or down) in response to pathogen invasion.

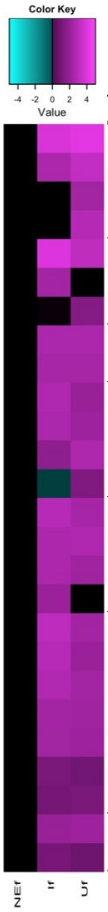

Sialome	Genbank	GTSid	Sequence Description	FPKM NEf	FPKM If	FPKM Uf
Kunitz domain-containing proteins	AAY66790.1	c33149_g2_i1	tissue factor pathway inhibitor 2	0	72.67	151.79
	AAY66790.1	c1364_g1_i1	kunitz domain-containing protein	0	4.02	15.51
	AAM93648.1	c34622_g1_i1	kunitz-type protease inhibitor 2	0	0	2.00
	AAY66790.1	c99354_g1_i1	aprotinin precursor	0	0	6.86
9- and 7-kDa families of peptides	AAY66742.1	c116545_g1_i1	secreted salivary protein	0	99.28	14.19
	AAY66742.1	c94160_g1_i1	secreted salivary protein	0	2.21	0
	AAY66742.1	c60872_g1_i1	secreted salivary protein	1.25	1.29	38.33
Metalloproteases	AAM93653.1	c23710_g1_i1	metalloprotease 5	0	3.53	4.17
	AAM93653.1	c24725_g1_i1	metalloprotease	0	2.61	2.45
Lipocalins	AAY66747.1	c76073_g1_i1	secreted protein	1.90	971.62	191.19
	AAY66754.1	c12236_g1_i1	tpa_inf: salivary lipocalin	0	3.50	1.40
	AAY66754.1	c29271_g1_i2	tpa_inf: salivary lipocalin	0.14	7.57	66.01
	AAY66754.1	c44474_g1_i1	tpa_inf: salivary lipocalin	0.35	0.29	7.40
Other putative antiprotease polypeptides	AAV80788.1	c2669_g1_i1	secreted salivary gland protein	0	7.61	2.73
	AAV80788.1	c37888_g1_i1	secreted salivary gland protein	0	4.16	4.92
	AAM93649.1	c49955_g1_i1	secreted salivary gland protein	0	3.80	1.75
	AAV80788.1	c113035_g1_i1	serpin 2	0	1.10	0.00
Other enzymes	AAM93650.1	c76511_g1_i1	venom serine carboxypeptidase-like	0	12.39	2.17
	AAM93650.1	c46705_g1_i1	Serine carboxypeptidase	0	8.18	1.14
	AAM93650.1	c107846_g1_i1	probable serine carboxypeptidase cpvl	0	5.88	2.15
	AAM93650.1	c52509_g1_i2	probable serine carboxypeptidase cpvl	0	2.15	1.67
	AAV63544.1	c56903_g1_i2	plasma kallikrein	0	1.96	1.41
	AAM93650.1	c52509_g1_i1	probable serine carboxypeptidase cpvl	0.26	4.13	2.62
	AAV63544.1	c56903_g1_i1	enteropeptidase- partial	0.38	4.19	5.61
Other polypeptides of unknown function	AAY66581.1	c60137_g1_i1	secreted salivary gland protein	0.31	31.39	43.81
	AAY66588.1	c50744_g1_i2	ixoderin	0.93	12.58	6.51

Figure 4-6. Up-regulated transcripts in the sialome.

Heatmap indicated the level of differential expressions of transcripts, which described as either magenta (up-regulation) or cyan (down-regulation). The values of color key indicated fold changes as log10. More details of the methods are in the text.

				FPKM		
Sialome	Genebank	GTSid	Sequence Description	NEf	If	Uf
Kunitz domain-containing proteins	AAY667G036.1	c112529_g1_i1	serine proteinase inhibitor	7.92	0	0.08
	AAY66790.1	c38307_g1_i1	tissue factor pathway inhibitor 2	60.61	0	0
9- and 7-kDa families of peptides	AAY66701.1	c107785_g1_i1	secreted salivary gland protein	985.30	0.13	0.13
	AAY66742.1	c76885_g1_i1	secreted salivary gland protein	181.65	0	0
Metalloproteases	AAM93653.1	c55917_g1_i1	salivary gland metalloprotease	21.26	1.58	1.13
	AAM93653.1	c63016_g1_i1	salivary gland metalloprotease	4.34	0.25	0
	AAP22067.1	c36037_g2_i1	tpa_inf: salivary gland metalloprotease	4.76	0.10	0.43
	AAM93653.1	c42895_g1_i2	salivary gland metalloprotease	8.54	0.17	1.25
	AAM93653.1	c47273_g1_i1	metalloprotease 2	153.73	2.72	0.69
	AAM93653.1	c50149_g1_i1	salivary gland metalloprotease	37.94	0.16	0.24
	AAM93653.1	c56824_g1_i2	salivary gland metalloprotease	5.15	0	2.13
	AAM93653.1	c45486_g1_i1	salivary gland metalloprotease	43.91	0.04	0
Lipocalins	AAY66819.1	c12620_g1_i1	secreted protein	4.48	0	0
	AAY66819.1	c48937_g1_i2	secreted protein	15.14	0	0
	AAY66819.1	c107733_g1_i1	secreted protein	2304.95	1.04	1.07
	AAY66639.1	c11558_g1_i1	tpa_inf: salivary lipocalin	11271.54	3.47	4.43
	AAY66754.1	c107851_g1_i1	tpa_inf: salivary lipocalin	4377.04	1.13	0.49
	AAY66819.1	c66079_g1_i1	secreted protein	77.13	0	0
	AAY66819.1	c93146_g1_i1	secreted protein	287.53	0	0
Other putative antiprotease polypeptides	AAM93649.1	c53813_g1_i6	serine proteinase inhibitor serpin	49.87	1.27	0.57
	AAM93649.1	c53813_g1_i5	serine proteinase inhibitor serpin	37.51	0.75	0.74
Other enzymes	AAM93650.1	c57627_g1_i1	venom serine carboxypeptidase-like	34.99	0.47	0.07
	AAM93650.1	c56259_g1_i1	probable serine carboxypeptidase cpvl	204.91	0.04	0.36
	AAM93650.1	c93769_g1_i1	probable serine carboxypeptidase cpvl	313.73	0.00	0.22
Other polypeptides of unknown function	AAY66826.1	c55174_g1_i3	secreted protein	19.30	0.85	0.39
	AAY66826.1	c49280_g1_i2	secreted protein	3.61	0.12	0.15
	AAY66591.1	c49066_g1_i1	protein pry1-like isoform x3	2.93	0.07	0.00
	AAY66827.1	c38574_g1_i3	secreted salivary gland protein	2.86	0	0.18
	AAY66605.1	c53680_g1_i2	secreted salivary gland protein	33.03	0	0

Figure 4-7. Down-regulated transcripts in the sialome.

Heatmap indicated the level of differential expressions of transcripts, which described as either magenta (up-regulation) or cyan (down-regulation). The values of color key indicated fold changes as log10. More details of the methods are in the text.

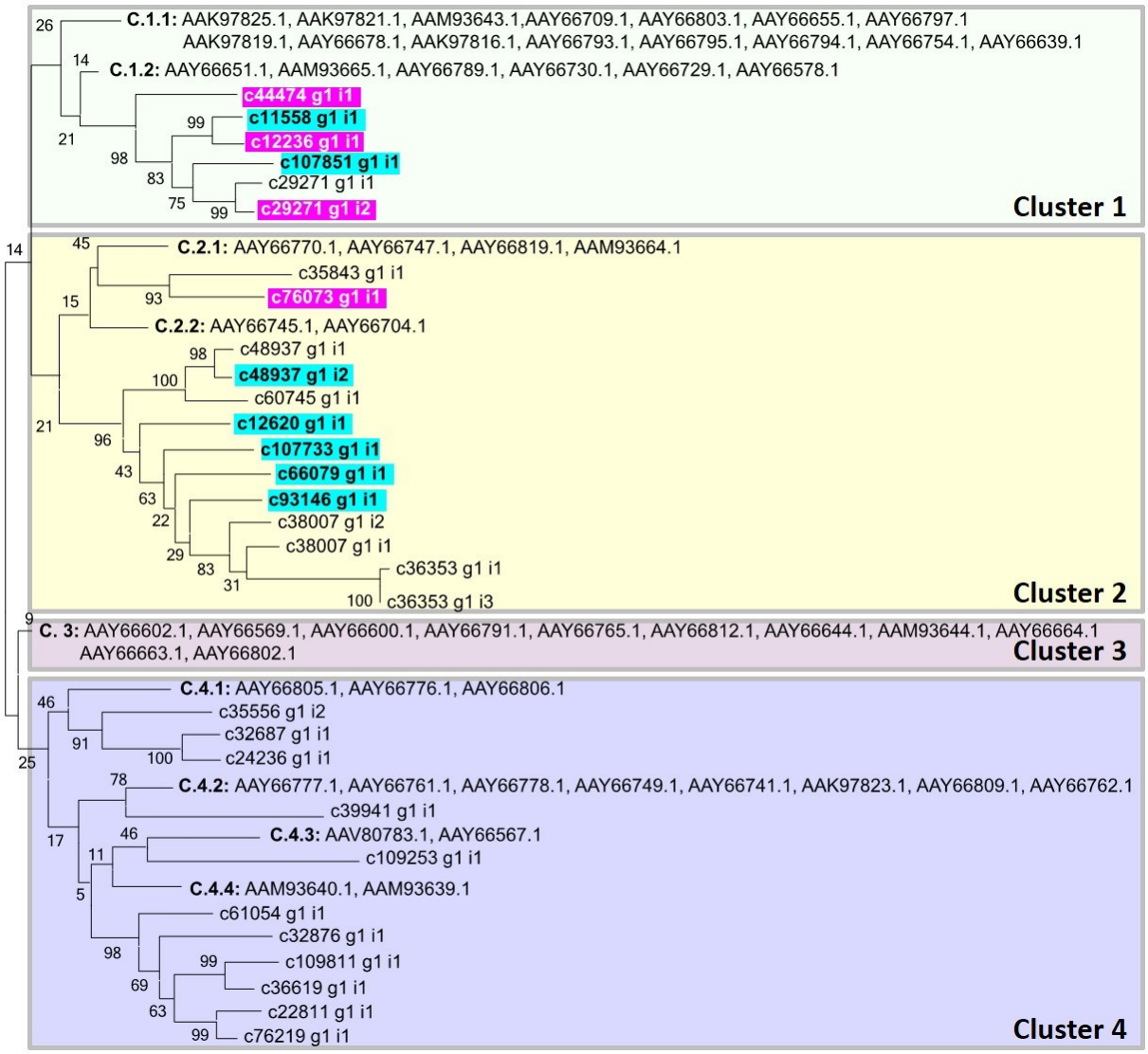

Figure 4-8. Phylogenetic relationship of transcripts for lipocalins of *A. americanum* and *I. scapularis*.

The phylogenetic tree was built by Maximum likelihood method with 500 bootstrap replicates. Four clusters are highlighted by different color boxes: Cluster 1 (C.1, green), Cluster 2 (C.2, yellow), Cluster 3 (C.3, dark red), and Cluster 4 (C.4, purple). Lipocalin genes of *I. scapularis* were shown by Genebank numbers, and the homologous transcripts of *A. ammericanum* are shown by the GTS number as c#####. Transcripts for differential expressions (FPKM > 1 and fold change >10x) were highlighted by red (upregulation) and blue (downregulation), respectively.

3) Comparison of neuropeptide-related genes (Fig. 4-9): Changes in many neuropeptide transcripts are associated with blood feeding (Egekwu et al., 2016), while expression levels in response to interactions with a pathogen have not been studied. In insects, neuropeptides such as bursicon and sex peptide (paralogy of allatostatin B or myoinhibitory peptide) induce the expression of genes encoding antimicrobial peptides as a part of an immune defense mechanism (An et al., 2012; Domanitskaya et al., 2007; Peng et al., 2005). A set of 71 tick neuropeptide genes has previously been identified in the *I. scapularis* genome annotation (Gulia-Nuss et al., 2016). Based on the neuropeptide gene set, our initial homology search identified 28 transcripts (0.04%) from our GTS as being putative neuropeptide transcripts. Only one of these transcripts, encoding an insulin-like peptide, was captured for DE in the same fashion with DE transcripts of immune-related in pairwise comparisons among NEf, If and Uf (Fig. 4-9). In mosquitoes, a hematophagous insect, it was demonstrated that an insulin-like peptide in *Aedes aegypti* functions in the proliferation of hemocytes as a defensive mechanism (Castillo et al., 2011), while insulin-like peptides (bombyxin) in other insects are well known for playing multiple roles in the regulation of digestion, growth, and egg formation in *Bombyx mori* (Iwami, 2000; Mizoguchi and Okamoto, 2013) and *Drosophila melanogaster* (Colombani et al., 2005). In comparing these two groups of blood feeding arthropods, the role of an insulin-like peptide serving as a factor responsible for activating hemocyte proliferation in mosquitoes may also be applicable to ticks having been exposed to pathogens.

4) Comparison of G-protein coupled receptor (GPCR)-related genes (Fig. 4-9): Like the cases of neuropeptide genes, changes in GPCR gene expressions are known to be associated with blood feeding, while their involvement in interactions with pathogens remains to be studied (Egekwu et al., 2016). Intracellular signaling via GPCR for calcium mobilization, leading to the activation of Duox, has been hypothesized (i.e., review in 46). GPCRs are involved in the expression of antimicrobial peptides (AMPs) as seen in the innate immune responses of insects (Buchon et al., 2014) and have been known to influence immunity by regulating the expression of noncanonical UPR (unfolded protein response) genes in nematodes (Sun et al., 2011).

A previous study in *I. scapularis* has identified a set of 186 genes in four classes of GPCR (Gulia-Nuss et al., 2016). Based on the GPCR gene set, our initial homology search identified 282 transcripts (0.5%) from our GTS as potentially being GPCR related genes. Of

these, the method described in section 1 identified nine transcripts as being DE in the pairwise comparisons among NEf, If and Uf (Fig. 4-9). A transcript (c107526_g1_i1) for bursicon receptor was upregulated in If and Uf (Fig. 4-9). Upregulation of a transcript for bursicon receptor may indicate its involvement in the expression of AMPs as a part of defense mechanisms against *E. chaffeensis,* as bursicon was reported in insects to induce expression of AMP genes (An et al., 2012). Also, transcriptome analysis of synganglion from hard ticks (*I. scapularis* and *Dermacentor variabilis*) confirmed the presence of transcripts for bursicon (Bissinger et al., 2011; Egekwu et al., 2014). Interestingly, metabotropic glutamate receptor (mGluR) was upregulated only in If. We speculate that *E. chaffeensis* may be modulating the regulation of the mGluR expressioin to facilitate the proliferation of the pathogen inside the tick. A similar situation is seen in Kaposi's sarcoma-associated herpesvirus (KSHV) infected primary human microvascular dermal endothelial cells (HMVEC-d) where an increased secretion of glutamate and expression of mGluR were documented in conjunction with virus infected cell proliferation (Valiya Veettil et al., 2014). In contrast, a transcript (c16075_g1_i1) for an ACP (AKH/corazonin-related peptide) receptor in class A GPCR (Fig. 4-9) and class D receptors were up- or down-regulated in pathogen-exposed ticks. It is possible that these genes regulate defensive functions against pathogen invasion or that *E. chaffeensis* modulates the expression of these GPCRs to facilitate its invasion of tick cells.

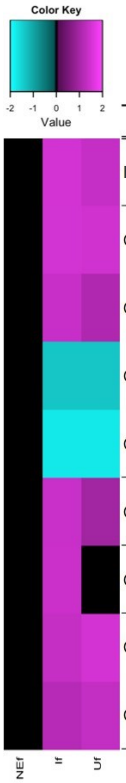

Neuropeptide/GPCRs	ISCW	GTSid	Sequence Description	FPKM NEf	FPKM If	FPKM Uf
Insulin-like peptide		c56947_g1_i1	bombyxin a-1-like partial	0	3.24	2.23
ClassA_orphan receptor	ISCW018990	c38274_g1_i1	alpha-2 adrenergic receptor	0	1.55	1.44
ClassA_Peptide receptor	ISCW015788	c107526_g1_i1	bursicon receptor	0	1.15	0.60
ClassA_orphan receptor	ISCW013584	c69665_g1_i1	neuropeptide y receptor	1.11	0	0
ClassA_Peptide receptor	ISCW019339 +ISCW019342	c16075_g1_i1	ACP receptor	2.77	0	0
ClassB_orphan receptor	ISCW023670	c73839_g1_i1	g-protein coupled receptor mth2	0	1.20	0.41
ClassC_Metabotropic glutamate receptor	ISCW016580	c68364_g1_i1	metabotropic glutamate receptor	0	1.26	0
ClassD receptor	ISCW022151	c115361_g1_i1	starry night	0	1.04	1.61
ClassD receptor	ISCW003177	c13638_g1_i1	frizzled	0.12	2.54	3.47

Figure 4-9. Differential expressions of the transcripts in neuropeptides or GPCRs.

Heatmap indicated the level of differential expressions of transcripts, which described as either magenta (up-regulation) or cyan (down-regulation). The values of color key indicated fold changes as log10. More details of the methods are in the text.

This study, focused on the DE of the lone star tick to examine the effects of the pathogen, *E. chaffeensis*, is summarized below:

- A Gold transcript set (GTS) of the transcriptome was established to minimize the noise in the analyses by using FPKM (>1) and high sequence similarity with to screen databases of peptides and ESTs from close/same species.
- Comparisons of GO term enrichment among NE, I, and U groups revealed upregulation of genes for tick defenses against pathogen invasion, but also for the genes supplying Ca^{++} for pathogen proliferation in the pathogen-exposed ticks.
- Analyses of DE of genes from several subcategories, including the immune pathway, sialome, neuropeptides, and GPCRs, revealed that the invasion of *E. chaffeensis* induced the expression of genes for the IMD pathway, AMPs, lysozyme, bacteriostatic properties of kunitz, insulin-like peptide, and a GPCR, bursicon receptor, involved in the expression of AMPs. DE of lipocalins revealed that clusters of similar lipocalins are co-regulated for up- or downregulation.

The current study uses comparative transcriptomics to provide insights into the molecular interactions of the arms race between the vector, the lone star tick, and the pathogen *E. chaffeensis*. Major categories of the DE genes indicated that the tick suppresses the pathogen population by changing transcriptional levels of immune related genes, while the pathogen may also modulate expression of tick genes that facilitate its invasion into tick cells and its eventual transmission into the mammalian host.

References

Alves, R. N., Levenhagen, M. A., Levenhagen, M. M. M. D., Rieck, S. E., Labruna, M. B. and Beletti, M. E. (2014). The spreading process of Ehrlichia canis in macrophages is dependent on actin cytoskeleton, calcium and iron influx and lysosomal evasion. *Vet. Microbiol.* **168**, 442-446.

An, S., Dong, S., Wang, Q., Li, S., Gilbert, L. I., Stanley, D. and Song, Q. (2012). Insect Neuropeptide Bursicon Homodimers Induce Innate Immune and Stress Genes during Molting by Activating the NF-?B Transcription Factor Relish. *PLoS One* **7**, e34510.

Anderson, B. E., Sims, K. G., Olson, J. G., Childs, J. E., Piesman, J. F., Happ, C. M., Maupin, G. O. and Johnson, B. J. (1993a). Amblyomma americanum: a potential vector of human ehrlichiosis. *The American journal of tropical medicine and hygiene* **49**, 239-244.

Anderson, B. E., Sims, K. G., Olson, J. G., Childs, J. E., Piesman, J. F., Happ, C. M., Maupin, G. O. and Johnson, B. J. B. (1993b). Amblyomma americanum: a Potential Vector of Human Ehrlichiosis. *The American Journal of Tropical Medicine and Hygiene* **49**, 239-244.

Andrews, S. FastQC A Quality Control tool for High Throughput Sequence Data.

Ayllón, N., Villar, M., Busby, A. T., Kocan, K. M., Blouin, E. F., Bonzón-Kulichenko, E., Galindo, R. C., Mangold, A. J., Alberdi, P., Pérez de la Lastra, J. M. et al. (2013). Anaplasma phagocytophilum Inhibits Apoptosis and Promotes Cytoskeleton Rearrangement for Infection of Tick Cells. *Infect. Immun.* **81**, 2415-2425.

Bissinger, B. W., Donohue, K. V., Khalil, S. M. S., Grozinger, C. M., Sonenshine, D. E., Zhu, J. and Roe, R. M. (2011). Synganglion transcriptome and developmental global gene expression in adult females of the American dog tick, Dermacentor variabilis (Acari: Ixodidae). *Insect Mol. Biol.* **20**, 465-491.

Blankenberg, D., Von Kuster, G., Coraor, N., Ananda, G., Lazarus, R., Mangan, M., Nekrutenko, A. and Taylor, J. (2010). Galaxy: a web-based genome analysis tool for experimentalists. *Curr. Protoc. Mol. Biol.* **Chapter 19**, Unit 19 10 1-21.

Buchon, N., Silverman, N. and Cherry, S. (2014). Immunity in Drosophila melanogaster [mdash] from microbial recognition to whole-organism physiology. *Nat. Rev. Immunol.* **14**, 796-810.

Castillo, J., Brown, M. R. and Strand, M. R. (2011). Blood Feeding and Insulin-like Peptide 3 Stimulate Proliferation of Hemocytes in the Mosquito *Aedes aegypti*. *PLoS Pathog.* **7**, e1002274.

Ceraul, S. M., Dreher-Lesnick, S. M., Mulenga, A., Rahman, M. S. and Azad, A. F. (2008). Functional Characterization and Novel Rickettsiostatic Effects of a Kunitz-Type Serine Protease Inhibitor from the Tick Dermacentor variabilis. *Infect. Immun.* **76**, 5429-5435.

Colombani, J., Bianchini, L., Layalle, S., Pondeville, E., Dauphin-Villemant, C., Antoniewski, C., Carre, C., Noselli, S. and Leopold, P. (2005). Antagonistic actions of ecdysone and insulins determine final size in Drosophila. *Science* **310**, 667-70.

de Hoon, M. J. L., Imoto, S., Nolan, J. and Miyano, S. (2004). Open source clustering software. *Bioinformatics* **20**, 1453-1454.

Dedonder, S. E., Cheng, C., Willard, L. H., Boyle, D. L. and Ganta, R. R. (2012). Transmission Electron Microscopy Reveals Distinct Macrophage- and Tick Cell-Specific Morphological Stages of <italic>Ehrlichia chaffeensis</italic>. *PLoS One* **7**, e36749.

Domanitskaya, E. V., Liu, H., Chen, S. and Kubli, E. (2007). The hydroxyproline motif of male sex peptide elicits the innate immune response in Drosophila females. *FEBS J.* **274**, 5659-5668.
Egekwu, N., Sonenshine, D. E., Bissinger, B. W. and Roe, R. M. (2014). Transcriptome of the Female Synganglion of the Black-Legged Tick *Ixodes scapularis* (Acari: Ixodidae) with Comparison between Illumina and 454 Systems. *PLoS One* **9**, e102667.
Egekwu, N., Sonenshine, D. E., Garman, H., Barshis, D. J., Cox, N., Bissinger, B. W., Zhu, J. and M. Roe, R. (2016). Comparison of synganglion neuropeptides, neuropeptide receptors and neurotransmitter receptors and their gene expression in response to feeding in Ixodes scapularis (Ixodidae) vs. Ornithodoros turicata (Argasidae). *Insect Mol. Biol.* **25**, 72-92.
Ewing, S. A., Dawson, J. E., Kocan, A. A., Barker, R. W., Warner, C. K., Panciera, R. J., Fox, J. C., Kocan, K. M. and Blouin, E. F. (1995). Experimental Transmission of Ehrlichia chaffeensis (Rickettsiales: Ehrlichieae) Among White-Tailed Deer by Amblyomma americanum (Acari: Ixodidae). *J. Med. Entomol.* **32**, 368-374.
Francischetti, I. M., Sa-Nunes, A., Mans, B. J., Santos, I. M. and Ribeiro, J. M. (2009a). The role of saliva in tick feeding. *Front. Biosci.* **14**, 2051-88.
Francischetti, I. M. B., Sá-Nunes, A., Mans, B. J., Santos, I. M. and Ribeiro, J. M. C. (2009b). The role of saliva in tick feeding. *Frontiers in Biosciences* **14**.
Giardine, B., Riemer, C., Hardison, R. C., Burhans, R., Elnitski, L., Shah, P., Zhang, Y., Blankenberg, D., Albert, I., Taylor, J. et al. (2005). Galaxy: a platform for interactive large-scale genome analysis. *Genome Res.* **15**, 1451-5.
Giraldo-Calderón, G. I., Emrich, S. J., MacCallum, R. M., Maslen, G., Dialynas, E., Topalis, P., Ho, N., Gesing, S., Consortium, t. V., Madey, G. et al. (2015). VectorBase: an updated bioinformatics resource for invertebrate vectors and other organisms related with human diseases. *Nucleic Acids Res.* **43**, D707-D713.
Goecks, J., Nekrutenko, A., Taylor, J. and Galaxy, T. (2010). Galaxy: a comprehensive approach for supporting accessible, reproducible, and transparent computational research in the life sciences. *Genome Biol* **11**, R86.
Gotz, S., Garcia-Gomez, J. M., Terol, J., Williams, T. D., Nagaraj, S. H., Nueda, M. J., Robles, M., Talon, M., Dopazo, J. and Conesa, A. (2008). High-throughput functional annotation and data mining with the Blast2GO suite. *Nucleic Acids Res* **36**, 3420-35.
Grabherr, M. G., Haas, B. J., Yassour, M., Levin, J. Z., Thompson, D. A., Amit, I., Adiconis, X., Fan, L., Raychowdhury, R., Zeng, Q. et al. (2011). Full-length transcriptome assembly from RNA-Seq data without a reference genome. *Nat. Biotechnol.* **29**, 644-52.
Gulia-Nuss, M., Nuss, A. B., Meyer, J. M., Sonenshine, D. E., Roe, R. M., Waterhouse, R. M., Sattelle, D. B., de la Fuente, J., Ribeiro, J. M., Megy, K. et al. (2016). Genomic insights into the Ixodes scapularis tick vector of Lyme disease. *Nat Commun* **7**.
Ha, E.-M., Lee, K.-A., Seo, Y. Y., Kim, S.-H., Lim, J.-H., Oh, B.-H., Kim, J. and Lee, W.-J. (2009). Coordination of multiple dual oxidase-regulatory pathways in responses to commensal and infectious microbes in drosophila gut. *Nat. Immunol.* **10**, 949-957.
Iwami, M. (2000). Bombyxin: An insect brain peptide that belongs to the insulin family. *Zool. Sci.* **17**, 1035-1044.
James, A. M., Liveris, D., Wormser, G. P., Schwartz, I., Montecalvo, M. A. and Johnson, B. J. B. (2001). Borrelia lonestari Infection after a Bite by an Amblyomma americanum Tick. *J. Infect. Dis.* **183**, 1810-1814.

Lai, R., Takeuchi, H., Lomas, L. O., Jonczy, J., Rigden, D. J., Rees, H. H. and Turner, P. C. (2004). A new type of antimicrobial protein with multiple histidines from the hard tick, Amblyomma hebraeum. *The FASEB Journal*.
Li, B. and Dewey, C. N. (2011). RSEM: accurate transcript quantification from RNA-Seq data with or without a reference genome. *BMC Bioinformatics* **12**, 323.
Liu, L., Narasimhan, S., Dai, J., Zhang, L., Cheng, G. and Fikrig, E. (2011). Ixodes scapularis salivary gland protein P11 facilitates migration of Anaplasma phagocytophilum from the tick gut to salivary glands. *EMBO Rep* **12**, 1196-1203.
Mans, B. J. and Ribeiro, J. M. C. (2008). A novel clade of cysteinyl leukotriene scavengers in soft ticks. *Insect Biochem. Mol. Biol.* **38**, 862-870.
Mans, B. J., Ribeiro, J. M. C. and Andersen, J. F. (2008). Structure, Function, and Evolution of Biogenic Amine-binding Proteins in Soft Ticks. *J. Biol. Chem.* **283**, 18721-18733.
Mizoguchi, A. and Okamoto, N. (2013). Insulin-like and IGF-like peptides in the silkmoth Bombyx mori: discovery, structure, secretion and function. *Front. Physiol.* **4**.
Motobu, M., Tsuji, N., Miyoshi, T., Huang, X., Islam, M. K., Alim, M. A. and Fujisaki, K. (2007). Molecular characterization of a blood-induced serine carboxypeptidase from the ixodid tick Haemaphysalis longicornis. *FEBS J.* **274**, 3299-3312.
Peng, J., Zipperlen, P. and Kubli, E. (2005). Drosophila Sex-Peptide Stimulates Female Innate Immune System after Mating via the Toll and Imd Pathways. *Curr. Biol.* **15**, 1690-1694.
Ramamoorthi, N., Narasimhan, S., Pal, U., Bao, F., Yang, X. F., Fish, D., Anguita, J., Norgard, M. V., Kantor, F. S., Anderson, J. F. et al. (2005). The Lyme disease agent exploits a tick protein to infect the mammalian host. *Nature* **436**, 573-577.
Ribeiro, J. M. C., Alarcon-Chaidez, F., B. Francischetti, I. M., Mans, B. J., Mather, T. N., Valenzuela, J. G. and Wikel, S. K. (2006). An annotated catalog of salivary gland transcripts from Ixodes scapularis ticks. *Insect Biochem. Mol. Biol.* **36**, 111-129.
Richardson, M. A., Smith, D. R. J., Kemp, D. H. and Tellam, R. L. (1993). Native and baculovirus-expressed forms of the immunoprotective protein BM86 from Boophilus microplus are anchored to the cell membrane by a glycosylphosphatidyl inositol linkage. *Insect Mol. Biol.* **1**, 139-147.
Robinson, M. D., McCarthy, D. J. and Smyth, G. K. (2010). edgeR: a Bioconductor package for differential expression analysis of digital gene expression data. *Bioinformatics* **26**, 139-40.
Saldanha, A. J. (2004). Java Treeview—extensible visualization of microarray data. *Bioinformatics* **20**, 3246-3248.
Shelby, K. S., Cui, L. and Webb, B. A. (1998). Polydnavirus-mediated inhibition of lysozyme gene expression and the antibacterial response. *Insect Mol. Biol.* **7**, 265-272.
Sultana, H., Neelakanta, G., Kantor, F. S., Malawista, S. E., Fish, D., Montgomery, R. R. and Fikrig, E. (2010). Anaplasma phagocytophilum induces actin phosphorylation to selectively regulate gene transcription in Ixodes scapularis ticks. *The Journal of Experimental Medicine* **207**, 1727-1743.
Sun, J., Singh, V., Kajino-Sakamoto, R. and Aballay, A. (2011). Neuronal GPCR Controls Innate Immunity by Regulating Noncanonical Unfolded Protein Response Genes. *Science* **332**, 729-732.
Valiya Veettil, M., Dutta, D., Bottero, V., Bandyopadhyay, C., Gjyshi, O., Sharma-Walia, N., Dutta, S. and Chandran, B. (2014). Glutamate Secretion and Metabotropic Glutamate

Receptor 1 Expression during Kaposi's Sarcoma-Associated Herpesvirus Infection Promotes Cell Proliferation. *PLoS Pathog.* **10**, e1004389.
Zivkovic, Z., Blouin, E. F., Manzano-Roman, R., Almazán, C., Naranjo, V., Massung, R. F., Jongejan, F., Kocan, K. M. and de la Fuente, J. (2009). Anaplasma phagocytophilum and Anaplasma marginale Elicit Different Gene Expression Responses in Cultured Tick Cells. *Comp. Funct. Genomics* **2009**, 9.

Chapter 5 - Conclusion

Ticks are hematophagous arthropod vectors that transmit pathogens causing numerous diseases, including Lyme disease, human monocytic ehrlichiosis, Rocky Mountain spotted fever, and southern tick-associated rash illness (STARI). Across the Unites States, the most commonly reported vector-borne disease is Lyme disease, transmitted by the blacklegged tick, *Ixodes scapularis*. Ticks can feed on their host for up to 2 weeks before detaching during which they increase their body weight up to 100 times. A successful long tick feeding duration, which may be the major reason of such efficient disease vectors, requires that the tick be capable of overcoming host defensive responses, mainly through salivation. Tick salivary secretion contains various bioactive components for compromising the hosts' immune responses. Salivation also functions to maintain homeostasis by removing excessive water and ions that are processed from large blood meals. Thus, tick salivary secretion is crucial for survival and for successful feeding. Control of tick salivary secretion involves autocrine/paracrine dopamine, the most potent stimulator of tick salivation. Our research group has recently characterized two dopamine receptors in the salivary glands of the blacklegged tick, *I. scapularis*: dopamine receptor (D1) and invertebrate-specific D1-like dopamine receptor (InvD1L). My dissertation focused on the physiological mechanism of tick salivary secretion, as induced by dopamine, and upon characterizing the tick transcriptome during tick-borne pathogen interaction.

In Chapter 2, my study identified pharmacological agents that distinguish D1 and InvD1L receptors in heterologous receptor expression. The agents discriminating the two dopamine receptors successfully revealed different physiological actions in salivary gland acini *in vitro*. In dopamine-mediated salivary secretion, my study determined that two combinatory physiological actions occurred in the salivary gland type 3 acini: inward fluid transport and release of the luminal content. Utilizing a specific agonist and antagonist for D1 and InvD1L, these two distinct physiological functions of dopamine-induced salivary secretion were linked to the activation of two dopamine receptors. D1 and InvD1L receptors mediated distinct physiological actions; influx of water and solutes in type 2 and 3 acini by low dose of dopamine, and efflux of water and solutes via the acinar duct in type 2 and 3 acini by high dose of dopamine, respectively. Thus, ticks coordinated salivary secretion with duo dopamine receptors.

In Chapter 3, my study further characterized the physiological roles of Na/K-ATPase in salivary secretion. The intracellular signaling pathways for dopamine are only partially known. Na/K-ATPase plays a role in salivary glands function as evidenced by the pharmacological agent ouabain, Na/K-ATPase blocker, to abolish dopamine-induced salivary secretion Na/K-ATPase in previous studies. Also, Na/K-ATPase transcript was highly expressed in the salivary glands according to our tick EST database. The locations of Na/K-ATPase revealed in immunohistochemistry indicate that the Na/K-ATPase in type I acini is located in the basolateral infoldings, implying its typical Na^+ resorptive function of epithelial model. However, the Na/K-ATPase in type III is located in the apical labyrinth-like infolding, implying Na^+ secretion function of epithelial model. A major downstream physiology in the dopamine-mediated salivary secretion is the action of Na/K-ATPase in the epithelial cells in the type III (and likely also in type II) acini for sodium-rich primary saliva formation, while Na/K-ATPase in type I acini is dopamine-independent for the resorptive function. Furthermore, type I acini function in direct water absorption when drinking water in off-host ticks. This is an important finding, because the salivary glands may serve as a direct route for acaricide delivery.

In Chapter 4, my study aimed to understand the differences of tick gene expression caused by exposure to the pathogen in order to understand the interaction between the vector *Amblyomma americanum* and the pathogen *Erhlichia chaffeensis*. Gold transcript set (GTS) of transcriptome was established to minimize the noise in the analyses by using FPKM (>1) and high sequence similarity with to screen database of peptide and ESTs from close/same species. Comparisons of GO term enrichment among pathogen-free, pathogen-infected, and pathogen-uninfected tick groups revealed upregulation of the genes for tick defense against pathogen invasion, but also for the genes supplying Ca^{++} for pathogen proliferation in the pathogen-exposed ticks. Analyses of differential expressions (DE) of genes from several subcategories (immune pathway, sialome, neuropeptides, and GPCRs) revealed that the invasion of *E. chaffeensis* induced expression of genes for the IMD pathway, AMPs, lysozyme, bacteriostatic property of kunitz, insulin-like peptide, and a GPCR, bursicon receptor, involved in the expression of AMP. DE of lipocalins revealed that clusters of similar lipocalins are co-regulated for up- or downregulation. My study provided insight for molecular interactions in the course of arms race between the vector lone star tick and the pathogen *E. chaffeensis* by using comparative transcriptomics. Major categories of the DE genes indicated that the tick suppresses the

pathogen population by changing transcriptional levels of immune related genes, while the pathogen may also modulates expression of genes that facilitate its invasion into tick cells and its eventual transmission into the mammalian host.

The mechanisms controlling tick salivary secretion have been studied for more than four decades. Using classic physiological techniques, the hypotheses and data generated from these studies have laid the groundwork for today's research. In my dissertation research, I reexamine a number of these hypotheses using modern techniques and technologies to study old problems. Using modern techniques, such as confocal microscopy, real time imaging of salivary glands, and Next Generation sequencing, I have built a unique and innovative tool set which, combined with new skills, concepts, and theories, provides a solid foundation for further studies into the mechanisms of tick salivary secretion. Among those, a new hypothesis that I have introduced and continued for further investigations is that of an absorptive function of type 1 acini in off-host ticks. Based on this observation, previous studies have misunderstood the function of type 1 acini for excretion of hygroscopic saliva for absorption of atmospheric water. Furthermore, this type 1 mediated absorptive function may provide a potential route for the delivery of acaricidal compounds in off-host ticks. The roles of one of the major molecular components, Na/K-ATPase, in the water/ion absorption process are being studied by utilizing a combination of tools, such as pharmacological agents, RNAi, and water tracer dyes. I am also expanding upon previous transcriptomics data for ticks by performing acini type-specific studies, taking advantage of my unique ability to dissect and separate type 1, 2, and 3 acini.

My ultimate goal is to develop novel modes of action for the disruption of tick feeding and pathogen transmission via the understanding the fundamentals of physiological and genomic responses to pathogens. I believe the knowledge obtained from my studies makes it possible. In addition, the results of my studies can be expanded to the salivary glands of additional arthropod vectors that transmit pathogens, causing not only human and zoonotic disease, but also to those implicated in plant disease.

Appendix A - Supplementary Movie 1

http://www.biologists.com/movies/JEB_Movies/JEB109462/Movie1.mov

Dopamine triggers acini size increases in the salivary gland of the blacklegged tick, *Ixodes scapularis*. The movie is in 30x speed.

Appendix B - Supplementary Movie 2

http://www.biologists.com/movies/JEB_Movies/JEB109462/Movie2.mov

The movie demonstrates pumping action of an acinus (indicated by arrow) in the salivary gland of the blacklegged tick, *Ixodes scapularis*. The movie is in real time with 1 frame captured per second.

Appendix C - Supplementary Movie 3

http://www.biologists.com/movies/JEB_Movies/JEB109462/Movie3.mov

The movie demonstrates gating action of an acinus in the salivary gland of the blacklegged tick, *Ixodes scapularis*. The periodic movement of acinar valve flaps is indicated by arrow. The movie is in 30x speed.

Appendix D - Supplementary Figure S1

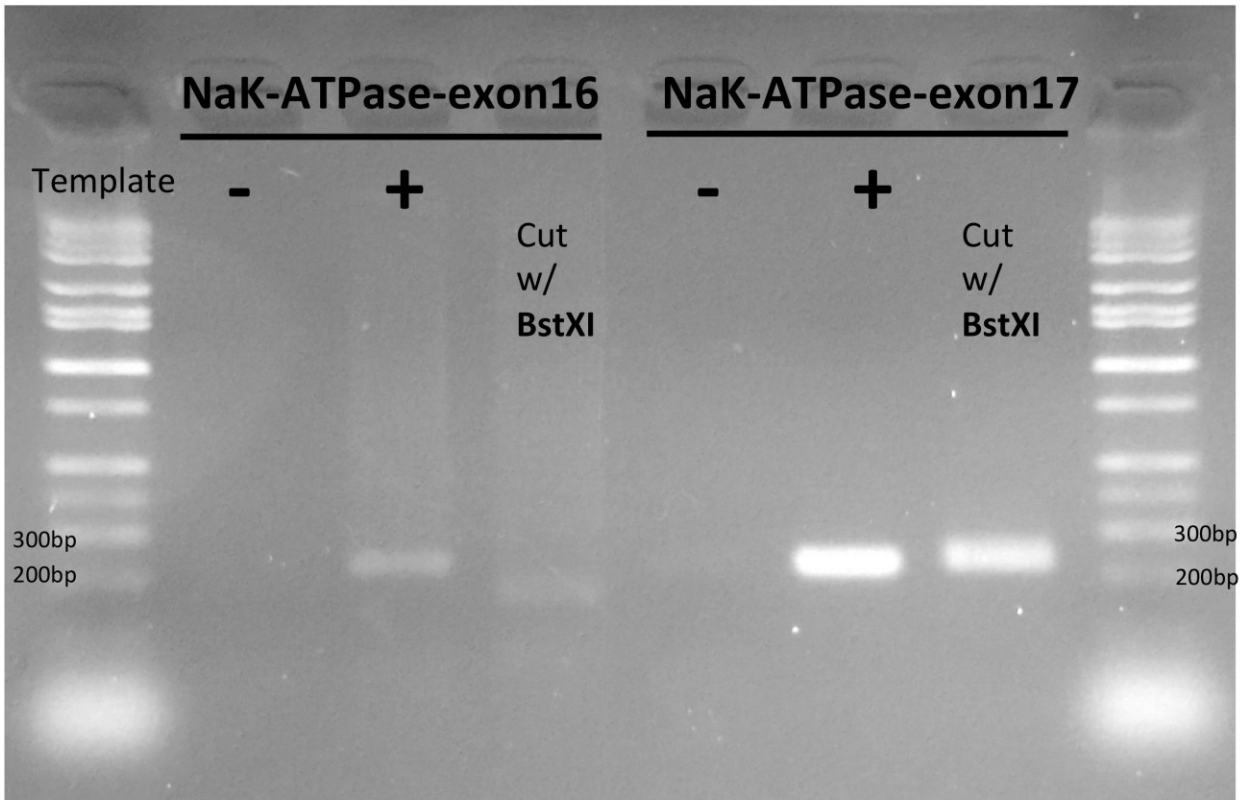

Na/K-ATPase in the salivary glands utilizes mainly exon 17, while low levels of transcripts using exon 16 also exist. Only exon 16 carries the BstXI restriction motif and the BstXI-cut was confirmed by electrophoresis of the exon 16 PCR product and subsequent digestion.

Appendix E - Supplementary Figure S2

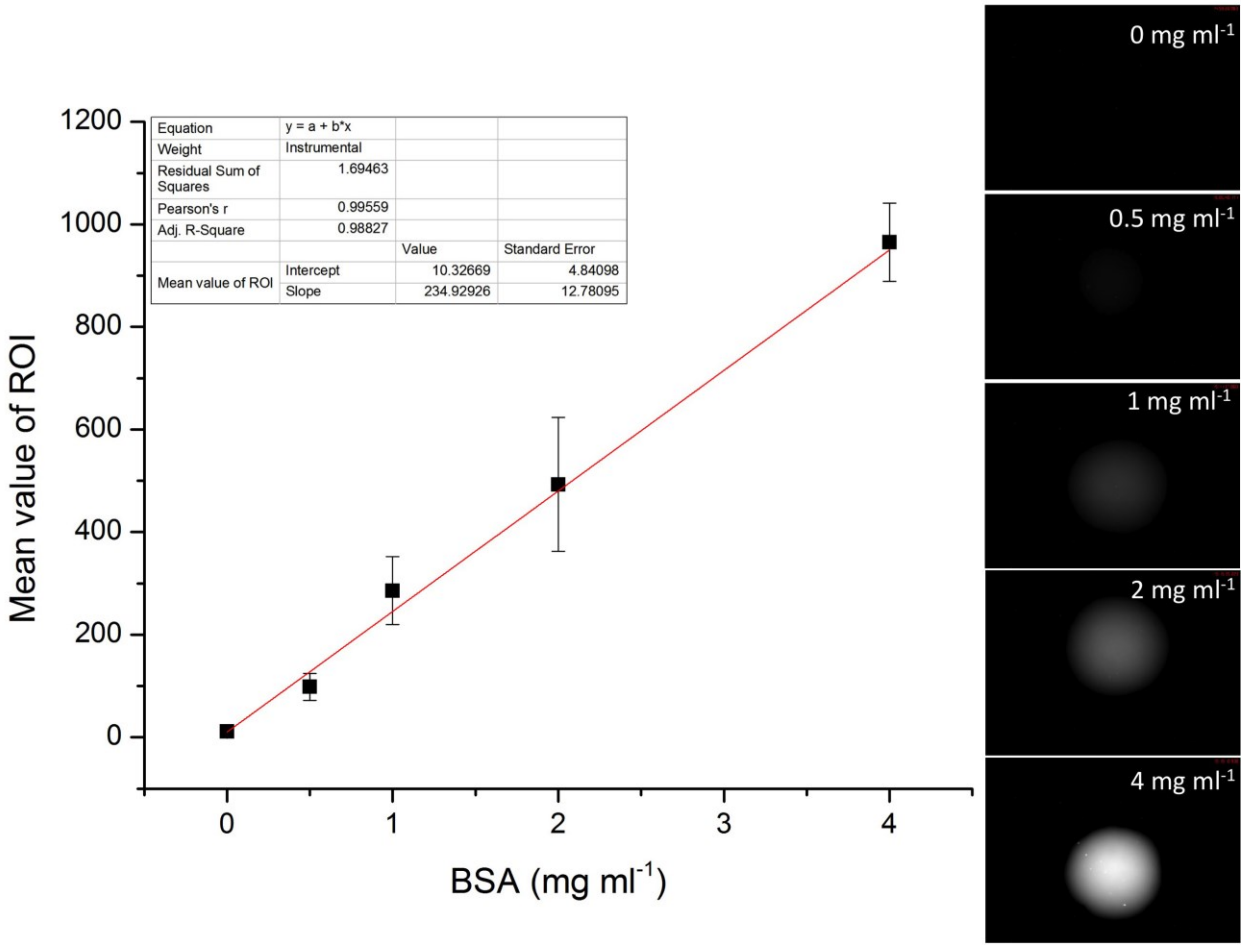

Protein quantification using fluorescence-dye based method (CBQCA). Standard curve: bovine serum albumin (BSA, Serial 2-fold dilutions from 0 mg ml^{-1} – 4 mg ml^{-1}) and captured images of fluorescence from each concentration of BSA.

Appendix F - Supplementary Figure S3

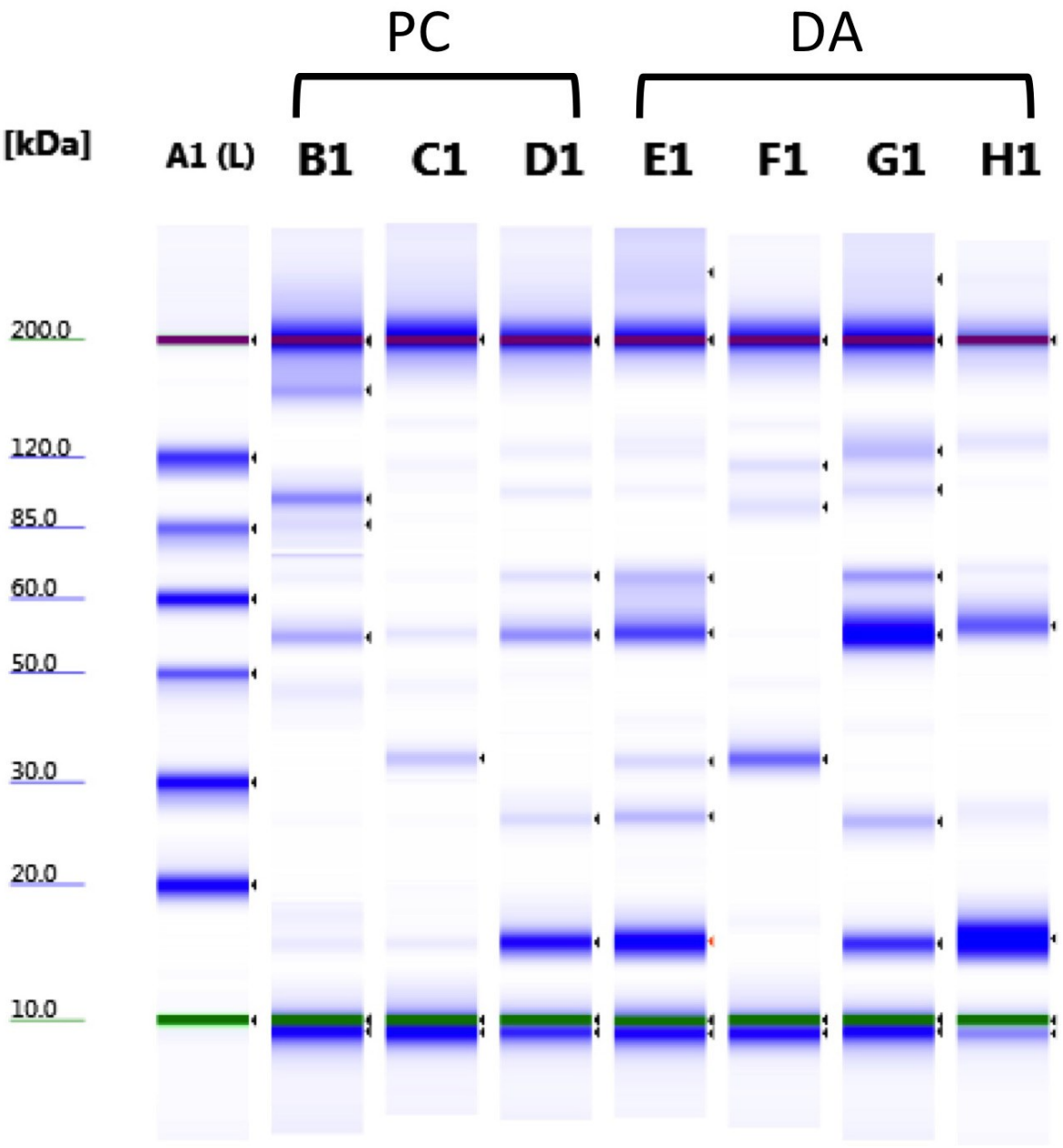

Variations in the salivary proteins shown by Agilent 2200 TapeStation. Each lane represents pooled saliva collected from two individuals. A1: P200 ladder. B1-D1: saliva induced by injection of 2µl of pilocarpine (10mg/ml). E1-H1: saliva induced by injection of 2µl of dopamine (10µmol l^{-1}). The band pattern indicated large variations among different individuals, but not between different methods of inducing salivation.

Appendix G - Supplementary Figure S4

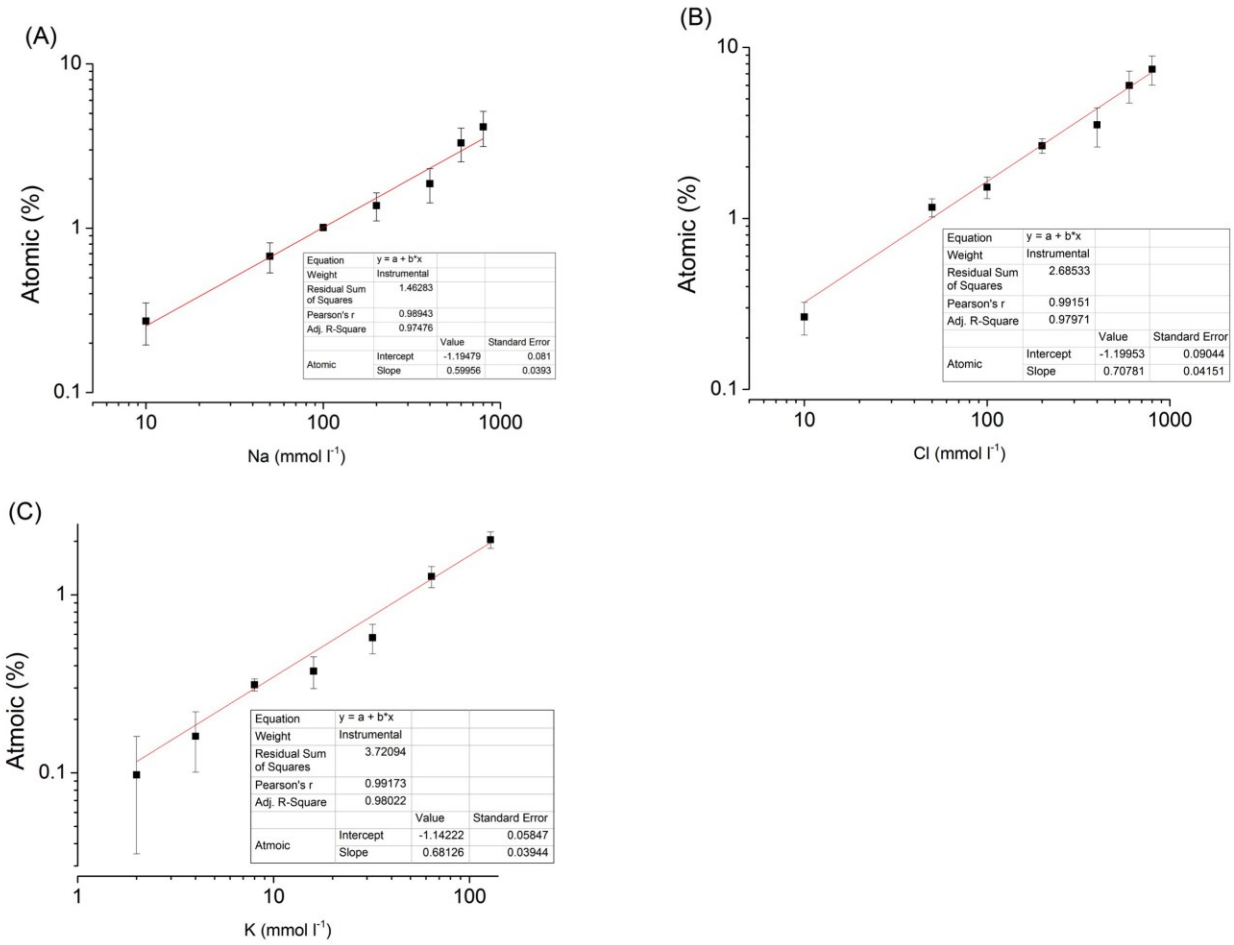

Standard curves of major ions analyzed by SEM/EDS. (A) Na^{+}; (B) Cl^{-}; (C) K^{+}.

Appendix H - Supplementary Figure S5

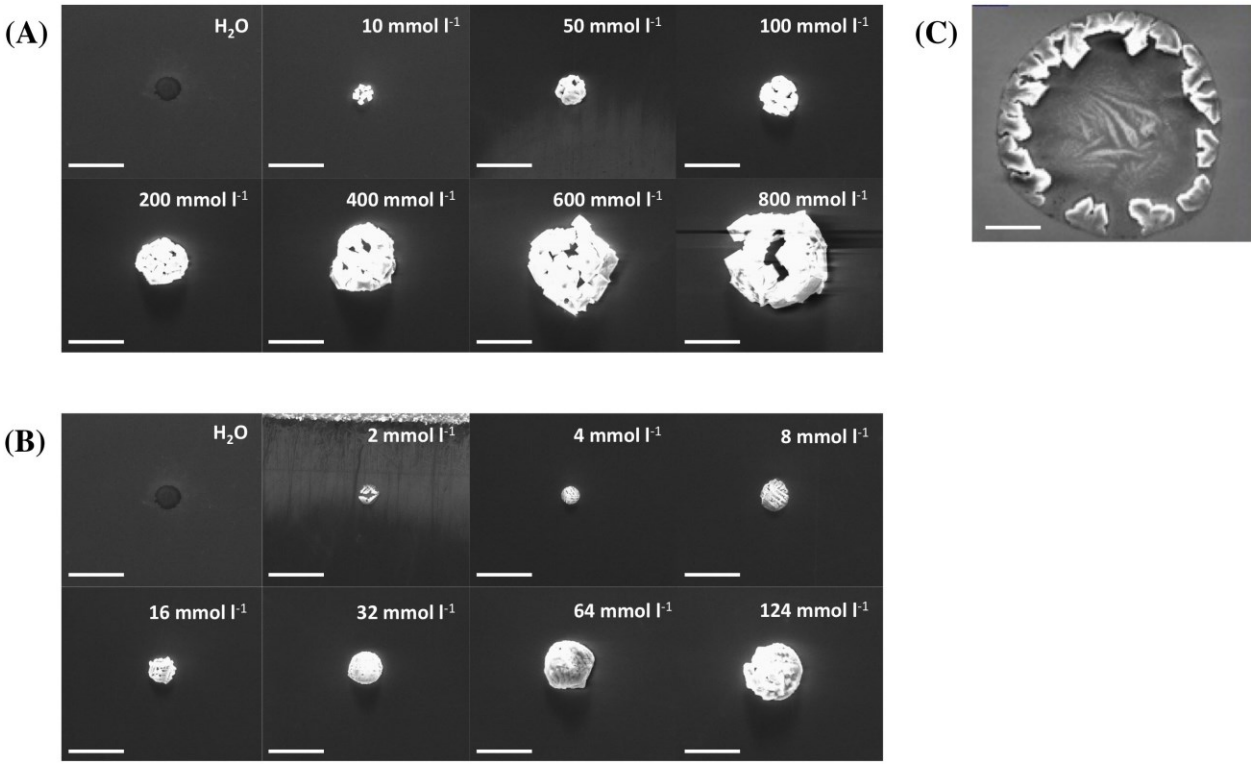

SEM images. A Nanoliter2000 (WPI) was used to place a drop (2 nL) of either standard solution or saliva onto the silicon grid. (A) NaCl standard (10mM to 800mM); (B) KCl standard (2mM to 124mM); (C) Representative image of a drop of saliva. The scale bar indicated is 45µm in length.

Appendix I - Supplementary Figure S6

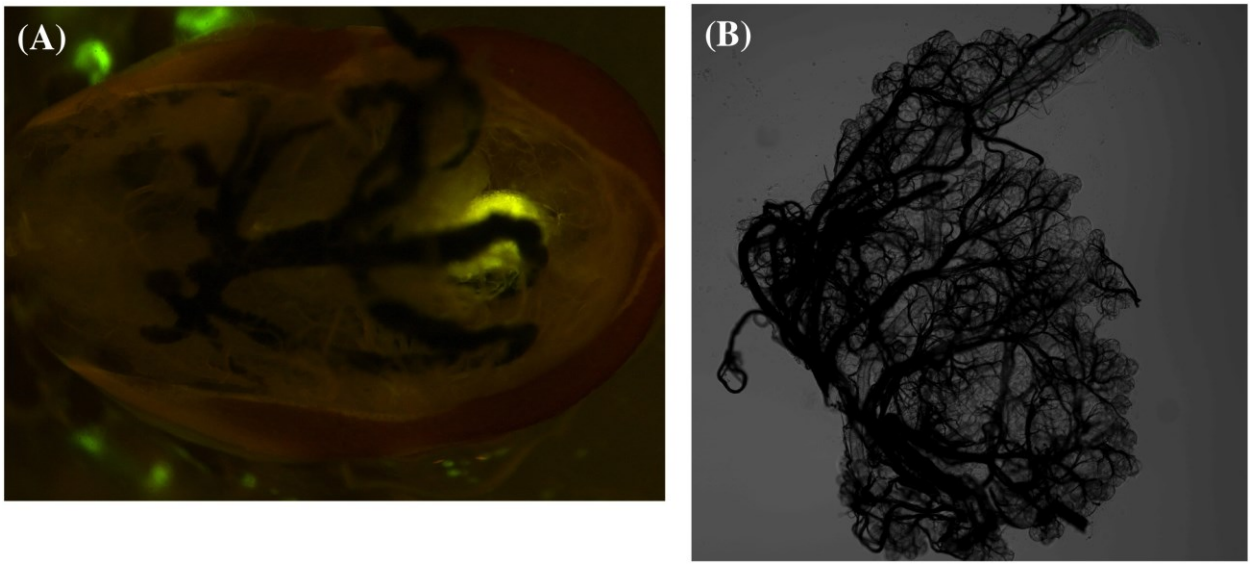

Fluorescence observation from water ingested (negative control) unfed tick. Auto-fluorescence was observed from the hindgut and rectal sac of a water ingested tick. (A) Overview of fluorescence from water ingested tick. (B) Lack of fluorescence from intact isolated salivary gland.

Appendix J - Supplementary Table 1-4

https://ksuemailprod-my.sharepoint.com/personal/kp5091_ksu_edu/_layouts/15/guestaccess.aspx?guestaccesstoken=JJPhbzSRb0PF8XD0BxrFBGccjIbvYgsOCw8tgC2cJAI%3d&docid=2_1a2ea3636935649a484c9c14b528366d2

Supplementary table 1. List of transcripts as being putative immune-related genes from GTS. Table indicated best hits yielded via reciprocal blast searches (e-value <1e-10 for tblastn) of the GTS to *I. scapularis* genes. GTSids were sorted by group name of the immune pathways.

Supplementary table 2. List of transcripts as being putative tick sialome from GTS. Table indicated best hits yielded via tblastn searches (e-value <1e-10 for tblastn) of the *I. scapularis* genes to GTS. GTSids were sorted by group name of sialome (G03, Kunitz; G07, 9&7 families, G08, metalloprotease; G10, Ixostatin family; G11, lipocalin; G12, neuropeptide like poly peptide; G13, oxidant metabolism; G17, other antiprotease; G19, IS6 family; G22, 30kDa family; G25, other enzyme; G26, other known function).

Supplementary table 3. List of transcripts as being putative neuropeptide from GTS. Table indicated best hits yielded via reciprocal blast searches (e-value <1e-10 for tblastn) of the GTS to *I. scapularis* genes. GTSids were sorted by name of neuropeptides in alphabetical order. The table included neuropeptide names, ISCW number, GTSid number, sequence description in Blast2GO annotation, and FPKM values for NEf, If, and Uf.

Supplementary table 4. List of transcripts as being putative GPCR from GTS. Table indicated best hits yielded via reciprocal blast searches (e-value <1e-10 for tblastn) of the GTS to *I. scapularis* genes. GTSids were sorted by the order of class of GPCR. The table included GPCR classes, short names for GPCR, ISCW number, GTSid number, sequence description in Blast2GO annotation, and FPKM values for NEf, If, and Uf.